

Air Force Institute of Technology

AFIT Scholar

Theses and Dissertations

Student Graduate Works

3-16-2007

Modeling In Situ Bioremediation of Perchlorate-Contaminated Groundwater

Roland E. Secody

Follow this and additional works at: <https://scholar.afit.edu/etd>



Part of the [Environmental Engineering Commons](#)

Recommended Citation

Secody, Roland E., "Modeling In Situ Bioremediation of Perchlorate-Contaminated Groundwater" (2007).
Theses and Dissertations. 3019.
<https://scholar.afit.edu/etd/3019>

This Thesis is brought to you for free and open access by the Student Graduate Works at AFIT Scholar. It has been accepted for inclusion in Theses and Dissertations by an authorized administrator of AFIT Scholar. For more information, please contact AFIT.ENWL.Repository@us.af.mil.



**MODELING *IN SITU* BIOREMEDIATION
OF PERCHLORATE-CONTAMINATED
GROUNDWATER**

THESIS

Roland E. Secody, Major, USAF
AFIT/GEM/ENV/07-M13

**DEPARTMENT OF THE AIR FORCE
AIR UNIVERSITY**

AIR FORCE INSTITUTE OF TECHNOLOGY

Wright-Patterson Air Force Base, Ohio

APPROVED FOR PUBLIC RELEASE; DISTRIBUTION UNLIMITED

The views expressed in this thesis are those of the author and do not reflect the official policy or position of the United States Air Force, Department of Defense, or the United States Government.

AFIT/GEM/ENV/07-M13

MODELING *IN SITU* BIOREMEDIATION OF
PERCHLORATE-CONTAMINATED GROUNDWATER

THESIS

Presented to the Faculty

Department of Systems and Engineering Management

Graduate School of Engineering and Management

Air Force Institute of Technology

Air University

Air Education and Training Command

In Partial Fulfillment of the Requirements for the
Degree of Master of Science in Engineering and Environmental Management

Roland E. Secody, BS

Major, USAF

March 2007

APPROVED FOR PUBLIC RELEASE; DISTRIBUTION UNLIMITED

AFIT/GEM/ENV/07-M13

MODELING *IN SITU* BIOREMEDIATION OF
PERCHLORATE-CONTAMINATED GROUNDWATER

Roland E. Secody, BS
Major, USAF

Approved:

//Signed//

Dr. Mark N. Goltz (Chairman)

16 March 07

date

//Signed//

Dr. Jungi Huang (Member)

16 March 07

date

//Signed//

Maj Jeffrey Heiderscheidt, PhD. (Member)

16 March 07

date

Abstract

Perchlorate-contaminated groundwater is a significant problem for the Department of Defense and the United States Air Force. An innovative technology was recently developed which uses dual-screened treatment wells to mix an electron donor into perchlorate-contaminated groundwater in order to effect *in situ* bioremediation of the perchlorate by indigenous perchlorate reducing bacteria without the need to extract the contaminated water from the subsurface. In this study, a model that simulates operation of the technology is calibrated and validated using 761 days of observational data obtained from a field-scale technology evaluation project. A genetic algorithm was used with the first 113 days of data to derive a set of best-fit parameters to describe perchlorate reduction kinetics for the electron donor, citrate, utilized in the evaluation study. The calibrated parameter values were then used to predict technology performance from day 114 through day 761. Measurements of goodness-of-fit statistics indicate the model appears to qualitatively reproduce the salient characteristics of the observed data when utilizing the new best-fit parameter values. Therefore, it appears the model may be a useful tool for designing and operating this technology at other perchlorate-contaminated sites.

Acknowledgements

There are many individuals I would like to thank for the support they've provided as I've worked to complete this thesis. First, I want to thank my wife and daughter for their love, encouragement and patience as I toiled away on the computer working on this thesis. I also owe my sincere gratitude and thanks to Dr. Goltz, whose guidance was incalculable in making this an enjoyable learning experience. Dr. Huang spent numerous hours with me going over the nuances of GMS, genetic algorithms and learning how to use the High Performance Computing Shared Resource Center. Maj. Heiderscheidt was a great resource while getting up and running on GMS and provided valuable insight into modeling. And finally, a gracious word of thanks to all the individuals involved in the ESTCP *In situ* Bioremediation of Perchlorate in Groundwater (ER-0224) Project. For, without their hard work and expertise, none of this would have been possible.

Roland Secody

Table of Contents

	Page
Abstract	iv
Acknowledgements	v
List of Figures	viii
List of Tables	xi
1.0 INTRODUCTION	1
1.1 MOTIVATION	1
1.2 EARLIER STUDIES	8
1.3 RESEARCH OBJECTIVES:	10
1.4 RESEARCH APPROACH	10
1.5 SCOPE AND LIMITATIONS OF RESEARCH	11
2.0 LITERATURE REVIEW	12
2.1 INTRODUCTION	12
2.2 PERCHLORATE CONTAMINATION	12
2.3 HEALTH RISKS	13
2.4 STATE AND FEDERAL PERCHLORATE REGULATIONS	17
2.5 TREATMENT TECHNOLOGIES	18
2.5.1 REMOVAL	18
2.5.2 DESTRUCTION	19
2.5.3 <i>EX SITU</i> VERSUS <i>IN SITU</i> REMEDIATION	21
2.6 HORIZONTAL FLOW TREATMENT WELL (HFTW) SYSTEM	23
2.7 TECHNOLOGY MODEL	25
2.8 AEROJET PILOT STUDY	26
2.9 MODEL CALIBRATION/VALIDATION	30
2.9.1 GOODNESS-OF-FIT ERROR STATISTICS	30
2.10 EVOLUTIONARY COMPUTING (EC)	32
2.11 EVOLUTIONARY/GENETIC ALGORITHMS (GA)	33
2.11.1 GENES/CHROMOSOMES/INDIVIDUALS	34
2.11.2 OBJECTIVE FUNCTION	34
2.11.3 POPULATION	34
2.11.4 PARENT SELECTION	34
2.11.5 VARIATION OPERATORS	35
2.11.6 TERMINATION	35
2.12 SUMMARY	36
3.0 METHODOLOGY	37
3.1 INTRODUCTION	37
3.2 TECHNOLOGY MODEL	37
3.2.1 GROUNDWATER FLOW MODEL	38
3.2.2 RT3D	39
3.3 ELECTRON DONOR SCHEDULE	41
3.4 MEASURES OF PERFORMANCE	42
3.5 GENETIC ALGORITHM (GA) CONFIGURATION	46
3.5.1 GA INDIVIDUAL DEFINITION	46
3.5.2 GA OBJECTIVE FUNCTION	47
3.5.3 POPULATION AND PARENT SELECTION	47

	Page
3.5.4 VARIATION	47
3.5.5 SURVIVOR SELECTION/REPLACEMENT	48
3.5.6 TERMINATION.....	49
3.6 DIFFERING SITE CONDITIONS IMPACTS ON TECHNOLOGY PERFORMANCE	49
4.0 RESULTS AND ANALYSIS.....	50
4.1 INTRODUCTION	50
4.2 PARAMETER SENSITIVITY ANALYSIS	50
4.3 MODEL CALIBRATION	52
4.3.1 GA OPERATION	52
4.3.2 CALIBRATION RESULTS	53
4.3.3 GOODNESS-OF-FIT ERROR STATISTIC RESULTS.....	54
4.4 BREAKTHROUGH CURVES AT MONITORING WELLS	57
4.4.1 SHALLOW UPGRADIENT MONITORING WELL.....	57
4.4.2 DEEP UPGRADIENT MONITORING WELL	59
4.4.3 SHALLOW DOWNGRAIENT MONITORING WELLS	61
4.4.4 DEEP DOWNGRAIENT MONITORING WELLS.....	65
4.5 MODEL APPLICATION TO INVESTIGATE EFFECT OF DIFFERING SITE CONDITIONS ON TECHNOLOGY PERFORMANCE	69
4.5.1 PERCHLORATE CONCENTRATION VS TIME RESULTS.....	69
4.5.2 PERCHLORATE CONTOUR PLOTS	73
5.0 CONCLUSIONS.....	77
5.1 SUMMARY	77
5.2 CONCLUSIONS.....	77
5.3 RECOMMENDATIONS	79
APPENDIX A: DETAILED DESCRIPTION OF THE PARR (2002) HORIZONTAL FLOW TREATMENT WELL (HFTW) TECHNOLOGY MODEL	81
A.1 INTRODUCTION	81
A.2 FLOW AND TRANSPORT MODEL	81
A.3 ELECTRON DONOR.....	82
A.4 ELECTRON ACCEPTORS.....	82
A.5 MICROBIAL GROWTH/DECAY	83
A.6 PARAMETER VALUES.....	83
A.7 DEFINITION OF TERMS.....	85
APPENDIX B: MONITORING WELL BREAKTHROUGH GRAPHS	88
BIBLIOGRAPHY	108
Vita.....	113

List of Figures

	Page
FIGURE 1.1 KNOWN PERCHLORATE RELEASES AND PERCHLORATE DETECTIONS UNDER THE UCMR PROGRAM (BRANDHUBER, 2005)	2
FIGURE 1.2 HORIZONTAL FLOW TREATMENT WELL (HFTW) SYSTEM	7
FIGURE 1.3 AEROJET SITE WITH PERCHLORATE ISOCONCENTRATION CONTOURS INDICATED IN PPB	9
FIGURE 2.1 PROPOSED EPA MODE-OF-ACTION MODEL (EPA, 2002)	14
FIGURE 2.2 PROPOSED NRC MODE-OF-ACTION MODEL (NRC, 2005)	16
FIGURE 2.3 GENERAL PERCHLORATE TECHNOLOGY TREATMENT TYPES (GWR TAC, 2001)	20
FIGURE 2.4 PERCHLORATE REDUCTION PATHWAY (XU ET AL., 2003 ADAPTED FROM RIKKEN ET AL., 1996)	21
FIGURE 2.5 IN-SITU VERSUS <i>EX SITU</i> TREATMENT (KINGSCOTT AND WEISMAN, 2002)	22
FIGURE 2.6 STREAMLINES REPRESENTING GROUNDWATER CAPTURE/RECIRCULATION IN LOWER PORTION OF AN AQUIFER WHERE UPFLOW WELL (U) EXTRACTS AND DOWNFLOW WELL (D) INJECTS WATER. ASTERISKS REPRESENT STAGNATION POINTS (CUNNINGHAM ET AL., 2004)	24
FIGURE 2.7 PLAN VIEW OF HFTW AND MONITORING WELL LAYOUT AT AEROJET SITE (HATZINGER AND DIEBOLD, 2005)	28
FIGURE 2.8 PERCHLORATE LEVELS IN SHALLOW AND VERY SHALLOW MONITORING WELLS (HATZINGER AND DIEBOLD, 2005; SHAW, 2006)	29
FIGURE 2.9 PERCHLORATE LEVELS IN DEEP MONITORING WELLS (HATZINGER AND DIEBOLD, 2005; SHAW, 2006)	30
FIGURE 2.10 GENERAL SCHEME OF AN EVOLUTIONARY ALGORITHM (EIBAN AND SMITH, 2003)	33
FIGURE 3.1 MODFLOW RECTILINEAR GRID	38
FIGURE 3.2 PERCHLORATE CONCENTRATION VS TIME AT SHALLOW MONITORING WELL 3628 (SEE FIGURE 2.7 FOR LOCATION)	44
FIGURE 3.3 PERCHLORATE CONCENTRATION VS TIME AT SHALLOW MONITORING WELL 3631 (SEE FIGURE 2.7 FOR LOCATION)	44
FIGURE 3.4 PERCHLORATE CONCENTRATION VS TIME AT DEEP MONITORING WELL 3630 (SEE FIGURE 2.7 FOR LOCATION)	45
FIGURE 3.5 PERCHLORATE CONCENTRATION VS TIME AT DEEP MONITORING WELL 3633 (SEE FIGURE 2.7 FOR LOCATION)	46
FIGURE 4.1 OBJECTIVE FUNCTION VALUE OF MOST FIT INDIVIDUAL AND POPULATION AVERAGE VS GA GENERATION	53
FIGURE 4.2 CHANGES IN MEAN ERROR OVER GA GENERATIONS	55
FIGURE 4.3 CHANGES IN MEAN ABSOLUTE ERROR OVER GA GENERATIONS	56
FIGURE 4.4 CHANGES IN ROOT MEAN-SQUARED ERROR OVER GA GENERATIONS	56
FIGURE 4.5 OXYGEN CONCENTRATION VS TIME AT WELL NMW3	58
FIGURE 4.6 NITRATE CONCENTRATION VS TIME AT WELL NMW3	58
FIGURE 4.7 PERCHLORATE CONCENTRATION VS TIME AT WELL NMW3	59
FIGURE 4.8 OXYGEN CONCENTRATION VS TIME AT WELL NMW4	60
FIGURE 4.9 NITRATE CONCENTRATION VS TIME AT WELL NMW4	60
FIGURE 4.10 PERCHLORATE CONCENTRATION VS TIME AT WELL NMW4	61
FIGURE 4.11 OXYGEN CONCENTRATION VS TIME AT WELL 3632	62
FIGURE 4.12 NITRATE CONCENTRATION VS TIME AT WELL 3632	62
FIGURE 4.13 PERCHLORATE CONCENTRATION VS TIME AT WELL 3632	63

	Page
FIGURE 4.14 OXYGEN CONCENTRATION VS TIME AT WELL NMW7	64
FIGURE 4.15 NITRATE CONCENTRATION VS TIME AT WELL NMW7	64
FIGURE 4.16 PERCHLORATE CONCENTRATION VS TIME AT WELL NMW7	65
FIGURE 4.17 OXYGEN CONCENTRATION VS TIME AT WELL 3519	66
FIGURE 4.18 NITRATE CONCENTRATION VS TIME AT WELL 3519	66
FIGURE 4.19 PERCHLORATE CONCENTRATION VS TIME AT WELL 3519	67
FIGURE 4.20 OXYGEN CONCENTRATION VS TIME AT WELL NMW10	68
FIGURE 4.21 NITRATE CONCENTRATION VS TIME AT WELL NMW10	68
FIGURE 4.22 PERCHLORATE CONCENTRATION VS TIME AT WELL NMW10	69
FIGURE 4.23 SIMULATED PERCHLORATE CONCENTRATION VS TIME AT WELL NMW3 FOR HYPOTHETICAL SITES 1 AND 2 AND AEROJET	70
FIGURE 4.24 SIMULATED PERCHLORATE CONCENTRATION VS TIME AT WELL NMW4 FOR HYPOTHETICAL SITES 1 AND 2 AND AEROJET	71
FIGURE 4.25 SIMULATED PERCHLORATE CONCENTRATION VS TIME AT WELL 3632 FOR HYPOTHETICAL SITES 1 AND 2 AND AEROJET	71
FIGURE 4.26 SIMULATED PERCHLORATE CONCENTRATION VS TIME AT WELL NMW7 FOR HYPOTHETICAL SITES 1 AND 2 AND AEROJET	72
FIGURE 4.27 SIMULATED PERCHLORATE CONCENTRATION VS TIME AT WELL 3519 FOR HYPOTHETICAL SITES 1 AND 2 AND AEROJET	72
FIGURE 4.28 SIMULATED PERCHLORATE CONCENTRATION VS TIME AT WELL NMW10 FOR HYPOTHETICAL SITES 1 AND 2 AND AEROJET	73
FIGURE 4.29 PERCHLORATE “HOLE” (DEFINED BY 2.4 MG/L CONTOUR) AT LAYER 5 AND DAY 63	74
FIGURE 4.30 PERCHLORATE “HOLE” (DEFINED BY 2.4 MG/L CONTOUR) AT LAYER 5 AND DAY 182	75
FIGURE 4.31 PERCHLORATE “HOLE” (DEFINED BY 2.4 MG/L CONTOUR) AT LAYER 5 AND DAY 364	76
FIGURE B.1 AEROJET HFTW AND MONITORING WELL SITE LAYOUT	88
FIGURE B.2 NMW1 OXYGEN BREAKTHROUGH	89
FIGURE B.3 NMW1 NITRATE BREAKTHROUGH	89
FIGURE B.4 NMW1 PERCHLORATE BREAKTHROUGH	89
FIGURE B.5 NMW2 OXYGEN BREAKTHROUGH	90
FIGURE B.6 NMW2 NITRATE BREAKTHROUGH	90
FIGURE B.7 NMW2 PERCHLORATE BREAKTHROUGH	90
FIGURE B.8 NMW3 OXYGEN BREAKTHROUGH	91
FIGURE B.9 NMW3 NITRATE BREAKTHROUGH	91
FIGURE B.10 NMW3 PERCHLORATE BREAKTHROUGH	91
FIGURE B.11 NMW4 OXYGEN BREAKTHROUGH	92
FIGURE B.12 NMW4 NITRATE BREAKTHROUGH	92
FIGURE B.13 NMW4 PERCHLORATE BREAKTHROUGH	92
FIGURE B.14 NMW5 OXYGEN BREAKTHROUGH	93
FIGURE B.15 NMW5 NITRATE BREAKTHROUGH	93
FIGURE B.16 NMW5 PERCHLORATE BREAKTHROUGH	93
FIGURE B.17 NMW7 OXYGEN BREAKTHROUGH	94
FIGURE B.18 NMW7 NITRATE BREAKTHROUGH	94
FIGURE B.19 NMW7 PERCHLORATE BREAKTHROUGH	94
FIGURE B.20 NMW8 OXYGEN BREAKTHROUGH	95
FIGURE B.21 NMW8 NITRATE BREAKTHROUGH	95
FIGURE B.22 NMW8 PERCHLORATE BREAKTHROUGH	95
FIGURE B.23 NMW9 OXYGEN BREAKTHROUGH	96
FIGURE B.24 NMW9 NITRATE BREAKTHROUGH	96
FIGURE B.25 NMW9 PERCHLORATE BREAKTHROUGH	96
FIGURE B.26 NMW10 OXYGEN BREAKTHROUGH	97
FIGURE B.27 NMW10 NITRATE BREAKTHROUGH	97

	Page
FIGURE B.28 NMW10 PERCHLORATE BREAKTHROUGH	97
FIGURE B.29 3514 OXYGEN BREAKTHROUGH	98
FIGURE B.30 3514 NITRATE BREAKTHROUGH	98
FIGURE B.31 3514 PERCHLORATE BREAKTHROUGH.....	98
FIGURE B.32 3519 OXYGEN BREAKTHROUGH	99
FIGURE B.33 3519 NITRATE BREAKTHROUGH	99
FIGURE B.34 3519 PERCHLORATE BREAKTHROUGH.....	99
FIGURE B.35 3627 OXYGEN BREAKTHROUGH	100
FIGURE B.36 3627 NITRATE BREAKTHROUGH	100
FIGURE B.37 3627 PERCHLORATE BREAKTHROUGH.....	100
FIGURE B.38 3628 OXYGEN BREAKTHROUGH	101
FIGURE B.39 3628 NITRATE BREAKTHROUGH	101
FIGURE B.40 3628 PERCHLORATE BREAKTHROUGH.....	101
FIGURE B.41 3629 OXYGEN BREAKTHROUGH	102
FIGURE B.42 3629 NITRATE BREAKTHROUGH	102
FIGURE B.43 3629 PERCHLORATE BREAKTHROUGH.....	102
FIGURE B.44 3630 OXYGEN BREAKTHROUGH	103
FIGURE B.45 3630 NITRATE BREAKTHROUGH	103
FIGURE B.46 3630 PERCHLORATE BREAKTHROUGH.....	103
FIGURE B.47 3631 OXYGEN BREAKTHROUGH	104
FIGURE B.48 3631 NITRATE BREAKTHROUGH	104
FIGURE B.49 3631 PERCHLORATE BREAKTHROUGH.....	104
FIGURE B.50 3632 OXYGEN BREAKTHROUGH	105
FIGURE B.51 3632 NITRATE BREAKTHROUGH	105
FIGURE B.52 3632 PERCHLORATE BREAKTHROUGH.....	105
FIGURE B.53 3633 OXYGEN BREAKTHROUGH	106
FIGURE B.54 3633 NITRATE BREAKTHROUGH	106
FIGURE B.55 3633 PERCHLORATE BREAKTHROUGH.....	106
FIGURE B.56 4440 OXYGEN BREAKTHROUGH	107
FIGURE B.57 4440 NITRATE BREAKTHROUGH	107
FIGURE B.58 4440 PERCHLORATE BREAKTHROUGH.....	107

List of Tables

	Page
TABLE 1.1 STATE ADVISORY LEVELS FOR PERCHLORATE (ADEQ, 2007. EPA, 2005; CDHS, 2007; MASS DEP, 2006; NDEP, 2006)	4
TABLE 1.2 PERCHLORATE TREATMENT/REMEDATION TECHNOLOGIES (EPA 2005, ITRC 2005)—ITALICS INDICATE INNOVATIVE TECHNOLOGIES.....	5
TABLE 2.1 PERCHLORATE EXPOSURE CAUSAL RELATIONSHIPS (NRC, 2005)	15
TABLE 2.2 TECHNOLOGY MODEL PARAMETERS.....	25
TABLE 2.3 MONITORING WELL SCREEN INTERVALS (SHAW, 2003)	28
TABLE 2.4 BASIC EVOLUTIONARY COMPUTING METAPHOR (EIBAN AND SMITH, 2003)	33
TABLE 3.1 BIOLOGICAL REACTION PARAMETERS (HATZINGER ET AL., 2005)	39
TABLE 3.2 AVERAGE OXYGEN, NITRATE, AND PERCHLORATE CONCENTRATIONS AT AEROJET SITE ON 30 SEPTEMBER 2004 (SHAW, 2006).....	40
TABLE 3.3 UPFLOW HFTW INJECTION SCHEDULE.....	41
TABLE 3.4 DOWNFLOW HFTW INJECTION SCHEDULE	41
TABLE 3.5 SENSITIVITY ANALYSIS BASELINE ERROR STATISTICS	42
TABLE 3.6 MODEL PERFORMANCE BASELINE ERROR STATISTICS	43
TABLE 3.7 GA PARAMETER RANGE.....	48
TABLE 4.1 DIFFERENCE IN ERROR STATISTICS AS PARAMETER VALUE IS INCREASED FROM LOW TO HIGH VALUES	51
TABLE 4.2 GA PARAMETER VALUES.....	54
TABLE 4.3 GA ERROR STATISTIC RESULTS	54
TABLE A.1 KINETIC PARAMETERS USED IN MODEL SIMULATIONS (PARR, 2002)	84
TABLE A.2 ENVIRONMENTAL PARAMETERS USED IN MODEL SIMULATIONS (PARR, 2002).....	84
TABLE A.3 ENGINEERING PARAMETERS USED IN MODEL SIMULATIONS (PARR, 2002).....	84

MODELING *IN SITU* BIOREMEDIATION OF PERCHLORATE-CONTAMINATED GROUNDWATER

1.0 INTRODUCTION

1.1 MOTIVATION

The Safe Drinking Water Act (SDWA) serves to protect public health by regulating the nation's public drinking water supplies. The Act authorizes the Environmental Protection Agency (EPA) to set national health-based standards for drinking water to protect against both naturally-occurring and man-made contaminants. The EPA currently regulates over 90 contaminants which may be found in drinking water and also establishes a Contaminant Candidate List (CCL) to identify and list unregulated contaminants which may require future regulation (EPA, 2006). Perchlorate (ClO_4^-) salts have been used in solid rocket fuels, highway safety flares, air bag inflators, fireworks and matches (Trumpolt, 2005) and were first listed on the EPA's CCL in 1998 (EPA, 1998). The EPA uses the Unregulated Contaminant Monitoring Regulation (UCMR) program to collect data for contaminants suspected to be present in drinking water, but that do not have health-based standards established. Since its first listing on the CCL, the EPA reports that 152 public water systems in 35 states have tested positive for perchlorate in water, with over 11 million people exposed to perchlorate at concentrations of 4 ppb ($4\mu\text{g/L}$) or higher (EPA 2005; NRC 2005). Reported instances of perchlorate detection are indicated on the map in Figure 1.1. It is likely that the extent of perchlorate contamination of water supplies is actually greater than the EPA report indicates, as the report is limited to those instances where a release has been reported or perchlorate has been detected through sampling (GAO, 2005).

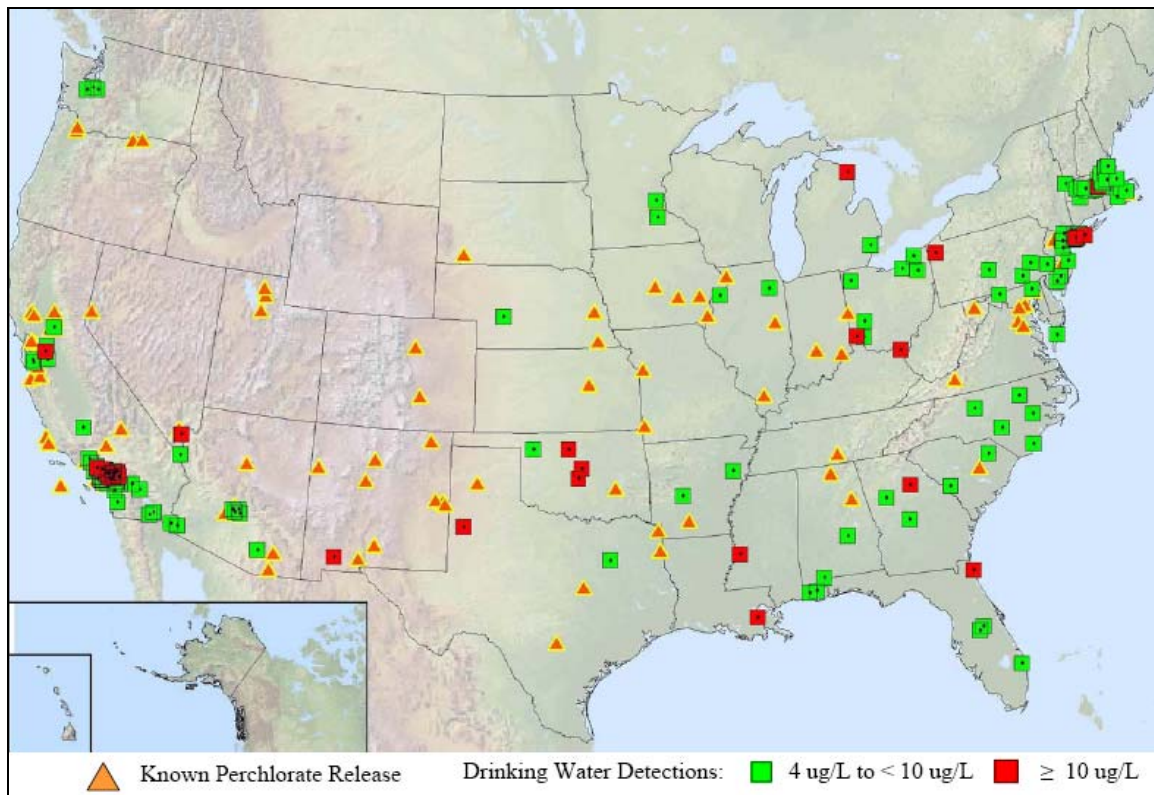


Figure 1.1 Known Perchlorate Releases and Perchlorate Detections under the UCMR Program (Brandhuber, 2005)

Perchlorate is a negatively charged ion that can affect thyroid function through competitive inhibition of the transport of iodide into the thyroid gland. This is the only effect that has been consistently documented in humans exposed to perchlorate (EPA, 2005; NRC, 2005). Iodide transport inhibition can lead to iodide deficiencies and decreased synthesis of thyroid hormones, which are critical determinants of growth and development in fetuses, infants and young children. For this reason, the National Research Council (NRC) has identified fetuses, infants and pregnant women as the sensitive populations most susceptible to the adverse effects of perchlorate (NRC, 2005). Sustained changes to thyroid hormone production and fluctuating thyroid stimulating hormone secretions can result in thyroid hypertrophy and hyperplasia, possibly followed by hypothyroidism in people unable to compensate with an increase in thyroid iodide uptake (EPA, 2005).

Following recommendations of the NRC (2005), the EPA adopted a reference dose (RfD) for perchlorate of 0.0007 milligrams/kilogram-day (mg/kg-day) which translates to a Drinking Water Equivalent Level (DWEL) of 24.5 micrograms/liter ($\mu\text{g/L}$) or 24.5 parts per billion (ppb). The oral RfD is an estimate of a daily oral exposure to the human population, including sensitive subgroups, that is likely to be without an appreciable risk of deleterious effects during a lifetime (EPA, 2006).

Following the EPA's adoption of the RfD, both the Department of Defense (DoD) (DoD, 2006), and the United States Air Force (USAF) (USAF, 2006) published guidance on sampling, analysis, and restoration/remediation requirements for varying levels of perchlorate contamination.

Even with the establishment of EPA's RfD, there are no federal cleanup standards for perchlorate-contaminated groundwater or soil except for site specific standards established under federal statutes such as the Comprehensive Environmental Response, Compensation, and Liability Act (CERCLA), Resource Conservation and Recovery Act (RCRA), and Safe Drinking Water Act (SDWA) (EPA, 2005). In addition, several states as indicated in Table 1.1 have identified state specific perchlorate advisory levels, with Massachusetts going as far as establishing a Maximum Contaminant Level (MCL) of 2 $\mu\text{g/L}$, which DoD organizations in the state must comply with for Comprehensive Environmental Response, Compensation, and Liability Act (CERCLA) site remediations (DoD, 2006; USAF 2006).

Table 1.1 State Advisory Levels for Perchlorate (ADEQ, 2007; EPA, 2005; CDHS, 2007; Mass DEP, 2006; NDEP, 2006)

State	Advisory Level	Comment
Arizona	14 µg/L	1998 health-based guidance level; based on child exposure; following EPA established RfD, state task force formed to investigate possibility of developing water quality standard for perchlorate
California	6 µg/L – public health goal (PHG) for perchlorate in drinking water	California Department of Health Services has proposed an MCL of 6 µg/L; currently in regulatory process
Massachusetts	2 µg/L	MCL for drinking water and waste site cleanup established in Jul 06
Maryland	1 µg/L	
New Mexico	1 µg/L – only for monitoring	Drinking water screening level
New York	5 and 18 µg/L	5 µg/L for drinking water planning; 18 µg/L for public notification
Nevada	18 µg/L – public notice standard	For contaminated groundwater
Texas	17 and 51 µg/L	17 µg/L for residential protective cleanup level (PCL); 51µg/L for industrial/commercial PCL

If remediation of perchlorate-contaminated groundwater is required, a variety of treatment technologies are available as summarized in Table 1.2. Treatment technologies

can be categorized as either destruction or removal and as either *ex situ* or *in situ*. Destruction technologies transform the contaminant into less harmful compounds, while removal treatments simply concentrate the contaminant (typically in a different phase). The concentrated contaminant then must be managed, either through additional treatment or disposal (EPA 2005). *Ex situ* technologies involve bringing the contaminant to the surface for treatment, while *in situ* treatment occurs in place, i.e. in the subsurface (ITRC, 2005). Italicized treatment technologies in Table 1.2 are identified as still being in the experimental/research phases. Of the numerous remediation technologies available, bioremediation has been identified as having the greatest potential for perchlorate treatment (Logan, 2001; Urbansky, 2002); hence much current research focuses on *ex situ* and *in situ* bioremediation (EPA, 2005).

Table 1.2 Perchlorate Treatment/Remediation Technologies (EPA 2005, ITRC 2005)—Italics Indicate Innovative Technologies

	Destruction	Removal
<i>Ex situ</i>	Bioreactors Composting <i>Catalytic Gas Membrane</i> <i>Electrochemical Reduction</i> <i>Zero-Valent Iron Reduction under</i> <i>Ultraviolet Light</i>	Ion Exchange Liquid Phase Carbon Adsorption (GAC) Reverse Osmosis Electrodialysis <i>Nanofiltration/Ultrafiltration</i> <i>Capacitive Deionization</i>

<i>In situ</i>	Permeable Reactive Barriers (Fixed Biobarriers/Biowalls) Bioremediation (Mobile Amendments) <i>Vapor Phase Electron Donor Injection</i> <i>Constructed Wetlands</i> <i>Monitored Natural Attenuation</i> <i>Nanoscale Bimetallic Particles</i>	Phytoremediation
----------------	---	------------------

Perchlorate bioremediation occurs when microorganisms, in the presence of an electron donor and a microbial growth-supporting substrate, reduce perchlorate into chloride and oxygen along the following pathway:



For *in situ* bioremediation, the electron donor is mixed into perchlorate-contaminated groundwater so indigenous microorganisms can reduce the perchlorate. One innovative method of accomplishing this mixing is to use two dual-screened treatment wells as part of a so-called horizontal flow treatment well (HFTW) system. Figure 1.2 illustrates the operation of a HFTW system, showing how an electron donor may be mixed into perchlorate-contaminated groundwater without the need to pump the water to the surface.

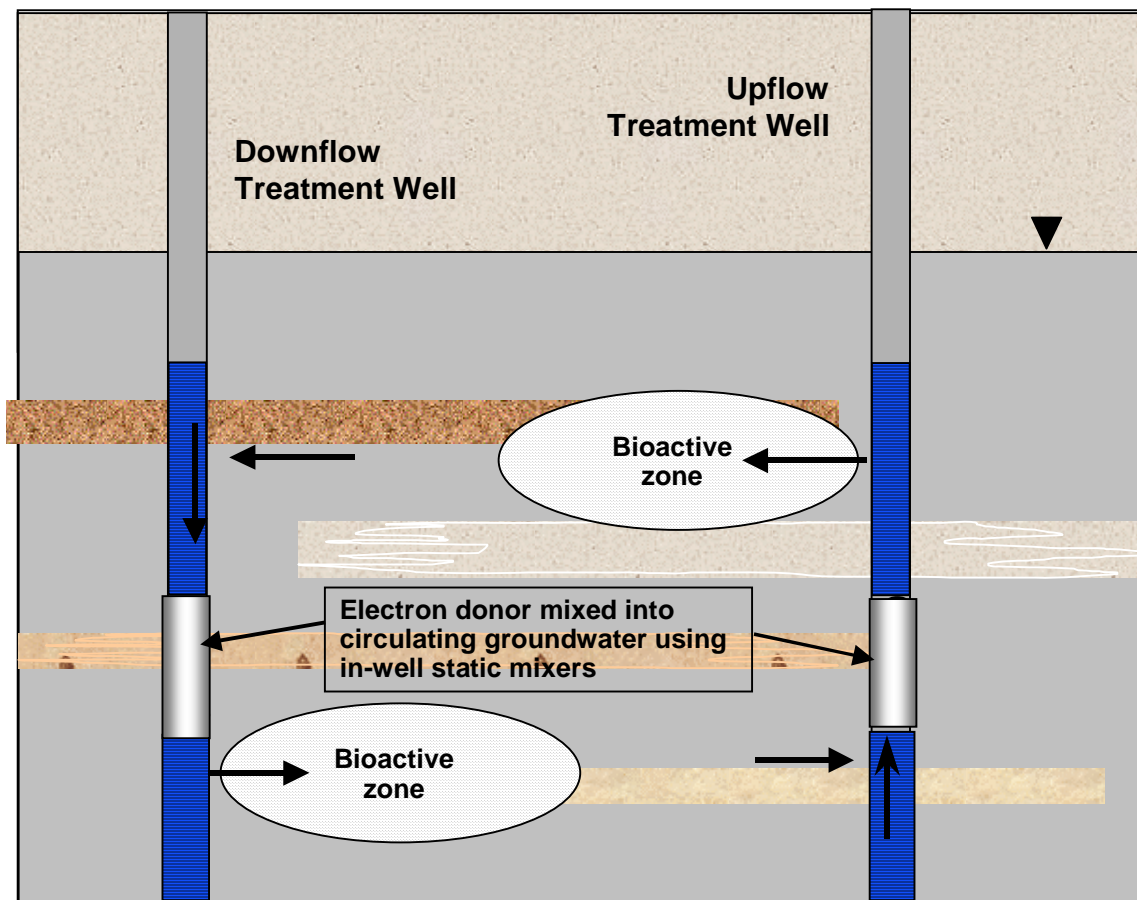


Figure 1.2 Horizontal Flow Treatment Well (HFTW) System

A HFTW system was successfully used to treat trichloroethylene-contaminated groundwater at Edwards AFB (McCarty et al., 1998) and is, as discussed below, has been applied to treat perchlorate-contaminated groundwater at the Aerojet Facility in Rancho Cordova, CA (Hatzinger, 2005). The Environmental Security Technology Certification Program (ESTCP), whose goal is to demonstrate and validate promising and innovative technologies that target Department of Defense (DoD) environmental requirements, has identified HFTW systems as having the potential of being widely applicable for *in situ* perchlorate treatment at DoD locations. ESTCP is interested in evaluating HFTWs because of the cost and operational advantages of being able to treat the contaminant in the subsurface without having to pump contaminated water to the surface for treatment. Both the pilot study at the Aerojet site, and this research are parts of an ESTCP-funded

project to evaluate the performance of an HFTW system in promoting *in situ* biodegradation of perchlorate-contaminated groundwater.

Based on the above discussion regarding the prevalence of perchlorate in the subsurface environment, the potential health effects of perchlorate contamination, and regulations mandating cleanup, it seems clear that there is a growing need for remediation technologies to manage perchlorate-contaminated groundwater. *In situ* bioremediation using HFTWs holds promise as a candidate technology. However, in order to facilitate technology transfer and commercialization of this innovative technology, a technology model that can be used to predict performance is extremely useful. Such a model, constructed using data obtained from the field evaluation, may be used by site owners, designers and consultants, and regulators, to optimize a HFTW system.

1.2 EARLIER STUDIES

A previous study was conducted to develop a technology model to mathematically simulate *in situ* bioremediation of perchlorate-contaminated groundwater using HFTWs (Parr, 2002). The technology model is based on a dual-Monod multi-electron acceptor model developed by Envirogen, using acetate as the electron donor, and coupled with a numerical model of advective/dispersive transport of sorbing solutes in the groundwater flow field resulting from HFTW operation (Envirogen, 2002; Parr, 2002).

The technology model was utilized to help design the HFTW system that was installed at the Aerojet Facility. The project investigators used the model to simulate the performance of several HFTW designs. Ultimately, modeling helped the investigators choose such engineered parameters as the treatment well locations, well spacing, pumping rates, and electron donor injection schedule (Shaw, 2003).

Once the design features were specified, a demonstration system was installed in Area D of Aerojet General Corporation's (Aerojet) 8,500-acre Sacramento, California facility that had been used for rocket engine development, testing, and production since 1951. The site selected for the pilot study, as indicated in Figure 1.3, had a large perchlorate plume. Sampling conducted just prior to the HFTW system, showed initial perchlorate concentrations at the demonstration site ranged from approximately 3,100 to 3,600 $\mu\text{g/L}$.

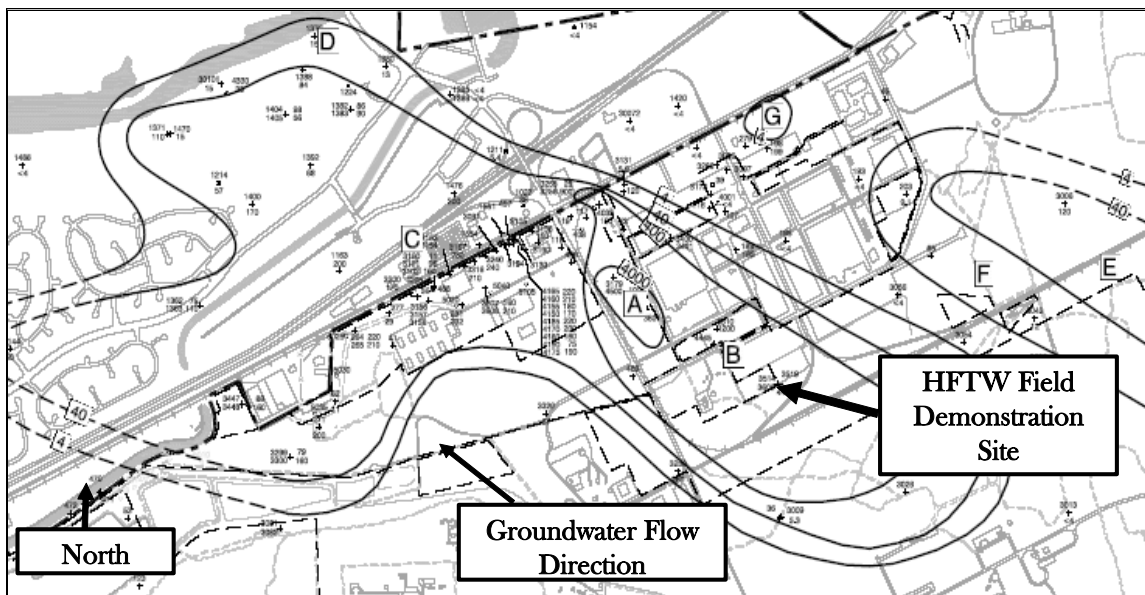


Figure 1.3 Aerojet Site with Perchlorate Isoconcentration Contours Indicated in ppb

The HFTW system was installed in June 2004, and began operating in August 2004. During operation, groundwater samples were collected for analysis of volatile organic compounds (VOCs) (since trichloroethylene (TCE) was present at the site as a co-contaminant), anions, including perchlorate, total iron and manganese, and field geochemical parameters, including pH, dissolved oxygen, conductivity, and redox potential.

1.3 RESEARCH OBJECTIVES:

The main objective of this research is to use the data obtained from the ongoing field trial at the Aerojet facility to calibrate, validate and refine the existing technology model that was used to design the HFTW installation. Specifically, this research will:

- (1) Determine how applicable parameters developed in the lab using acetate as an electron donor must be modified to be appropriate for citrate, which was used as the electron donor in the field evaluation.
- (2) Determine if the model adequately simulates system performance in the field at the Aerojet facility.
- (3) Evaluate the applicability of the HFTW technology under a variety of differing site conditions.

1.4 RESEARCH APPROACH

- (1) The literature review will focus on how models have been applied to interpret the results of remediation technology field evaluations and methods utilized for calibration. Questions to be answered include: how models are developed for such evaluations, how data are interpreted, and how can technology models be used to better facilitate technology transfer. The literature review will also address recent developments and current applications of HFTW systems for remediation of other contaminants.
- (2) Obtain remediation results from the Aerojet site technology evaluation and compare/contrast field data to model predictions.
- (3) Should the model results not match field observations, a determination will be made as to the reason(s) for the discrepancies. Utilizing that information, the technology model parameters will be modified to accurately represent HFTW *in situ* bioremediation operation.

- (4) Use the refined model to predict technology performance at other sites, over a range of environmental and operating conditions.

1.5 SCOPE AND LIMITATIONS OF RESEARCH

- (1) Calibration and validation of the technology model will be accomplished utilizing field data obtained from the Aerojet project. Thus, model validation will be limited to using data from a single site.
- (2) No independent laboratory studies will be conducted as part of this research.
- (3) Some limitation of the initial technology model is that various physical and environmental parameters utilized in the model were obtained from external sources and that Parr utilized substrate parameters from various acetate lab studies, whereas the field demonstration utilized citrate as the substrate. Extended maintenance shutdowns of the system and the frequency of sampling may impact validation results.
- (4) Due to computational resource and time constraints, a limited number of simulations are conducted. With additional resources, optimization techniques used in the model calibration could be continued.

2.0 LITERATURE REVIEW

2.1 INTRODUCTION

This chapter will provide a brief review of perchlorate health effects and regulatory issues associated with perchlorate contamination. A review of the extent to which perchlorate contaminates U.S. groundwaters will be provided along with descriptions of the treatment technologies currently available for remediation, with specific focus on how the innovative Horizontal Flow Treatment Well (HFTW) technology may be applied to effect *in situ* bioremediation of perchlorate-contaminated groundwater. We will also look at development and use of an HFTW technology model to design a pilot study that was conducted to treat perchlorate-contaminated groundwater at the Aerojet site in California.

2.2 PERCHLORATE CONTAMINATION

An excellent oxidizer, perchlorate is used extensively in industry, the Department of Defense (DoD), and the National Aeronautics and Space Administration (NASA). Approximately 90 percent by weight of industrial perchlorate production is utilized in the production of ammonium perchlorate for use as an oxidizing agent for solid propellant rockets and missiles (Trumpolt et al., 2005). Since production began in the United States in 1908, perchlorate has found its way into a diverse array of products. For example, in addition to its use as an oxidizer in rockets and missiles, perchlorate is used in vehicles as an air bag initiator, as a flash powder in photography, in road flares, in matches, in fireworks, as well as in myriad other products (EPA, 2005).

Past management practices during the production, use, and disposal of perchlorate resulted in its release to the environment. Perchlorate is highly soluble and does not appreciably adsorb to soils. It is also kinetically stable under environmental conditions and typically will not react or degrade under ambient conditions (Trumpolt et al., 2005). In addition, biodegradation of perchlorate will not occur unless there are significant

levels of organic carbon present, oxygen and nitrate are depleted and perchlorate-degrading anaerobic bacteria are present. Due to all of these characteristics, perchlorate releases to the subsurface result in dissolved perchlorate plumes that are large, persistent and difficult to remediate (Trumpolt et al., 2005).

2.3 HEALTH RISKS

Perchlorate contamination is a concern because perchlorate competitively inhibits the transport of iodide into the thyroid gland, which may potentially result in adverse health effects. Much recent research has centered on what those health effects are and what concentration levels pose acceptable risks from a regulatory standpoint.

From 1992 through 1998, the EPA published three separate provisional or proposed oral reference doses (RfDs) for perchlorate ranging from 0.00003 mg/kg-day to 0.0009 mg/kg-day. The oral RfD is an estimate of a daily oral exposure to the human population, including sensitive subgroups, that is likely to be without an appreciable risk of deleterious effects during a lifetime (EPA, 2006). In 2002, the EPA published a Draft Perchlorate Risk Assessment which included a mode-of-action model (Figure 2.1) representing a continuum of possible health effects resulting from perchlorate exposure. The model indicated that continued perchlorate exposure ultimately led to birth defects in children and tumors in adults. Based upon their analysis, the EPA proposed an oral reference dose of 0.00003 mg/kg-day, which translates to a concentration in drinking water of 1 µg/L (ppb) as the lowest observed adverse effect level (LOAEL). The LOAEL is the lowest level of a substance that causes statistically and biologically significant differences in test samples as compared to other samples subjected to no substance.

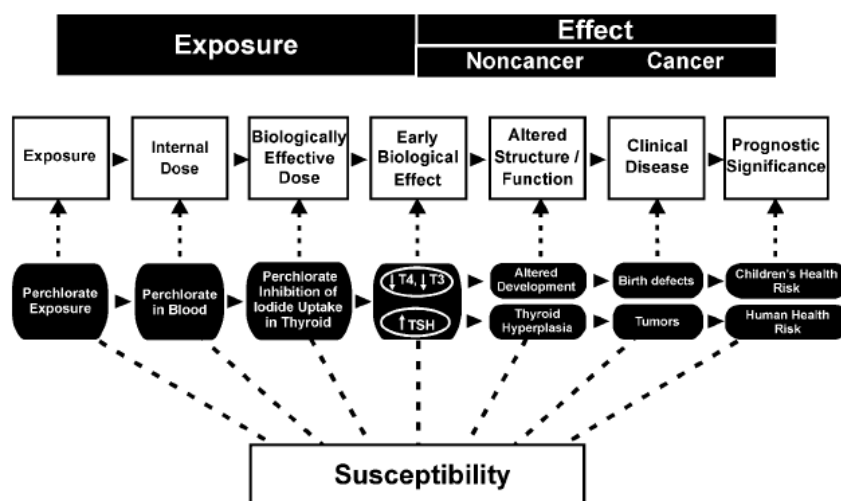


Figure 2.1 Proposed EPA Mode-of-action Model (EPA, 2002)

Following the release of the EPA draft risk assessment report in 2002, differing interpretations of the science associated with perchlorate exposure impacts came to light. In response, in 2003, the Environmental Protection Agency (EPA), the Department of Defense (DoD), the Department of Energy (DOE), and the National Aerospace and Space Administration (NASA) asked the National Research Council (NRC) to independently assess the adverse effects of perchlorate ingestion from clinical, toxicological, and public health perspectives (EPA, 2003). The NRC formed the Committee to Assess the Health Implications of Perchlorate Ingestion. During their review, the committee focused on four main areas: the mode-of action models of perchlorate toxicity, the definition of adverse effect, the point of departure defining the dose-response point that marks the beginning of an adverse effect, and the use of uncertainty factors to derive a reference dose (RfD) for daily oral exposures to perchlorate.

The committee determined there was insufficient evidence to support several causal relationships between perchlorate exposure and adverse effects as noted in Table 2.2, but that there was enough evidence to imply possible associations (NRC, 2005).

Table 2.1 Perchlorate Exposure Causal Relationships (NRC, 2005)

Perchlorate Exposure Health Impacts	Committee Conclusion
Congenital Hypothyroidism	Epidemiologic evidence is not consistent with a causal association between perchlorate exposure and congenital hypothyroidism
Changes in thyroid function in newborns	Epidemiologic evidence is not consistent with a causal association between exposure during gestation to perchlorate in the drinking water at up to 120 ppb and changes in thyroid hormone and TSH production in normal-birth weight, full-term newborns.
Neurodevelopmental outcomes	Epidemiologic evidence is inadequate to determine whether or not there is a causal association between perchlorate exposure and adverse neurodevelopmental outcomes in children
Hypothyroidism and other thyroid disorders in adults	Evidence from chronic, occupational-exposure studies and ecologic investigations in adults is not consistent with a causal association between perchlorate exposure at the doses investigated and hypothyroidism or other thyroid disorders in adults
Thyroid cancer in adults	Epidemiologic evidence is insufficient to determine whether or not there is a causal association between exposure to perchlorate and thyroid cancer
Adversely affect immune system	No evidence for a causative relationship between perchlorate ingestion and any biologically meaningful stimulatory or inhibitory effect on the immune system in rodents, and concludes that the side effects in humans were probably toxic effects of the very high doses of perchlorate given to those patients.

Based upon their review, the NRC proposed a modified mode-of-action model, Figure 2.2. The new model emphasizes that the inhibition of iodide uptake in the thyroid is the only effect that has been observed in humans and is represented in Figure 2.2 as solid arrows. Dashed arrows within the model represent outcomes that have not been clearly demonstrated, but are biologically plausible should the body not be able to adequately adjust to iodide deficiencies (NRC, 2005).

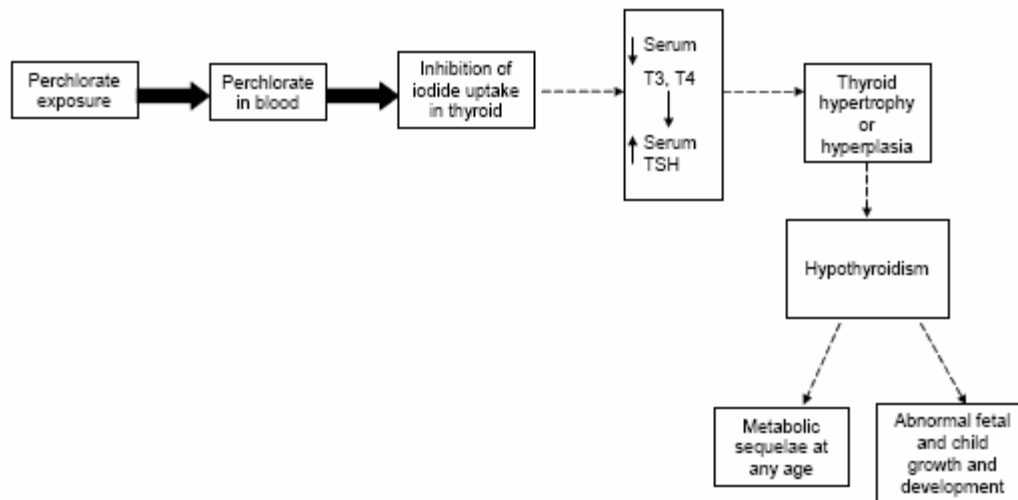


Figure 2.2 Proposed NRC Mode-of-Action Model (NRC, 2005)

Based upon their analysis, the committee decided to provide an RfD recommendation based upon a no observable adverse effect level (NOAEL) as compared to the EPA's RfD which was based upon a lowest observed adverse effect level (LOAEL). A NOAEL represents an exposure level at which there is no statistically or biologically significant difference in the frequency or severity of any effect in the exposed or control populations (EPA, 2006). Thus, by establishing a NOAEL-based RfD, the committee took a more conservative approach than the EPA did (NRC, 2005). The committee's recommendation of an RfD of 0.0007 mg/kg per day should protect the health of the most sensitive populations, defined as pregnant women and their fetuses. A RfD of 0.0007 mg/kg per day is equivalent to 24.5 µg/L per day or 24.5 ppb.

2.4 STATE AND FEDERAL PERCHLORATE REGULATIONS

As indicated in Chapter 1, the EPA reports that 152 public water systems in 35 states have tested positive for perchlorate in water, with over 11 million people exposed to perchlorate at concentrations of 4 ppb (4µg/L) or higher (EPA 2005; NRC 2005). To date, only 9 states have established guidance levels with Massachusetts being the only state to define actual cleanup standards.

The Arizona Department of Health Services (ADHS) has established a Health Based Guidance Level (HBGL) of 14 ppb for perchlorate in drinking water. This level is meant to represent contaminant concentrations in drinking water that are protective of public health during long-term exposures. The HBGLs are not enforceable drinking water standards, but rather are advisory levels identifying concentrations below which contaminants can be present in drinking water and considered safe for human consumption. The Arizona HBGL was established to be protective of children who have higher daily water intake rates and lower body weights (ADEQ, 2004).

The California Department of Health Services (CDHS) has established a Public Health Goal (PHG) and notification level of 6 µg/L which represents the perchlorate concentration in drinking water that poses no significant health risk if consumed for a lifetime, based on current risk assessment principles, practices, and methods (CDHS, 2007). PHGs represent health-protective goals based solely on public health considerations and are not regulatory requirements and as such, there are no consequences to drinking water providers if they cannot meet PHGs. Maximum Contaminant Levels (MCLs), on the other hand, are regulatory drinking water standards that drinking water suppliers must comply with. Once the MCL is established, systems exceeding the MCL are required to notify the CDHS and the public and take steps to immediately come back into compliance. CDHS has proposed an MCL for perchlorate in drinking water of 6 µg/L which is currently making its way through the state regulatory process (CDHS, 2007).

In July 2006, Massachusetts established drinking water and waste site cleanup standards at 2 parts per billion (ppb). The new regulations require most public water systems to regularly test for perchlorate, and if contamination is found to notify the Massachusetts Department of Environmental Protection (MassDEP) of the contamination and conduct appropriate environmental assessment and cleanup. The standard adopted seeks to protect public health, including sensitive populations such as pregnant women, nursing mothers, infants and individuals with low levels of thyroid hormones (MassDEP, 2006).

The Nevada Division of Environmental Protection (NDEP) established 18 ppb as a provisional action level based upon 1999 EPA guidance (NDEP, 2006).

2.5 TREATMENT TECHNOLOGIES

With the widespread perchlorate contamination of groundwater being discovered throughout the United States, as indicated in Figure 1.1, and the increased interest by both federal and state regulatory agencies, a variety of solutions for the treatment of perchlorate contamination have been developed. As indicated in Table 1.2, there are *in situ* and *ex situ* approaches for treating perchlorate-contaminated groundwater, and technologies may be applied that either remove or destroy the perchlorate.

2.5.1 REMOVAL

Typically applied aboveground (*ex situ*), perchlorate removal can be accomplished utilizing anion exchange, filtering or electrodialysis technologies. An early problem with anion exchange was that the ion exchange resins were not selective and removed competing ions along with perchlorate, making them uneconomical. However, ion exchange resins that are selective for perchlorate have been developed to help combat this problem, and currently, anion exchange is the technology that is conventionally used to treat perchlorate-contaminated water (Urbansky, 2002). Filtering technologies such as reverse osmosis or nanofiltration are able to remove perchlorate by forcing the

contaminated water through a filter or membrane that traps the contaminants. Problems with these approaches are that the removal is not selective for perchlorate, and the demineralized water can be corrosive to equipment and piping (Urbansky, 2002). Electrodialysis passes the contaminated groundwater through different membranes while exposing it to an electric field which causes the perchlorate to separate from the water. A problem common to all removal technologies is that perchlorate-contaminated waste is generated which must be treated and disposed of properly, adding complexity and cost to projects (GWRTAC, 2001).

2.5.2 DESTRUCTION

In a review of perchlorate treatment projects, the Ground-Water Remediation Technologies Analysis Center (GWRTAC) found that over 75% of the case studies involved application of destruction technologies (GWRTAC, 2001). Destruction technologies include chemical, electrochemical and biological reduction of perchlorate into its constituent parts; oxygen and chloride.

Chemical reduction of perchlorate is a difficult endeavor because while certain chemical reductants react with perchlorate to reduce it to either chlorate or chloride, only extremely reactive air-sensitive transition metal species, such as ruthenium(II), chromium(II), and titanium(III) have shown any observable redox reactions, and because of the nonlabile properties of perchlorate, any observed redox reactions occur too slowly to be of any practical use (Urbansky, 1998). Electrochemical reduction of perchlorate occurs when an electrical current is applied directly to the contaminated water by a cathode at high potential. This method has challenges of its own which detract from its usefulness; the lengthy time required for the treatment process, electrode corrosion, surface passivation, and natural organic matter adsorption to the electrode surface (Urbansky, 1998).

Of the available technologies utilized for perchlorate remediation, biological degradation has shown the most promise (Urbansky, 1998; Logan, 2001). Figure 2.3 shows that of

the 65 case studies reviewed by the GWRTAC involving perchlorate contamination, 67% focused on biological degradation technologies (GWRTAC, 2001).

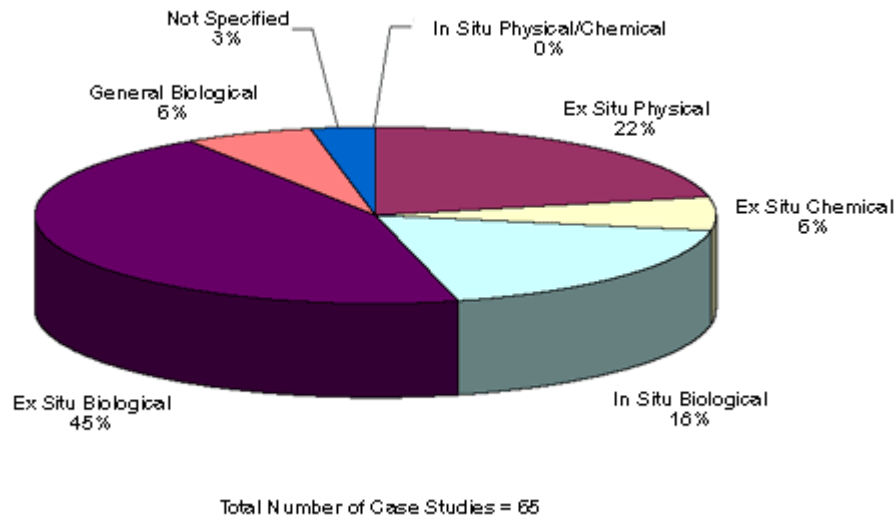


Figure 2.3 General Perchlorate Technology Treatment Types (GWRTAC, 2001)

In biological degradation, perchlorate is used as an electron acceptor by some bacteria for cellular respiration (Logan, 1998; 2001; Coates, 2000). Figure 2.4 presents the pathway used by perchlorate reducing bacteria (PRB) to degrade perchlorate using acetate as an electron donor (Xu et al., 2003). Perchlorate is first reduced to chlorate, then to chlorite, and finally chloride and oxygen.

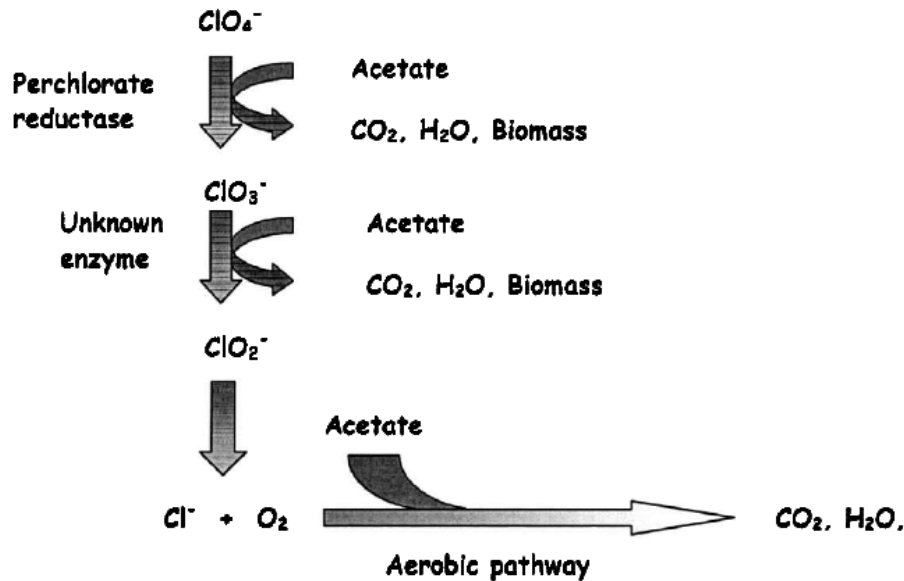


Figure 2.4 Perchlorate Reduction Pathway (Xu et al., 2003 adapted from Rikken et al., 1996)

For both perchlorate and chlorate, reduction does not occur in the presence of dissolved oxygen, meaning that environmental conditions must be anaerobic for perchlorate biodegradation to occur (Xu et al., 2003). It has also be noted that the presence of high concentrations of nitrate partially or completely inhibit perchlorate reduction (Logan, 1998).

2.5.3 EX SITU VERSUS IN SITU REMEDIATION

As mentioned in Chapter 1, *ex situ* technologies entail extracting the contaminated groundwater to the surface for treatment while *in situ* technologies treat the contaminant in place. Although much past research and technology application has focused on *ex situ* technologies, a review by the Federal Remediation Technologies Roundtable (FRTR), as shown in Figure 2.5, indicates that there's a trend in recent years to deploy more and more *in situ* technologies (Kingscott and Weisman, 2002).

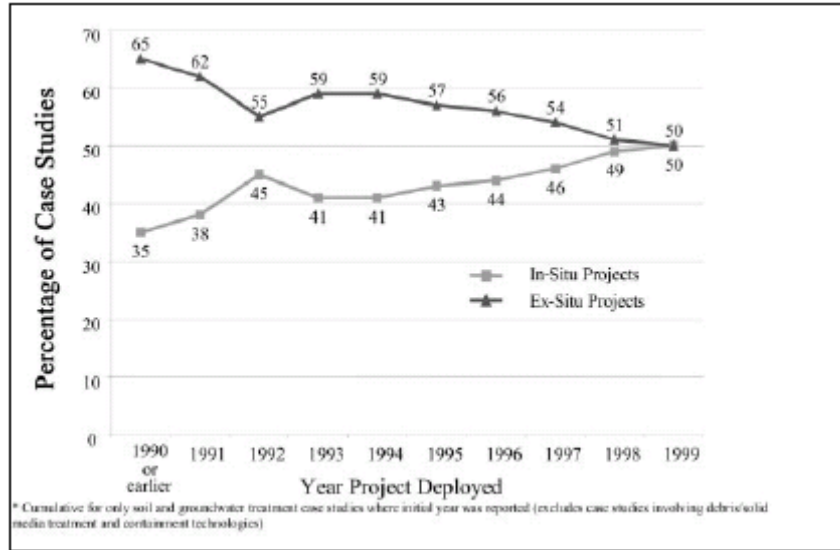


Figure 2.5 In-Situ versus *Ex situ* Treatment (Kingscott and Weisman, 2002)

With *ex situ* treatment technologies, the contaminant is brought to the surface for treatment. This requires significant infrastructure; piping, pumps, filters, tanks, etc., not to mention the costs of pumping the water aboveground. Treating the contaminant *in situ* can reduce or eliminate the aboveground infrastructure and pumping costs (Logan, 2001). As PRBs have been found to be widespread in the environment and are native to many groundwater aquifers, the utilization of *in situ* technologies can avoid the requirement of adding microorganisms to the subsurface (Hatzinger et al., 2002).

In situ biodegradation relies upon indigenous perchlorate reducing bacteria. While perchlorate reducing bacteria are widespread in the natural environment (Hatzinger et al., 2002), as noted earlier, natural degradation of perchlorate is extremely slow, since perchlorate is kinetically stable under ambient conditions (Trumpolt et al., 2005).

However, with the addition of an electron donor, the PRB can be stimulated to degrade perchlorate at a faster rate (Hatzinger et al., 2002). A challenge faced in designing an effective and cost efficient *in situ* biodegradation technology is the need to effectively deliver and mix the electron donor(s) into the perchlorate-contaminated groundwater

(Hatzinger et al., 2002). An innovative technology, known as Horizontal Flow Treatment Wells (HFTWs) was developed to meet this challenge.

2.6 HORIZONTAL FLOW TREATMENT WELL (HFTW) SYSTEM

As shown in Figure 1.2, the HFTW system utilizes two treatment wells, each of which has either an upper or lower injection or extraction screen. Looking at two adjacent wells, one well would be operated in an upflow mode and the second in a downflow mode. In the upflow mode, groundwater is extracted from the aquifer through the lower-well screen, mixed with an electron donor and then injected back into the aquifer through the upper-well screen. Operating in a downflow configuration, groundwater is extracted from the aquifer in the upper-well screen, mixed with an electron donor and then injected back into the aquifer through the lower-well screen.

When the amended groundwater is injected into the aquifer, under the anisotropic hydraulic conductivities typically found in aquifers (Christ et al., 1999), the water will flow horizontally toward the adjacent wells' extraction screen. A bioactive zone is established around the injection screens, where perchlorate is reduced by naturally occurring PRB. The two wells operate in tandem, recycling the contaminated groundwater between them. As represented in Figure 2.6, which shows streamlines in the lower aquifer, where the upflow well (u) is an extraction well and the downflow well (d) is an injection well, contaminated water from upgradient is captured by the upflow well and then recycled in the HFTW system (passing multiple times through the bioactive zones). Ultimately, the treated water is injected into the aquifer, where it flows downgradient (Cunningham et al., 2004).

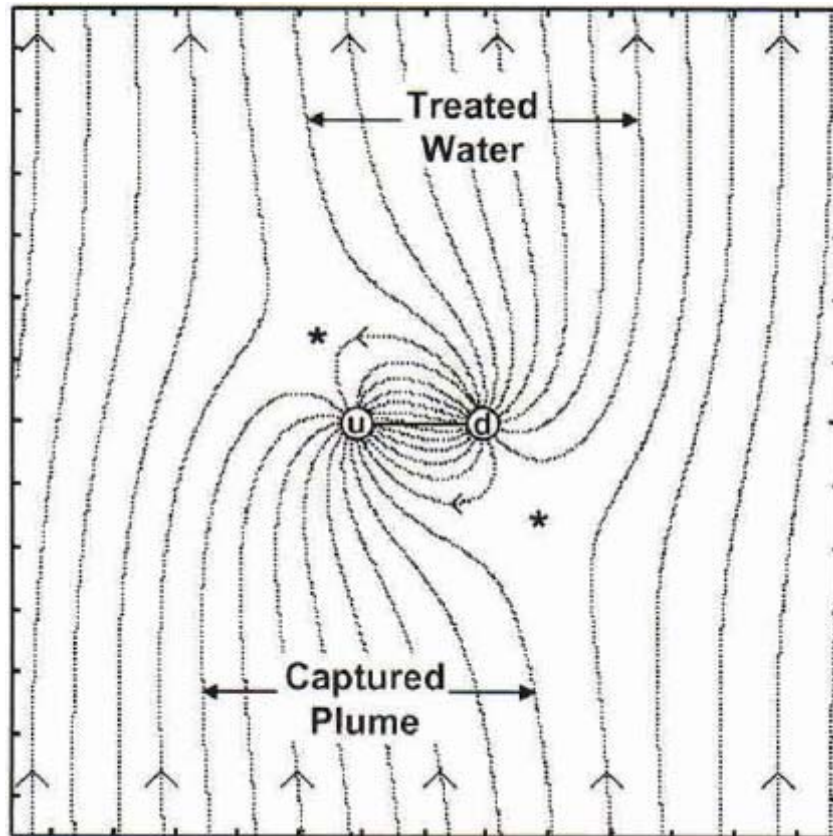


Figure 2.6 Streamlines Representing Groundwater Capture/Recirculation in Lower Portion of an Aquifer Where Upflow Well (u) Extracts and Downflow Well (d) Injects Water. Asterisks Represent Stagnation Points (Cunningham et al., 2004)

HFTWs were selected for use to treat perchlorate-contaminated groundwater at the Aerojet site for a number of reasons. Advantages of recirculating well pairs, or HFTWs, are that they act as an active hydraulic barrier to the flow of contaminated water, but without the need to extract water from the subsurface. The bioactive zones between the wells serve as bioreactors, one each in the upper and lower region of the aquifer. To induce perchlorate biodegradation in the bioactive zones, an electron donor can be efficiently mixed into the contaminated groundwater using mixers installed in the HFTWs (Cunningham et al., 2004). Application of HFTWs to stimulate *in situ* bioremediation by mixing an electron donor into contaminated groundwater was shown to be effective in a previous study by McCarty et al. (1998) where trichloroethylene-contaminated groundwater was successfully treated.

2.7 TECHNOLOGY MODEL

Parr (2002) combined a model that simulates the flow field induced by operation of an HFTW system (Huang and Goltz, 1998) with a submodel that simulates biodegradation of perchlorate by PRB (Envirogen, 2002). The biodegradation submodel uses dual Monod kinetics to simulate perchlorate reduction by PRB in the presence of an electron donor and competing electron acceptors (oxygen and nitrate). As noted earlier in Section 2.5.2, the rate of perchlorate reduction is slowed in the presence of oxygen and nitrate. This is modeled using an inhibition coefficient that slows the rate of nitrate reduction if oxygen is present, and slows the rate of perchlorate reduction if either oxygen or nitrate is present. The rate of perchlorate destruction is also dependent on microbial concentrations as well as the concentrations of both perchlorate and the electron donor (Schwartzbach et al., 1993). Microbial growth is modeled as a function of the rate of electron donor consumption less biomass decay, which is modeled as a first-order decay process. The model simulates advective/dispersive/reactive transport of the perchlorate, donor, and competing acceptors, while the PRB are assumed to be immobile (Parr, 2002). The parameters utilized in the model, along with a short description, are presented in Table 2.2, while a detailed description of the technology model developed by Parr is provided in Appendix A.

Table 2.2 Technology Model Parameters

Parameter	Definition
k_{\max}	Maximum specific rate of substrate utilization (mg donor/mg biomass/day)
K_S^{don}	Donor half saturation concentration (mg/L)
K_S^{oxy}	Half saturation concentration when oxygen (an electron acceptor) concentration is varied and limiting (mg/L)

K_S^{nit}	Half saturation concentration when nitrate (an electron acceptor) concentration is varied and limiting (mg/L)
K_S^{per}	Half saturation concentration when perchlorate (an electron acceptor) concentration is varied and limiting (mg/L)
K_i^{oxy}	Oxygen inhibition coefficient (mg/L)
K_i^{nit}	Nitrate inhibition coefficient (mg/L)
Y_{biomass}	Biomass yield per mass of donor consumed (mg biomass/mg electron donor consumed)
b	Biomass decay rate (1/day)

2.8 AEROJET PILOT STUDY

The completed technology model was utilized in the design of a HFTW system installed at the Aerojet General Corporation's (Aerojet) 8,500-acre Sacramento, California facility used for rocket engine development, testing and production. The site chosen for the pilot study was contaminated with perchlorate from a former propellant burn area. Samples taken from monitoring wells indicate initial perchlorate concentration levels ranging from approximately 3,100 to 3,600 $\mu\text{g/L}$ (Shaw, 2003).

The objective of the pilot study was to demonstrate and validate the combined use of two innovative technologies; bioremediation of perchlorate-contaminated groundwater through electron donor addition and application of HFTWs to achieve *in situ* mixing of the electron donor with the perchlorate-contaminated water and delivery of the mixture to indigenous PRB (Shaw, 2003). Many of the design parameters for the field

demonstration, including well spacing, pumping rates, and electron donor delivery schedule were selected based on model simulations (Shaw, 2003).

A HFTW system, as shown in Figure 2.7, was installed at the Aerojet site in June 2004. Groundwater at the site is encountered at a depth of 25 to 30 feet bls, with static groundwater at about 30 feet bls. Groundwater flow is towards the northwest with a gradient of approximately 0.017 ft/ft. The HFTW system consisted of two treatment wells installed approximately 10 m apart, oriented so that the line connecting the two wells was approximately perpendicular to groundwater flow. Nineteen monitoring wells were installed surrounding the HFTWs at the locations shown in Figure 2.7. Wells were screened at the depths indicated in Table 2.3. A description of site conditions and details regarding HFTW and monitoring well installation may be found in Shaw (2003). Initial operation and adjustment of the system began in August 2004. Addition of citric acid as the electron donor began on 28 October 2004 and sampling data from monitoring wells were collected and is available for dates through 28 November 2006.

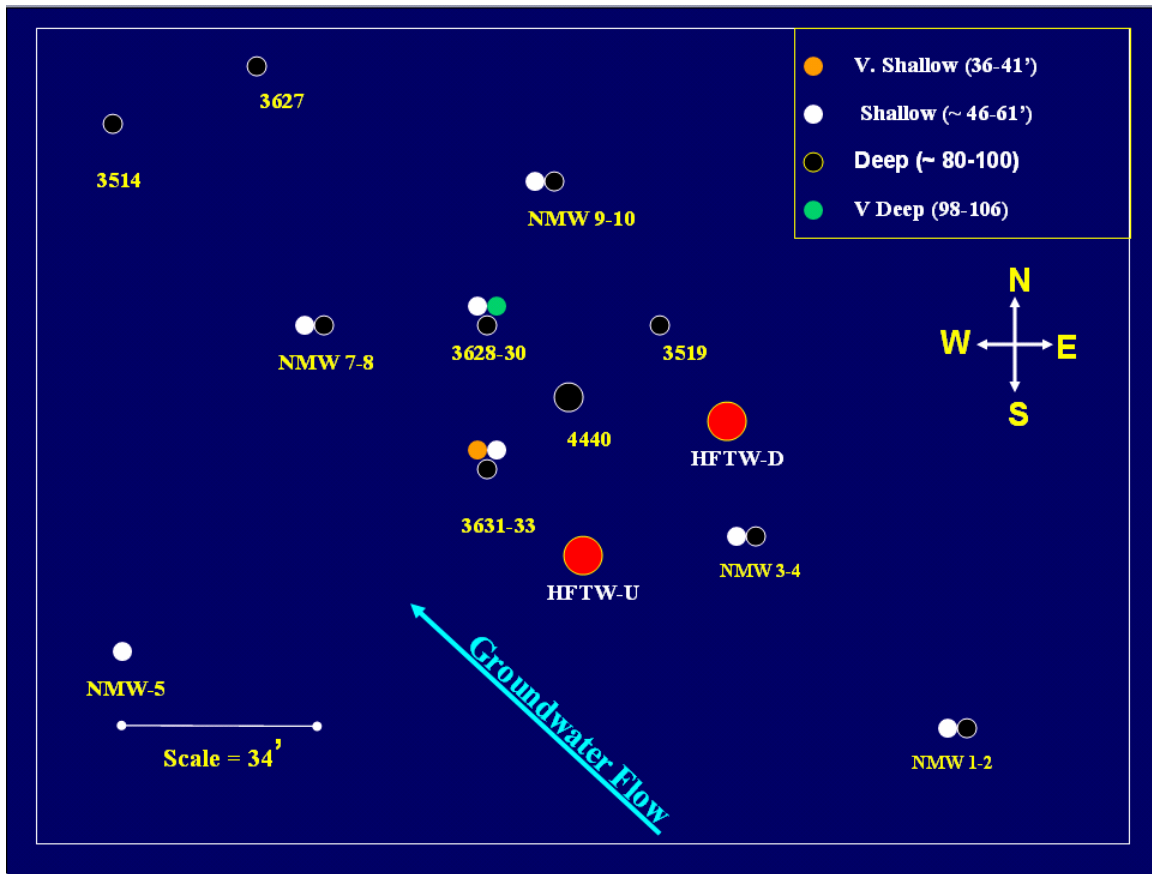


Figure 2.7 Plan View of HFTW and Monitoring Well Layout at Aerojet Site (Hatzinger and Diebold, 2005)

Table 2.3 Monitoring Well Screen Intervals (Shaw, 2003)

Well	Screen Interval (ft bls)
MW3628	52-57
MW3829	80-85
MW3630	96-101
MW3631	36-41
MW3632	52-57
MW3633	98-103
MW3627	75-95
MW3519	78-103
MW3514	77-90

MW4440	75-93 and 98-106
NMW1-2	46-61 and 80-100
NMW3-4	46-61 and 80-100
NMW5	46-61
NMW7-8	46-61 and 80-100
NMW9-10	46-61 and 80-100

Initial results shown in Figures 2.8 and 2.9 indicate that the system successfully degraded perchlorate, and that within the first three months, perchlorate levels in the shallow/very shallow monitoring wells (screened between 36 and 61 ft below ground surface) declined by an average of 94% from their starting levels, and 58% in the deep monitoring wells (screened between 80 and 106 ft below ground surface) (Hatzinger et al., 2005).

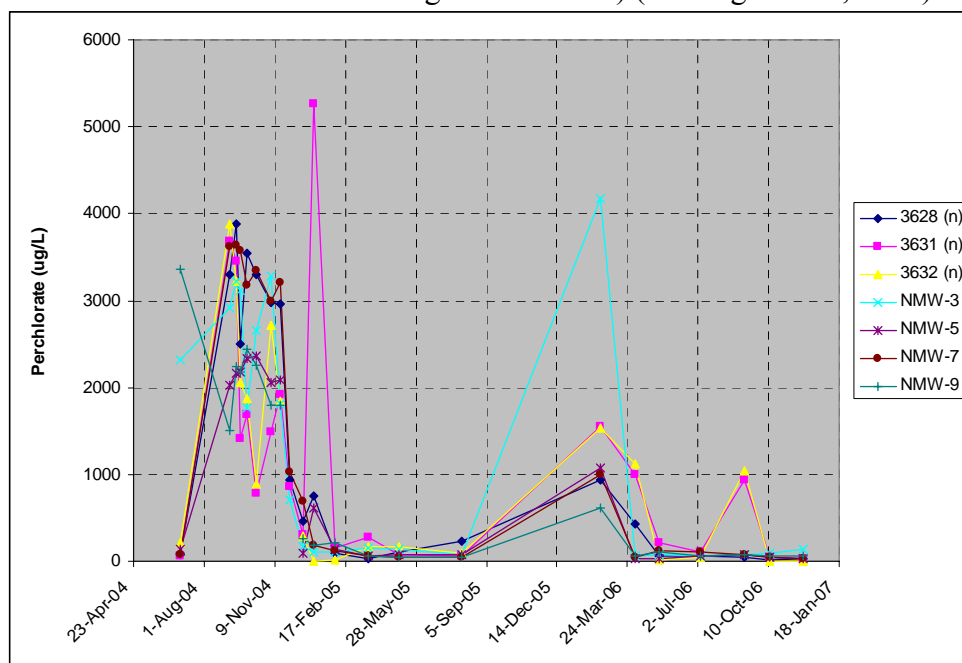


Figure 2.8 Perchlorate Levels in Shallow and Very Shallow Monitoring Wells (Hatzinger and Diebold, 2005; Shaw, 2006)

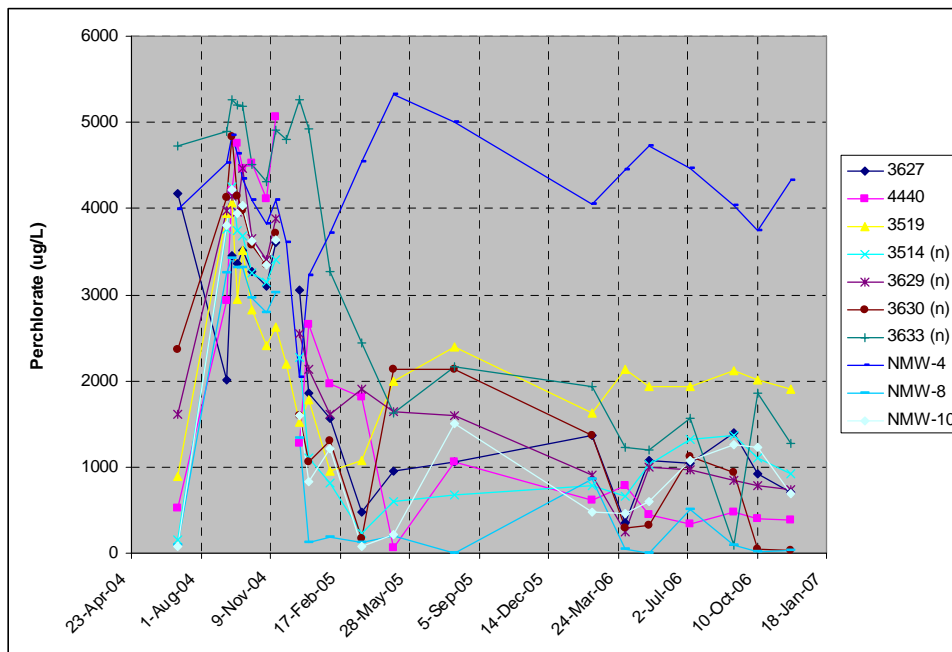


Figure 2.9 Perchlorate Levels in Deep Monitoring Wells (Hatzinger and Diebold, 2005; Shaw, 2006)

2.9 MODEL CALIBRATION/VALIDATION

Anderson and Woessner (1992) put forward that model calibration and verification demonstrate that a model can mimic past behavior while model validation determines whether the model can predict the future (Hassan, 2004). Calibration involves tuning the model by fitting the model results to field or experimental data. Calibration is accomplished by varying parameters, and seeing how parameter changes impact model results. Model validation is the process of using the model to make predictions, and then testing those predictions by comparing them with data, for the purpose of refining, enhancing and building confidence in the model (Hassan, 2004).

2.9.1 GOODNESS-OF-FIT ERROR STATISTICS

In order to calibrate a model, or to assess how well model simulations predict observations, measures of accuracy are required. It is commonly accepted that there is no single best measure of how “good” a model is, and that assessing model accuracy is

necessarily subjective (Collopy and Armstrong, 1992). However, there are a number of goodness-of-fit measures that are used to evaluate model accuracy: mean error (ME), mean absolute error (MAE), and root mean square error (RMSE). These error statistics (detailed in Equations 2.1, 2.2, and 2.4), require one or more observed values of the dependent variable against which to compare the simulation results.

2.9.1.1 MEAN ERROR (ME)

The ME of a number of observations is found by taking the mean value of the differences between actual (A) and computed (C) values without regard to sign. Because the difference between actual and computed values can be either positive or negative, it is possible that error values can cancel each other out, but the ME remains a valuable statistic because it indicates the bias of the model; whether it over or under estimates the actual values. A positive ME indicates that the model is consistently high in its prediction while a negative ME means that the model is consistently low in its predictions versus actual data. ME values closer to zero are desired.

$$ME = \frac{\sum_{t=1}^n (A_t - C_t)}{n} \quad (2.1)$$

2.9.1.2 MEAN ABSOLUTE ERROR (MAE)

In contrast to the ME, the MAE takes the absolute value of the differences between actual and computed values. Thus, the MAE considers all the errors present in the simulation, therefore providing an average prediction error.

$$MAE = \frac{\sum_{t=1}^n |A_t - C_t|}{n} \quad (2.2)$$

2.9.1.3 ROOT MEAN-SQUARED ERROR (RMSE)

One of the most commonly used measures for the average size of errors is the mean square error (MSE) which is computed by taking the average of the squared differences between computed and observed values. By taking the square of the differences, the

error cancelling present in the ME is avoided, but the resulting statistic is no longer in the same units as the values being evaluated. The root mean-squared error (RMSE) is the square root of the mean-squared-error and gives the error value the same dimensionality as the actual and computed values. MSE and subsequently RMSE tend to place more emphasis on larger errors and are a more conservative measure than MAE. The smaller the MSE/RMSE value, the closer the fit is to the observed data.

$$\text{MSE} = \frac{\sum_{t=1}^n (A_t - C_t)^2}{n} \quad (2.3)$$

$$\text{RMSE} = \sqrt{\frac{\sum_{t=1}^n (A_t - C_t)^2}{n}} \quad (2.4)$$

2.10 EVOLUTIONARY COMPUTING (EC)

In the past, calibration of models relied on manual trial-and-error methods to optimize model parameters for best-fit results. Automated calibration methods have received much interest because they introduce efficiency and allow quantitative estimation of the quality of calibration (Hassan, 2004). The automation that evolutionary computing and genetic algorithms provide make them the ideal solution to optimize model parameters. Evolutionary computing involves the study of a class of algorithms which are inspired by Darwinian principles of natural selection and molecular genetics (Eiban and Smith, 2003). Eiban and Smith (2003) present what they call the evolutionary computing metaphor, shown in Table 2.4, which equates the process of natural evolution to that of problem solving. They go on to provide a generic definition of natural evolution as follows; a given environment is filled with a population of individuals that strive for survival and reproduction, the fitness of these individuals represents their chances of survival and multiplying. This is very similar to the trial-and-error style of problem solving where a collection of candidate solutions exists, and how well they solve the

problem determines the chance that they will be kept and used as seeds for constructing additional candidate solutions.

Table 2.4 Basic Evolutionary Computing Metaphor (Eiban and Smith, 2003)

Evolution		Problem Solving
Environment	↔	Problem
Individual	↔	Candidate Solution
Fitness	↔	Quality

2.11 EVOLUTIONARY/GENETIC ALGORITHMS (GA)

An algorithm utilizing evolutionary principles is termed an evolutionary algorithm (EA). All evolutionary algorithms are comprised of several components illustrated in flowchart form in Figure 2.10.

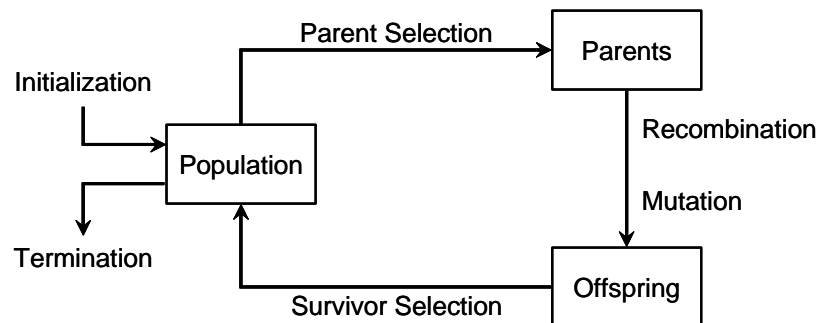


Figure 2.10 General Scheme of an Evolutionary Algorithm (Eiban and Smith, 2003)

This flowchart outlines how an evolutionary algorithm works (Eiban and Smith, 2003). Once a population is created, individuals are selected from the population to serve as parents for new offspring. Through mutation and recombination (defined below) parent characteristics are used to produce offspring, which hopefully have “better” traits, and are therefore fitter, than their parents. One individual is said to be fitter than another if it produces a result that has a higher value of the objective function (assuming the goal is to

maximize the objective function). During survivor selection, fitter individuals are chosen to reproduce as parents, thereby increasing the overall fitness of the population.

2.11.1 GENES/CHROMOSOMES/INDIVIDUALS

Individuals consist of a set of genes (parameter values), which make up a chromosome. A chromosome is a set of parameters that represent a solution to the problem under consideration. An individual is characterized by its chromosome.

2.11.2 OBJECTIVE FUNCTION

As noted above, the objective function forms the basis for determining which candidate solution (individual) should be selected for reproduction (Eibian and Smith, 2003). For example, when using a GA to optimize model parameters, the objective function might be the reciprocal of the RMSE, and the fitness of any particular individual will be evaluated by calculating the value of the objective function that results from using the individual's genes (parameter values) in the model.

2.11.3 POPULATION

In a GA, the role of a population is to hold the candidate solutions, or chromosomes. Individuals within a population do not change, but as individuals are replaced, the population changes and adapts.

2.11.4 PARENT SELECTION

To generate offspring two parents must be selected from the population and in EC, selection is generally accomplished randomly by use of probabilities. Selection combined with survivorship/replacement ensures that the population is continually moving towards a better fit against the objective function (Eibian and Smith, 2003).

2.11.5 VARIATION OPERATORS

Variation operators serve the function of creating new individuals from old ones. This can be accomplished via mutation, recombination and survivor selection. All evolutionary algorithms work by combining selection with a mechanism for introducing variations and the best known mechanism for producing variations is that of mutation (Eshelman, 2000), but crossover serves as the dominant function involved with introducing variation into new genotypes (Eiben and Smith, 2003). Crossover occurs when two individuals (parents) are combined to produce an offspring that has traits of both the parents. The idea is that when two parents have strong traits, there is the possibility the offspring will inherit the best of both parents, making a stronger member of the population. As generations advance, the quality of the population increases and eventually produces a candidate solution that minimizes the error between computed and observed values. Replacement occurs when a member of the population is replaced by an offspring of two parents. This can occur either stochastically, where an individual of the population is selected randomly, or deterministically, where an individual is placed in the population based upon their “fitness” using the objective function as an evaluation tool (Eiben and Smith, 2003).

2.11.6 TERMINATION

Once a GA has been started there must be a method to determine when the GA will terminate. In general, there are two ways to terminate the GA; when an acceptable fitness level is achieved or when the model has run for a specified amount of time. In the example of using a GA to determine best-fit parameters for a model, the GA might terminate when the error statistic is acceptably small or after the GA has run for a specified number of generations.

2.12 SUMMARY

We have reviewed the issues associated with perchlorate contamination; its potential health effects and why innovative treatment technologies are needed to deal with the problem. We have seen that *in situ* bioremediation using HFTWs is an innovative approach that may be useful in helping to manage the perchlorate contamination problem, and have discussed the details of a field evaluation of the technology. In the following chapter, we will present a methodology for applying the technology model described in this chapter and Appendix A, in conjunction with a genetic algorithm to calibrate the model, to help interpret the results of the field demonstration.

3.0 METHODOLOGY

3.1 INTRODUCTION

In this chapter, a technology model that simulates the *in situ* destruction of perchlorate-contaminated groundwater using a HFTW system will be evaluated and calibrated against observational data obtained at the Aerojet site in California. The effect of varying individual model parameters on how well simulation results compare to observation data will be evaluated utilizing goodness-of-fit statistics. Using a genetic algorithm (GA), best-fit parameters will be derived to maximize the goodness-of-fit statistic.

3.2 TECHNOLOGY MODEL

Developed by the Environmental Modeling Research Laboratory of Brigham Young University in partnership with the U.S. Army Engineer Waterways Experiment Station, the Groundwater Modeling System (GMS) provides tools for every phase of a groundwater simulation including site characterization, model development, calibration, post-processing, and visualization. Because of its modular design, the user is able to select modules in custom combinations, allowing the user to choose only those groundwater modeling capabilities that are required (EMS-I, 2007). Parr (2002) utilized GMS to develop a model that calculates hydraulic head and groundwater fluxes induced by operation of a HFTW system. These fluxes are then used as input to a fate and transport model which calculates how physical (advection/dispersion) and biochemical (microbially-mediated perchlorate reduction in the presence of competing electron acceptors) processes affect perchlorate concentrations in space and time. A detailed description of the equations utilized in the model is provided at Appendix A.

3.2.1 GROUNDWATER FLOW MODEL

MODFLOW is a three-dimensional finite-difference model in which groundwater flow within an aquifer can be simulated (Harbaugh et al., 2000). In a finite-difference model, a partial-differential equation representing groundwater flow is replaced by a system of simultaneous linear algebraic difference equations, and these equations are solved at a finite set of discrete points in space and time to calculate head values at those points. Layers can be simulated as confined, unconfined or a combination of both and flows from external stresses such as flow to wells can be simulated.

To use MODFLOW, a region to be simulated must be divided into a rectilinear grid of layers, rows and columns. To model the Aerojet site in California, a three-dimensional grid consisting of 35 rows, 35 columns and 10 layers was used to represent a 121.92 meters square by 54.86 meters deep aquifer volume (Figure 3.1). The density of the grid was designed so that a finer level of detail would be provided in the immediate area surrounding the HFTWs.

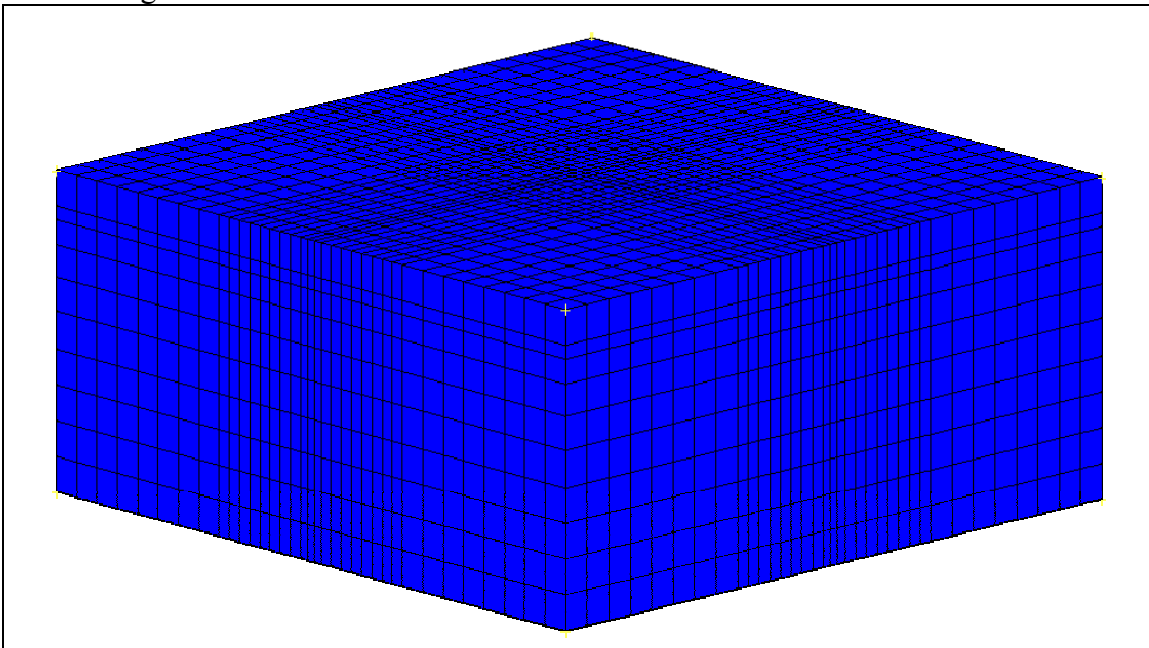


Figure 3.1 MODFLOW Rectilinear Grid

Hydraulic parameters (hydraulic conductivity, transmissivity, specific yield, etc.), boundary conditions (location of impermeable boundaries and constant heads), and stresses (pumping wells, recharge from precipitation, rivers, drains, etc.) are entered into the program. Pump tests were conducted at the Aerojet site to quantify the hydraulic conductivity of the aquifer. Using results for the pump tests, flow modeling and genetic algorithm optimization techniques were used to estimate layer horizontal and vertical hydraulic conductivities, K_h and K_v and specific storage coefficients (S_s) that provided a best-fit of model-simulated drawdowns to measured drawdown data (Hatzinger et al., 2005). For a more detailed description of the site model refer to Parr (2002) and Chosa (2004).

3.2.2 RT3D

RT3D is a software package for simulating three-dimensional, multispecies, reactive transport in groundwater (Clement, 1997; EMS-I, 2007). Initial estimates of the parameters in the biodegradation submodel were obtained directly from laboratory experiments or stoichiometry calculations, while two parameters (k_{max} and b) were fit to data collected during the first 113 days of the pilot study (Envirogen, 2002; Hatzinger et al., 2005). The initial parameters utilized in the technology model are provided in Table 3.1 along with the range of values used to test the model's sensitivity.

Table 3.1 Biological Reaction Parameters (Hatzinger et al., 2005)

Parameter	Original Values	Sensitivity Range Tested
k_{max}	12.5 d-1	0.1, 5, 15, 25
K_S^{don}	93 mg/L	1, 50, 150, 200
K_S^{oxy}	1 mg/L	10, 50, 100
K_S^{nit}	180 mg/L	1, 100, 200

K_S^{per}	150 mg/L	1, 100, 200
K_i^{oxy}	3 mg/L	1, 50, 100
K_i^{nit}	25 mg/L	1, 50, 100
Y_{biomass}	0.24 mg biomass/mg donor	0.1, 0.15, 0.3, 0.5
b	0.03 d-1	0.001, 0.01, 0.1

The initial parameter values identified in Table 3.1 differ from those used in Parr's model (Appendix A). The differences may be attributed to Parr's use of acetate as the electron donor as opposed to citrate, which was used at the Aerojet pilot study (Hatzinger et al., 2005).

Sampling data obtained before the HFTW system went into operation was extrapolated to the rectilinear grid described in Section 3.2.1 to establish the technology model's initial concentrations of oxygen, nitrate and perchlorate. Concentrations at the southern and eastern boundaries of the grid were held constant. This served as the constant concentration boundary condition, providing a source of contaminants. The average concentrations at the monitoring wells are presented in Table 3.2.

Table 3.2 Average Oxygen, Nitrate, and Perchlorate Concentrations at Aerojet Site on 30 September 2004 (Shaw, 2006)

	Average Concentration ($\mu\text{g/L}$)
Oxygen	1,370
Nitrate	4,626
Perchlorate	3,307

3.3 ELECTRON DONOR SCHEDULE

Citrate, as the electron donor, was injected into the HFTW system beginning 28 October 04 (day 0). Initial injection rates were based upon previous stoichiometric calculations and technology model simulation results. Injection slug lengths and frequency were varied throughout the operation of the system based upon sampling results. Tables 3.3 and 3.4 represent the electron donor injection schedule utilized during the pilot study from day 0 to day 113 (Huang, 2006). Although the system has been in continuous operation for 761 days with only short work stoppages since its inception, only the first 113 days of operational data are used to calibrate the model parameters. To help validate the model, the model is used to predict observed data from day 114 through 761. Model simulations for days 114 through 761 were based on the same injection rate/concentration and slug length that were used for days 106 through 113.

Table 3.3 Upflow HFTW Injection Schedule

Dates	Days	Injection Rate/ Concentration	Slug Length	Freq (per day)
28 Oct 04 – 13 Jan 05	0 - 77	78.7 ml/min (609 g/L)	20 min	1
13 Jan 05 – 11 Feb 05	77-106	78.7 ml/min (609 g/L)	30 min	1
11 Feb 05 – 18 Feb 05	106-113	78.7 ml/min (609 g/L)	38 min	1

Table 3.4 Downflow HFTW Injection Schedule

Dates	Days	Injection Rate/ Concentration	Slug Length	Freq (per day)
28 Oct 04 – 13 Jan 05	0 - 77	70.0 ml/min (609 g/L)	22 min	1
13 Jan 05 – 11 Feb 05	77-106	70.0 ml/min (609 g/L)	33 min	1
11 Feb 05 – 18 Feb 05	106-113	70.0 ml/min (609 g/L)	33 min	2

3.4 MEASURES OF PERFORMANCE

To evaluate the performance and accuracy of the technology model developed by Parr (2002), concentrations obtained from technology model simulations will be compared against observational data obtained from the HFTW system at the Aerojet site in California. In the analysis, the difference between simulated concentrations and observed values will be calculated and quantified using the error statistics described in Chapter 2. The technology model calibration will include time series plot comparisons and goodness-of-fit statistics to evaluate model performance. The calibration will be used to determine parameter values that result in a best-fit of model simulations to observed data.

There are no criteria which define a “good” value of RMSE or MAE, and as such, the original error values of the technology model as shown in Table 3.5 will serve as the basis for comparisons when evaluating the sensitivity of the model. These error statistics were obtained from the technology model utilizing the initial parameter values shown in Table 3.1, a continuous electron donor injection, and data for oxygen, nitrate, and perchlorate concentrations measured at the site.

Table 3.5 Sensitivity Analysis Baseline Error Statistics

	ME	MAE	RSME
Oxygen	-1.146	1.346	1.672
Nitrate	-1.222	2.048	2.678
Perchlorate	-0.488	1.039	1.566

Sensitivity analyses were conducted by varying the individual parameters in Table 3.1 over the identified ranges, and comparing the error statistics against the baseline statistics to determine if the model simulation improved or degraded. Following the sensitivity analysis, a GA was utilized to determine the parameters that obtain the best-fit between

simulated and observed concentrations. As noted in Section 3.2, observational data from the first 113 days of the study were utilized for calibration of the model.

Table 3.6 shows the error statistics obtained from the technology model utilizing the initial parameter values shown in Table 3.1 and the pulsed electron donor injection schedule detailed in Tables 3.3 and 3.4. These error statistics are used to evaluate changes in model predictions resulting from use of the best-fit parameters.

Table 3.6 Model Performance Baseline Error Statistics

	ME	MAE	RSME
Oxygen	-1.091	1.335	1.656
Nitrate	0.309	1.767	2.172
Perchlorate	0.477	1.227	1.562

Figures 3.2 and 3.3 show plots of simulated (using the technology model with baseline parameters) and observed perchlorate concentrations vs time at two shallow monitoring wells, 3628 (screened 52 – 57 feet below ground surface) and 3631 (screened 36 – 41 feet below ground surface). The shallow monitoring wells correspond with the upper screens of the HFTWs, while the deep monitoring wells coincide with the lower screens. Figure 2.7 shows approximate well locations in relation to the HFTWs.

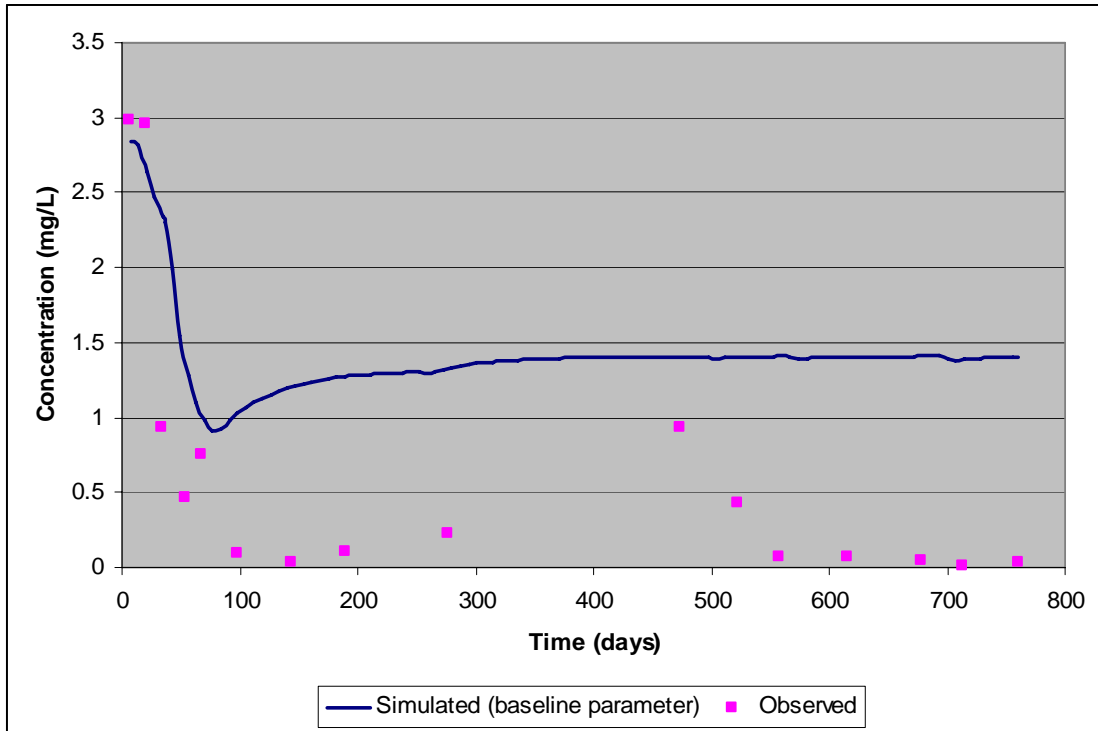


Figure 3.2 Perchlorate Concentration vs Time at Shallow Monitoring Well 3628 (see Figure 2.7 for location)

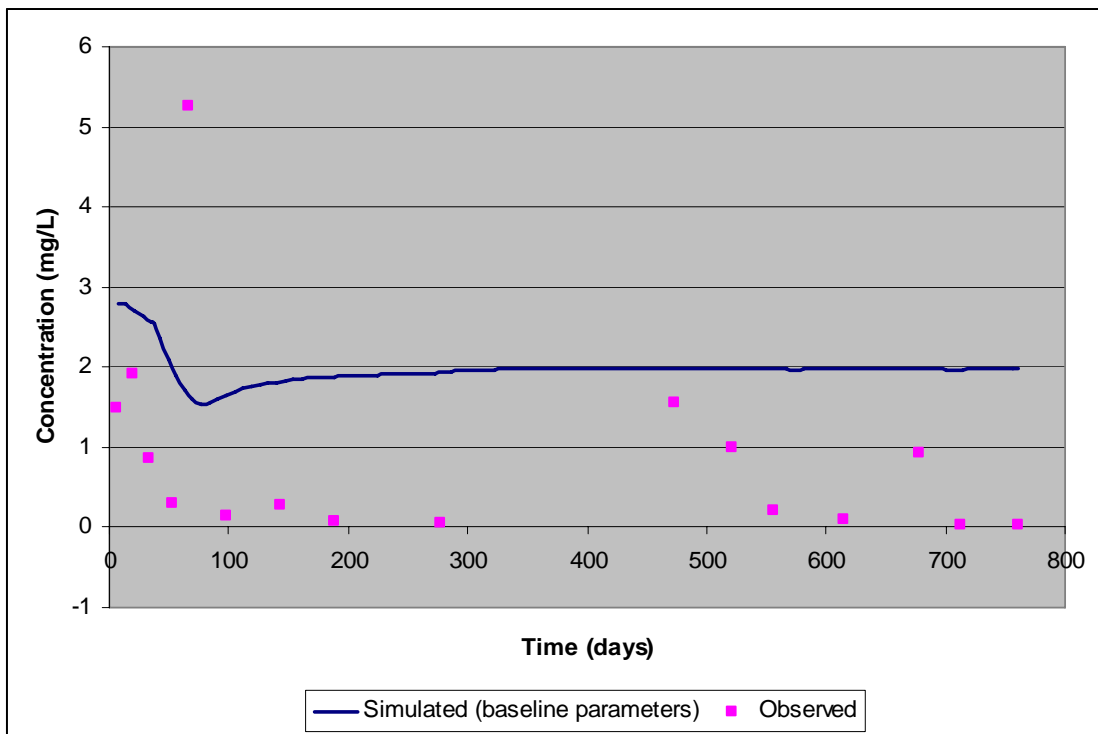


Figure 3.3 Perchlorate Concentration vs Time at Shallow Monitoring Well 3631 (see Figure 2.7 for location)

Figures 3.4 and 3.5 show plots of simulated (using the technology model with baseline parameters) and observed perchlorate concentrations vs time at two deep monitoring wells, 3630 and 3633, which are screened from 80 to 106 feet below ground surface.

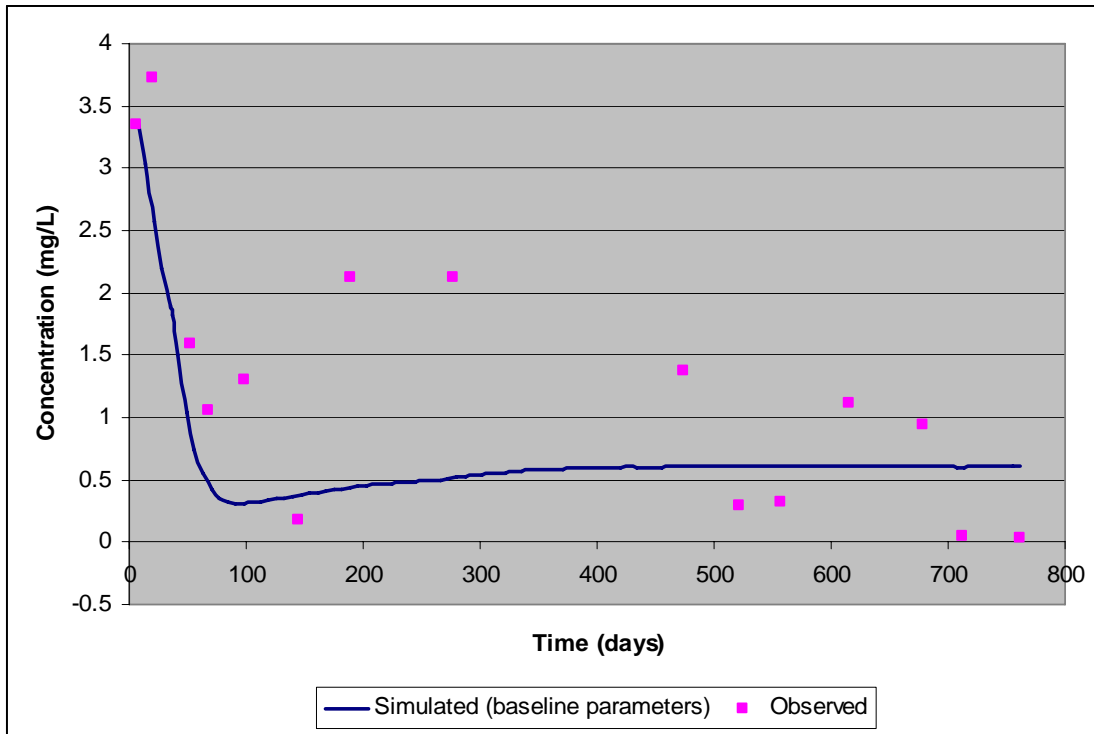


Figure 3.4 Perchlorate Concentration vs Time at Deep Monitoring Well 3630 (see Figure 2.7 for location)

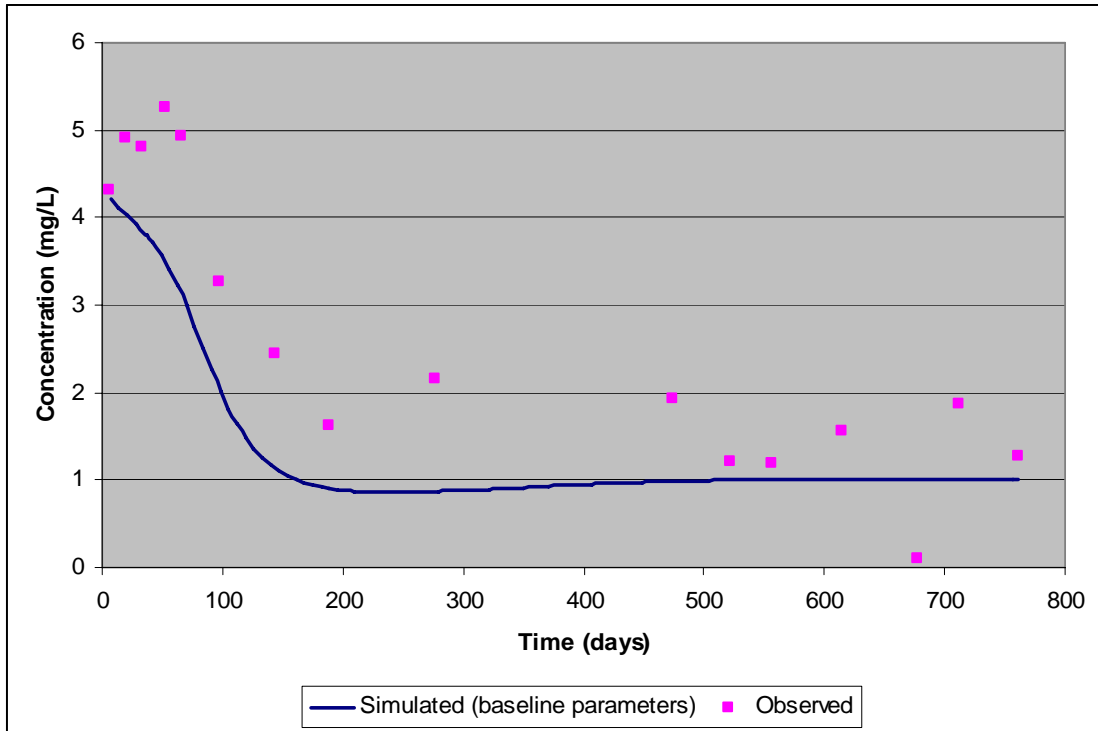


Figure 3.5 Perchlorate Concentration vs Time at Deep Monitoring Well 3633 (see Figure 2.7 for location)

3.5 GENETIC ALGORITHM (GA) CONFIGURATION

As indicated in Chapter 2, GAs are ideal optimization tools. A GA will be utilized in this analysis to determine the model parameters that result in the best-fit of the model to data observed in the first 113 days of the field evaluation. The GA configuration is provided in the following sections.

3.5.1 GA INDIVIDUAL DEFINITION

In reference to the technology model being evaluated, an individual is a set of the nine parameters identified in Table 2.2. In calibrating the model to determine the optimal parameters that best-fit the observed data, those individuals will be varied through use of a GA to minimize the model's error statistics.

3.5.2 GA OBJECTIVE FUNCTION

As mentioned in Chapter 2, a GA requires an objective function to evaluate the candidate solutions. In this study, the first 113 days of the observed oxygen, nitrate and perchlorate concentration data will be used, along with model predictions of those concentrations over the same time period, to calculate the RMSE. The RMSE will be used in a single objective function to be optimized. To frame the error statistic in a form for use in a GA, the RMSE will be inverted, as shown in Equation 3.1, so that the objective function increases as the RMSE approaches zero (Huang, 2006).

$$GA_{obj} = \frac{1}{1 + RMSE} \quad (3.1)$$

While the RMSE for the goodness-of-fit to oxygen, nitrate, and perchlorate concentrations will be used in the objective function to calibrate the model over the first 113 days of the technology evaluation, individual oxygen, nitrate and perchlorate goodness-of-fit error statistics (RMSE, ME and MAE) will be used to evaluate how well the parameterized model fits the observed data over the entire 761-day technology evaluation period.

3.5.3 POPULATION AND PARENT SELECTION

The population used for this evaluation is set at 30, and parent selection will be accomplished randomly by use of probabilities.

3.5.4 VARIATION

For a genetic algorithm to work, variation must be introduced into the population and reproduction process. The type of GA used in this research is called a MicroGA. MicroGA's method of introducing variation into the population is by use of

recombination, crossover and population regeneration, with no mutation factors applied. The crossover probability to be utilized in this GA is 0.5, meaning that genes from each parent are randomly selected to produce an offspring, with each parent contributing 50% of their genes to the child (Bäck, 2000). As the GA runs, the objective function will cause the population to converge on a set of parameters that provide the highest objective function value. In order to produce fitter (higher scoring) offspring, additional variation must be introduced into the population. This variation is introduced through population regeneration whereby the fittest individual is allowed to reproduce, while the rest of the population is randomly regenerated. With the new population, the GA can continue the recombination and crossover process. Table 3.7 shows the parameter ranges tested with the GA.

Table 3.7 GA Parameter Range

Parameter	Original Values	Range Tested
k_{\max}	12.5 d-1	1-50
K_S^{don}	93 mg/L	20-200
K_S^{oxy}	1 mg/L	20-200
K_S^{nit}	180 mg/L	20-200
K_S^{per}	150 mg/L	20-200
K_i^{oxy}	3 mg/L	5-50
K_i^{nit}	25 mg/L	5-50
Y_{biomass}	0.240 mg biomass/mg donor	0.01-1
b	0.030 d-1	0.001-0.1

3.5.5 SURVIVOR SELECTION/REPLACEMENT

Replacing members of the population is accomplished via a deterministic method. The candidate that scores highest against the objective function will be placed into the population.

3.5.6 TERMINATION

Due to resource limitations, time constraints and the possibility that the GA could run indefinitely without finding a set of parameters that produced a solution within specified tolerances (Eiban and Smith, 2003), the GA will run for 100 generations.

3.6 DIFFERING SITE CONDITIONS IMPACTS ON TECHNOLOGY PERFORMANCE

To evaluate the effect of differing site conditions on the models results, the Aerojet site model was modified to represent two very different hypothetical sites. The first hypothetical site (Site 1) was homogeneous, with high hydraulic conductivity (50 m/day), and no competing electron acceptors (oxygen and nitrate concentrations set at 0 mg/L). The second hypothetical site (Site 2) was configured to represent a location with high concentrations of competing electron acceptors in a homogeneous, low conductivity (5 m/day) aquifer. To achieve the high concentrations of competing electron acceptors, the initial Aerojet site concentrations identified in Table 3.2 were multiplied by a factor of 10.

4.0 RESULTS AND ANALYSIS

4.1 INTRODUCTION

This chapter presents the analyses that were conducted to determine the sensitivity of technology model results to changes in the model parameters identified in Table 3.7. The chapter also presents the results of the model calibration, obtained by using a genetic algorithm to find the parameter values that resulted in the best-fit of model simulations to concentration data measured during the initial 113 days of the field evaluation at the Aerojet site. The chapter concludes with an analysis of the effect of differing site conditions on simulated technology performance.

4.2 PARAMETER SENSITIVITY ANALYSIS

In this section, we explore the sensitivity of the technology model results to each of the kinetic parameters by varying the parameters identified in Table 3.7. Table 4.1 shows the differences in error statistics obtained by comparing simulations of the model (run for the range of parameter values) with measured data. The differences listed in Table 4.1 are the maximum differences in the error statistic values that were obtained from varying a given parameter. A positive value in the ME column indicates that the error statistic improved as the parameter value increased from low to high. For the MAE and RMSE error statistics, the opposite is true; a positive value indicates the error statistic gets worse as the parameter value increased from low to high.

Table 4.1 Difference in Error Statistics as Parameter Value is Increased from Low to High Values

	Oxygen			Nitrate			Perchlorate		
Parameter	ME	MAE	RMSE	ME	MAE	RMSE	ME	MAE	RMSE
k_{\max}	-0.541	0.270	0.281	-3.893	-0.637	-0.363	-2.526	-1.077	-0.658
K_s^{don}	0.014	0.006	0.005	0.199	-0.070	-0.122	0.107	-0.020	-0.047
K_s^{oxy}	0.061	-0.024	-0.030	0.019	-0.005	0.007	0.019	-0.009	-0.009
K_s^{nit}	0.468	-0.457	-0.641	0.233	-0.039	-0.128	-0.246	0.103	0.150
K_s^{per}	0.000	-0.001	-0.001	-0.131	0.045	0.082	0.198	-0.050	-0.083
K_i^{oxy}	0.000	0.000	0.000	0.000	0.001	0.000	0.000	0.000	0.000
K_i^{nit}	0.000	0.000	0.000	0.054	-0.023	-0.036	-0.105	0.018	0.044
Y_{biomass}	0.002	0.001	0.001	0.027	-0.013	-0.016	0.015	-0.008	-0.008
b	0.006	0.006	0.004	0.799	-0.280	-0.461	0.441	-0.055	-0.160

Table 4.1 shows that the model, as a whole, appears to be most sensitive to the k_{\max} and K_s^{nit} parameters, and relatively insensitive to the K_i^{oxy} parameter. Looking at each electron acceptor individually, simulated oxygen concentrations appear to be most sensitive to the k_{\max} and K_s^{nit} parameters, and relatively insensitive to all other parameters. Simulated nitrate concentrations appear to be most sensitive to changes in the b and k_{\max} parameters, and to a lesser degree, the K_s^{don} , K_s^{nit} parameters. All other parameters impact the technology model's nitrate error statistics to a small degree with the exception of the K_i^{oxy} , which has no impact. Simulated perchlorate concentrations, like oxygen and nitrate concentrations, are most sensitive to changes in the k_{\max} parameter, and to a lesser degree K_s^{nit} , and b. Like the other electron acceptors, simulated perchlorate concentrations are insensitive to the K_i^{oxy} parameter.

4.3 MODEL CALIBRATION

A GA, as described in Chapter 3, was utilized to determine the best-fit parameters that would enable the model to fit the observed data from the initial 113 days of the field evaluation. The GA found the set of nine parameter values that maximized the objective function in Equation 3-1. After finding the best-fit parameters, the calibrated model was run to simulate the entire 761 days of field data.

4.3.1 GA OPERATION

The graph of the GA objective function value vs generation number shown in Figure 4.1 indicates how well the GA is performing. As described previously, new offspring are created when crossover and recombination occurs between two parents. Depending on the offspring's objective function value, the offspring is either discarded or replaces a lower scoring individual in the population. As “fitter” offspring are put into the population, the overall fitness of the population gradually improves, as seen by the increasing population average line in Figure 4.1 (note that an objective function value of 1.0 represents perfect correspondence between the measured data and model calculations). Within every generation, there is one individual who has the highest objective function value. These individuals are represented on the graph as the individual maximum line in Figure 4.1. As the population average improves, eventually all individuals converge on a single objective function value and variation must be introduced into the population. When the population is regenerated, as described in section 3.4.4, the objective function value averaged over the entire population sharply decreases (as depicted in Figure 4.1 at generations 25, 48, and 79). Eventually, crossover and recombination improve the fitness of the entire population and the process continues.

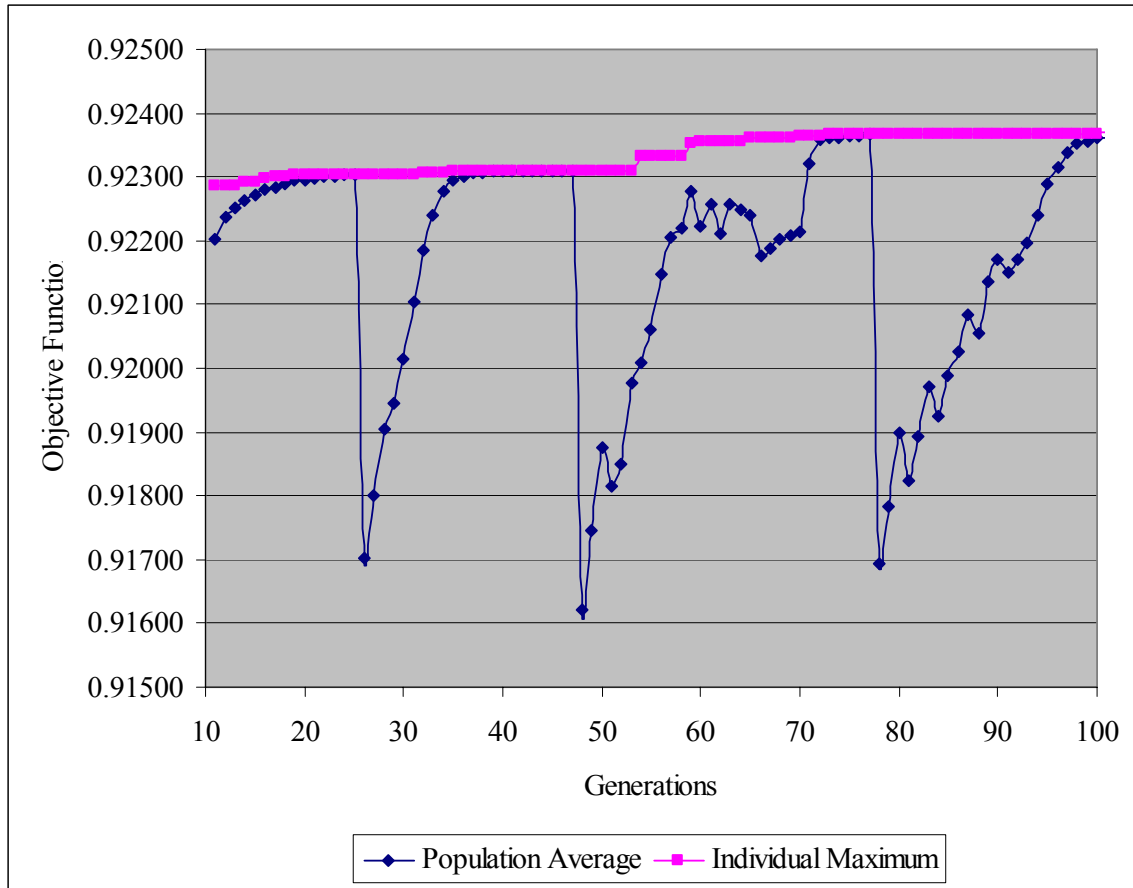


Figure 4.1 Objective function value of most fit individual and population average vs GA generation

4.3.2 CALIBRATION RESULTS

Parameter values calculated at various GA generations are shown in Table 4.2. The parameter values that will be used in subsequent model simulations, which we will refer to as the best-fit values, are the values identified after 100 GA generations. Of the range of values explored by the GA (see Table 3.7), only the best-fit value of K_s^{oxy} was at either the maximum or minimum end of the range (indicating that the best-fit value of K_{soxy} may be outside the specified range).

Table 4.2 GA Parameter Values

	Baseline	10 Gen	30 Gen	50 Gen	70 Gen	100 Gen	Units
k_{\max}	12.5	23.22	23.22	23.22	7.139	7.188	mg/mg/day
K_S^{don}	93	193.30	137.00	137.30	36.4	36.75	mg/L
K_S^{oxy}	1	186.20	187.60	187.80	184.4	200	mg/L
K_S^{nit}	180	125.60	199.40	198.70	151.1	150.9	mg/L
K_S^{per}	150	67.28	67.24	65.12	53.88	59.41	mg/L
K_i^{oxy}	3	20.61	43.11	43.28	43.66	44.36	mg/L
K_i^{nit}	25	27.22	49.89	49.89	38.05	35.44	mg/L
Y_{biomass}	0.24	0.01006	0.01006	0.01000	0.01100	0.01003	mg/mg
b	0.03	0.07938	0.09330	0.09986	0.09996	0.09948	1/day

4.3.3 GOODNESS-OF-FIT ERROR STATISTIC RESULTS

The parameter values in Table 4.2 were entered into the technology model to derive the goodness-of-fit statistics shown in Table 4.3 and Figures 4.2 through 4.4. In early generations, the GA improved the error statistics of the technology model's oxygen concentration calculations but made both the nitrate and perchlorate error statistics worse. As the generations advanced, the perchlorate error statistics began to improve slightly, while the nitrate statistics did not improve compared to their baseline values. Thus, we see that the GA was obtaining calibration parameters that improved the overall fit of the model calculations to the data, but the fit of the model to the concentration data for each of the individual electron acceptors did not necessarily improve with GA generation.

Table 4.3 GA Error Statistic Results

	Oxygen			Nitrate			Perchlorate		
	ME	MAE	RSME	ME	MAE	RSME	ME	MAE	RSME
Baseline	-1.091	1.335	1.656	0.309	1.767	2.172	0.477	1.227	1.562
30 Gen	-0.463	1.011	1.272	0.602	1.860	2.214	0.251	1.267	1.579
50 Gen	-0.451	1.006	1.266	0.642	1.867	2.220	0.260	1.271	1.578
70 Gen	-0.388	0.978	1.231	0.646	1.861	2.204	0.277	1.259	1.559
100 Gen	-0.377	0.975	1.227	0.621	1.865	2.206	0.310	1.267	1.561

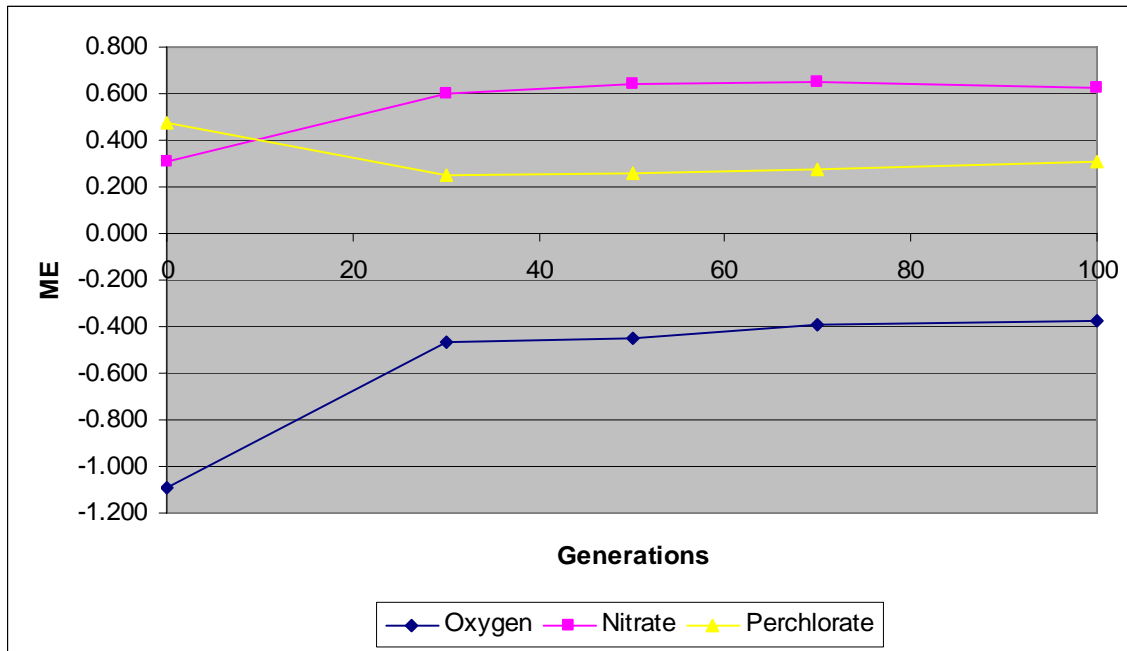


Figure 4.2 Changes in Mean Error over GA Generations

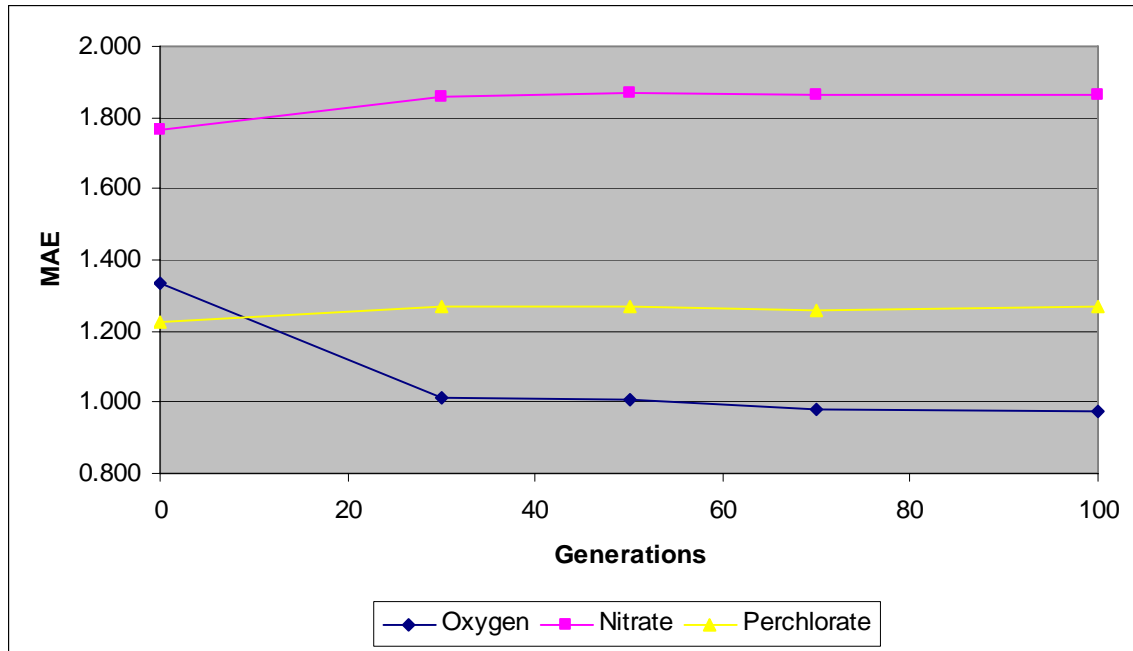


Figure 4.3 Changes in Mean Absolute Error over GA Generations

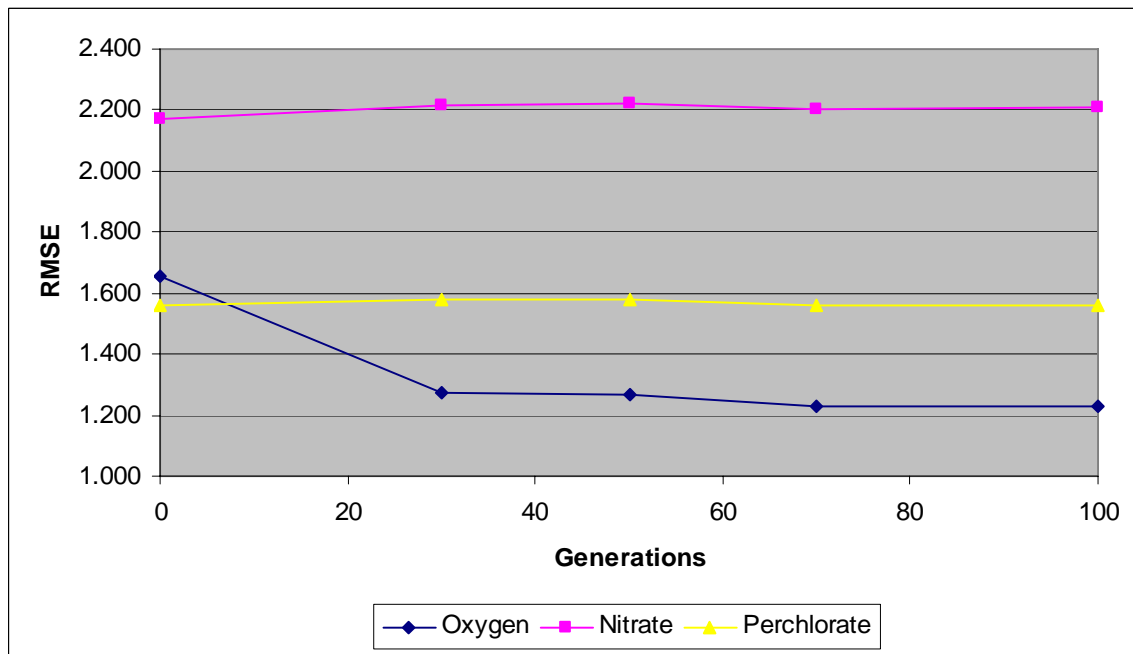


Figure 4.4 Changes in Root Mean-Squared Error over GA Generations

This behavior may be attributed to a combination of the objective function utilized by the GA along with the model structure itself. As described in Chapter 3, the GA maximizes a single objective function (Equation 3.1) based on minimizing the RMSE. The RMSE is

determined by calculating the difference between modeled and measured concentrations for all electron acceptor data, equally weighted. This, coupled with the model structure, where simulated oxygen concentrations affect the nitrate and perchlorate concentrations through competitive inhibition, but not vice versa (Appendix A, Equations A.10 – A.12), results in the GA giving additional weight to fitting the oxygen data.

4.4 BREAKTHROUGH CURVES AT MONITORING WELLS

The best-fit parameters obtained from the GA were used in the technology model to evaluate performance of the model over the entire 761-day period for which data are available. Oxygen, nitrate and perchlorate concentration time series graphs at monitoring wells upgradient and downgradient of the HFTWs are provided for both the shallow and deep parts of the aquifer. A complete set of time series plots for all monitoring wells is provided at Appendix C.

4.4.1 SHALLOW UPGRADIENT MONITORING WELL

NMW3 is a shallow (46-61 ft bls) monitoring well located upgradient of the HFTWs. Figures 4.5 – 4.7 show measured and simulated oxygen, nitrate, and perchlorate concentrations, respectively, versus time at NMW3. We see from Figure 4.5 that using the best-fit parameters improves the model fit for the oxygen data, compared to the baseline parameters. Use of the best-fit parameters results in little improvement for the nitrate or perchlorate simulations. We also note from Figure 4.7 that the perchlorate concentrations at this shallow upgradient well are significantly less than the concentrations predicted by the model.

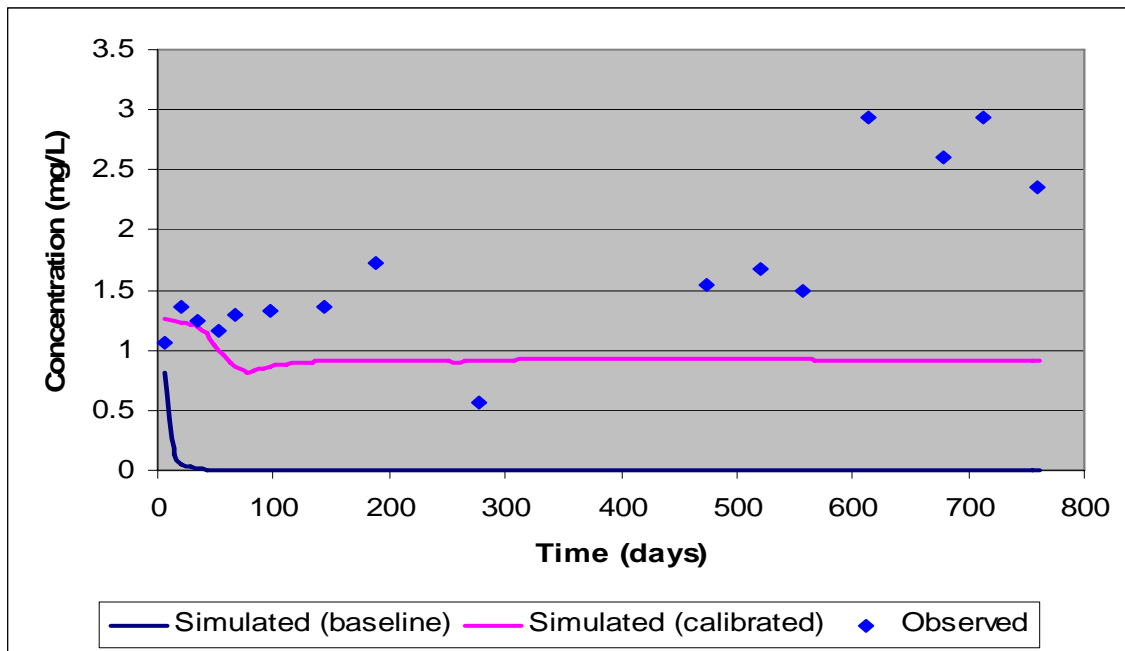


Figure 4.5 Oxygen Concentration vs Time at Well NMW3

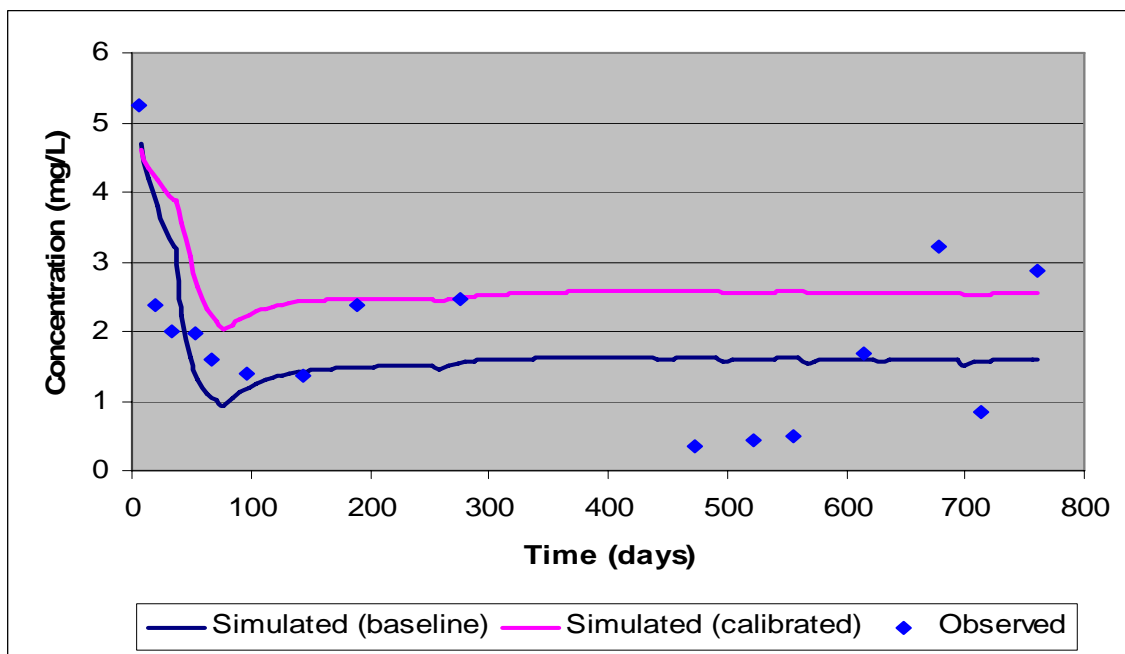


Figure 4.6 Nitrate Concentration vs Time at Well NMW3

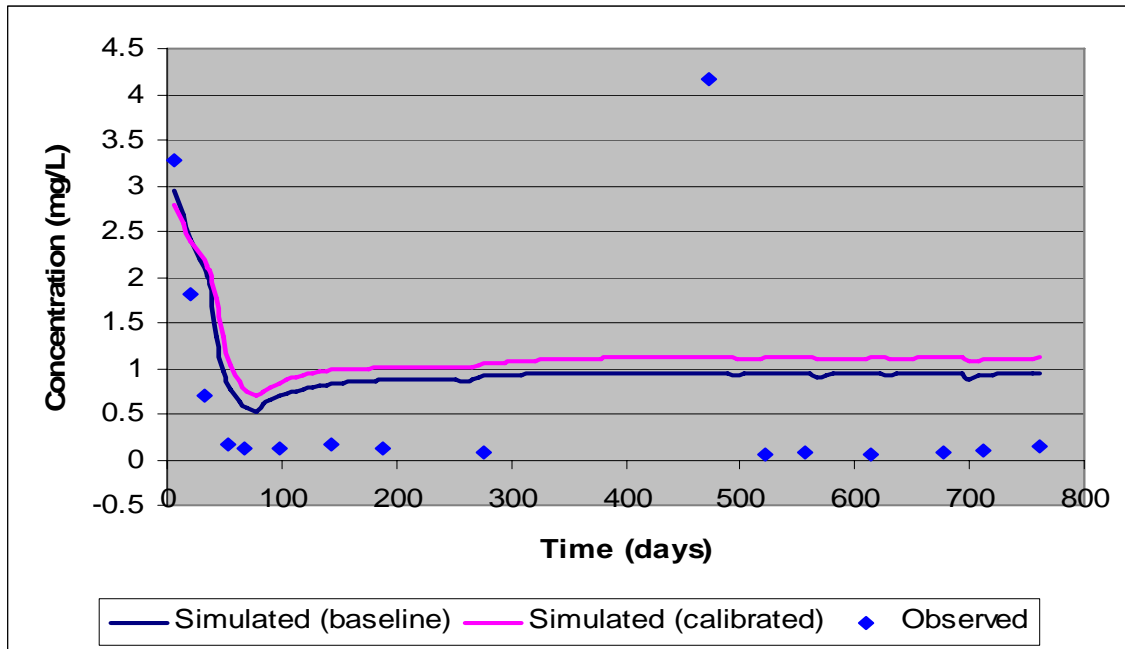


Figure 4.7 Perchlorate Concentration vs Time at Well NMW3

4.4.2 DEEP UPGRADIENT MONITORING WELL

NMW4 is a deep (80-100 ft bls) monitoring well located upgradient of the HFTWs.

Figures 4.8 – 4.10 show measured and simulated oxygen, nitrate and perchlorate concentrations, respectively, versus time at NMW4. We see from Figures 4.8 and 4.9 that using the best-fit parameters improves the model's fit for both oxygen and nitrate data, compared to the baseline parameters. Use of the best-fit parameters results in little improvement for the perchlorate simulations. We also note from Figures 4.9 and 4.10 that the measured nitrate and perchlorate concentrations at this deep upgradient well are significantly higher than the concentrations predicted by the model.

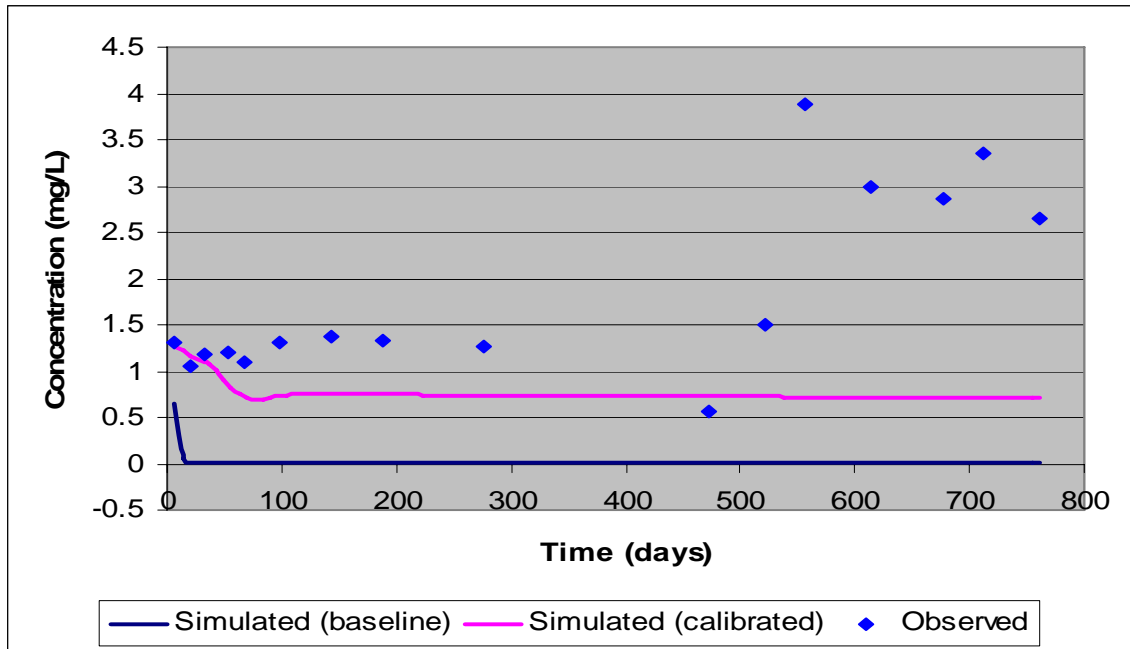


Figure 4.8 Oxygen Concentration vs Time at Well NMW4

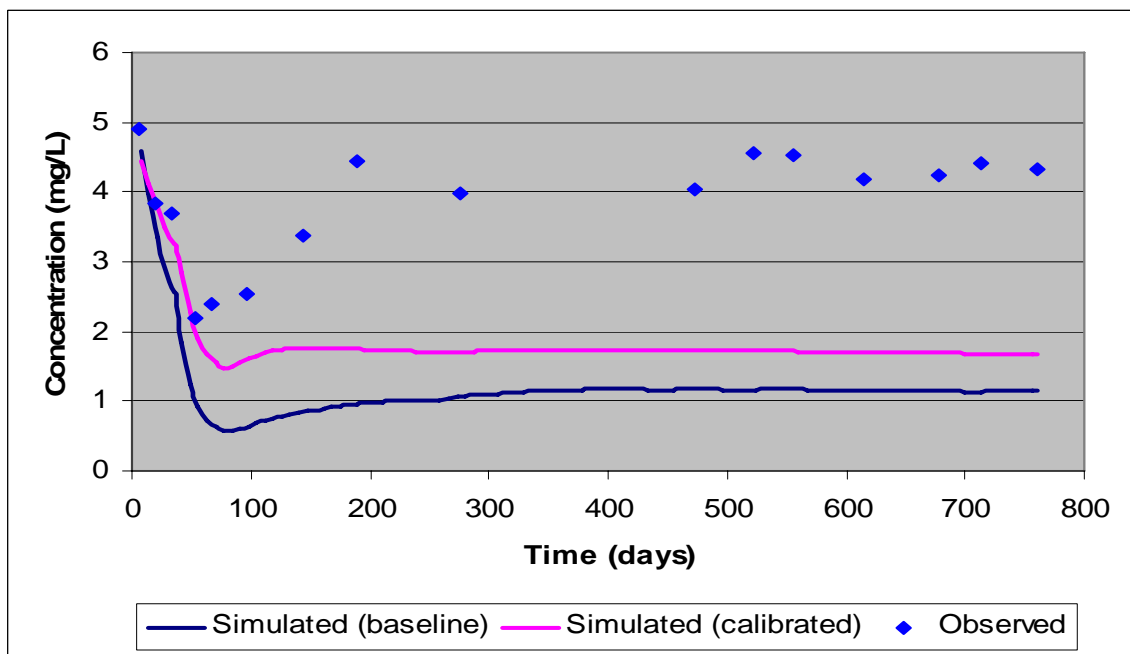


Figure 4.9 Nitrate Concentration vs Time at Well NMW4

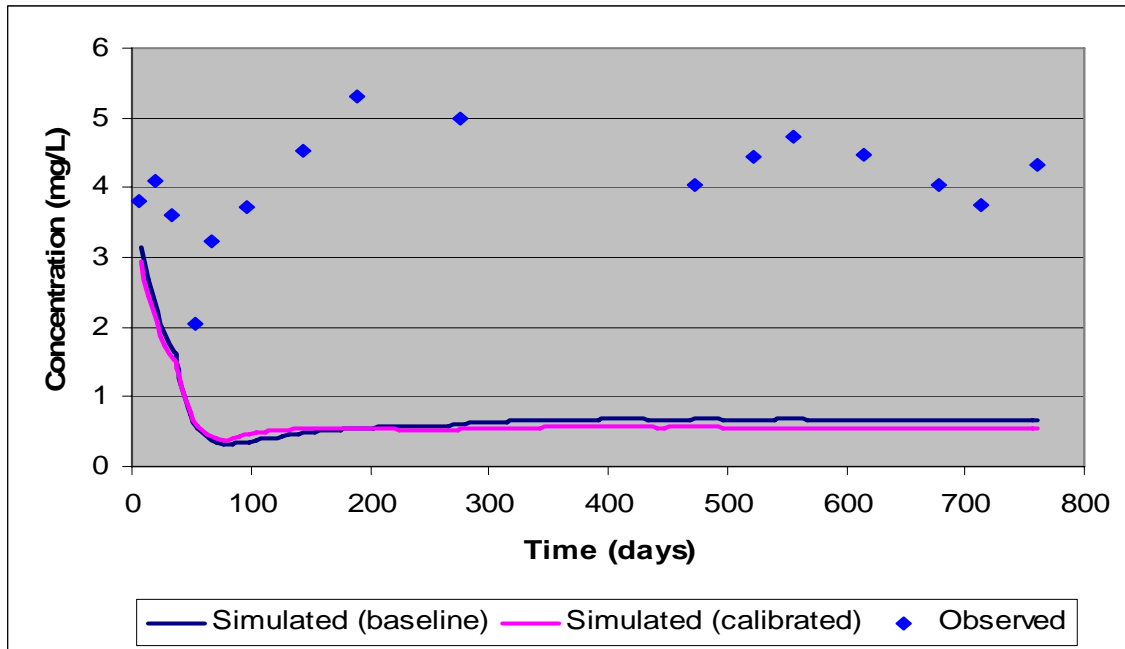


Figure 4.10 Perchlorate Concentration vs Time at Well NMW4

4.4.3 SHALLOW DOWNGRADIENT MONITORING WELLS

Monitoring well 3632 (52-57 ft bls) and NMW7 (46-61 ft bls) are shallow monitoring wells located downgradient of the upflow HFTW. Thus, these wells may be good indicators of the quality of treated water leaving the upflow HFTW. Figures 4.11 – 4.13 show measured and simulated oxygen, nitrate, and perchlorate concentrations, respectively, versus time at monitoring well 3632. We see from Figure 4.11 that using the best-fit parameters improves the model fit for the oxygen data, compared to the baseline parameters. Use of the best-fit parameters results in little improvement for the nitrate or perchlorate simulations. We also note from Figure 4.13 that the measured perchlorate concentrations at this shallow downgradient well are significantly less than the concentrations predicted by the model.

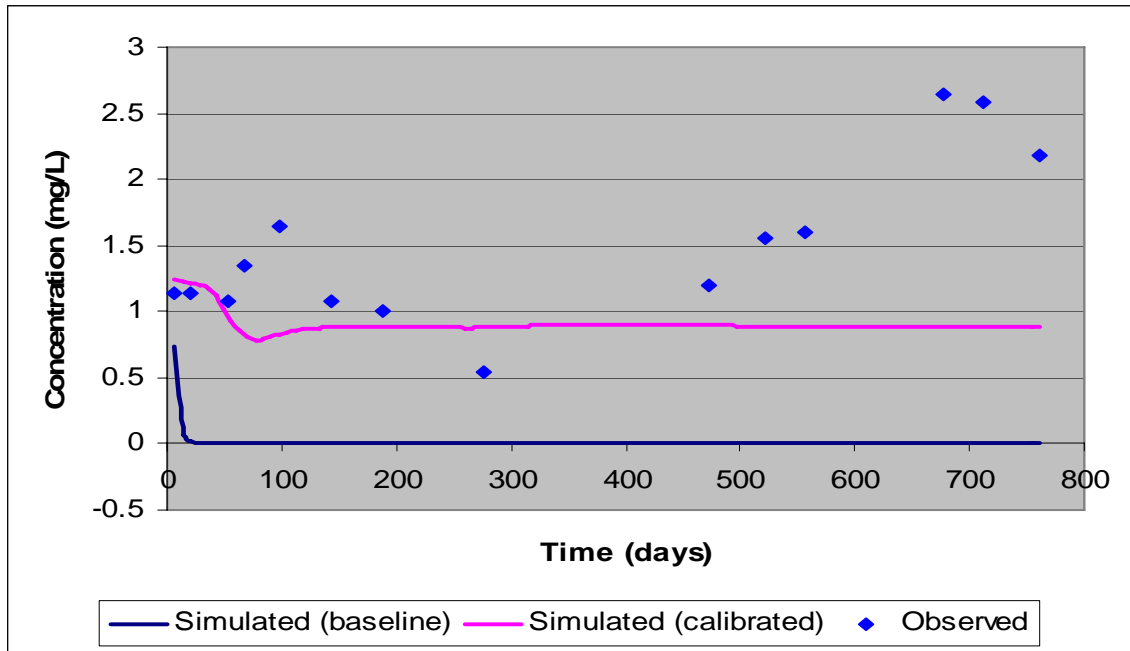


Figure 4.11 Oxygen Concentration vs Time at Well 3632

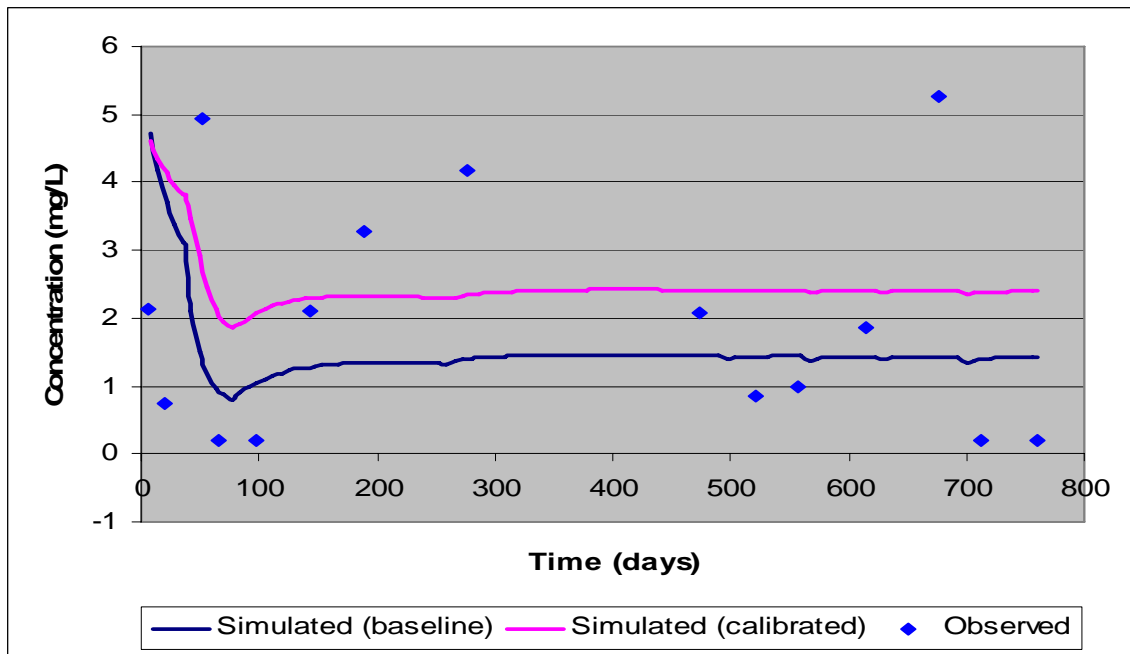


Figure 4.12 Nitrate Concentration vs Time at Well 3632

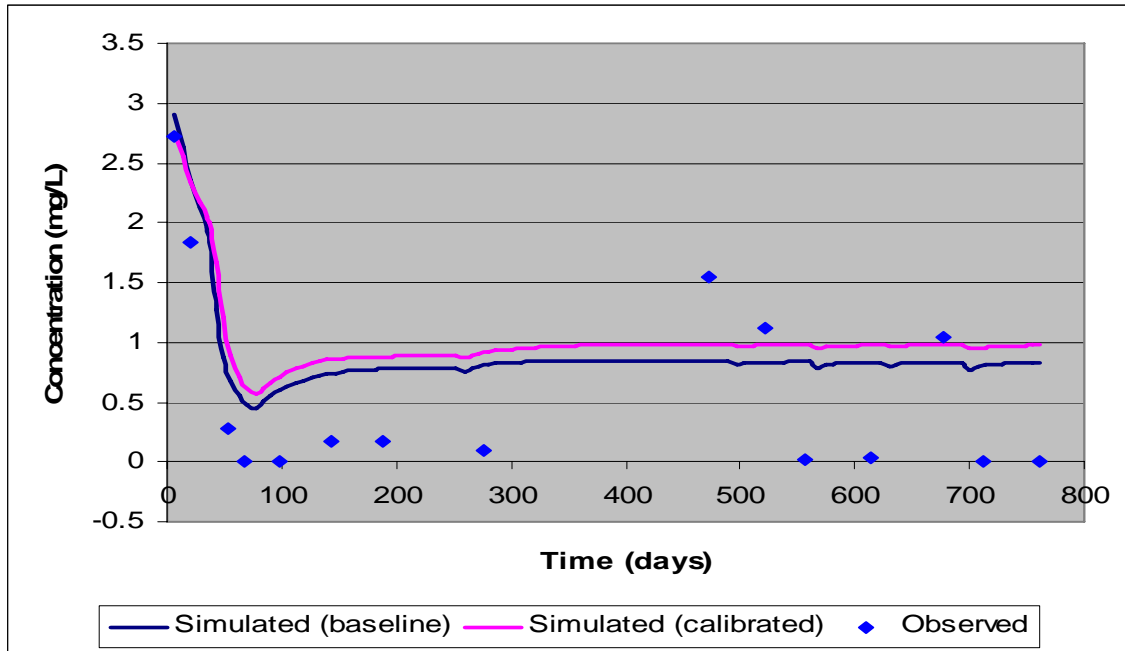


Figure 4.13 Perchlorate Concentration vs Time at Well 3632

NMW7 is a shallow well located further downgradient of the upflow HFTW than 3632. Figures 4.14 – 4.16 show measured and simulated oxygen, nitrate, and perchlorate concentrations, respectively, versus time at NMW7. Figure 4.14 indicates that using the best-fit parameters improves the model fit for the oxygen data, compared to the baseline parameters. Use of the best-fit parameters results in little improvement for the nitrate or perchlorate simulations. We also note from Figures 4.15 and 4.16 that the measured nitrate and perchlorate concentrations at this shallow downgradient well are significantly less than the concentrations predicted by the model.

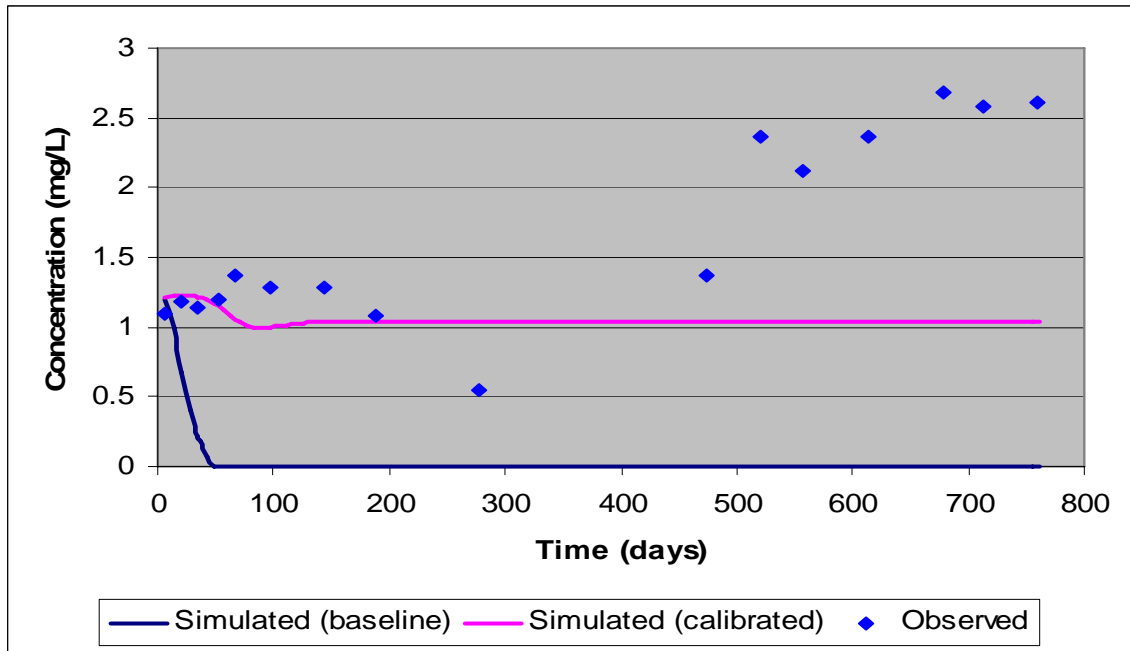


Figure 4.14 Oxygen Concentration vs Time at Well NMW7

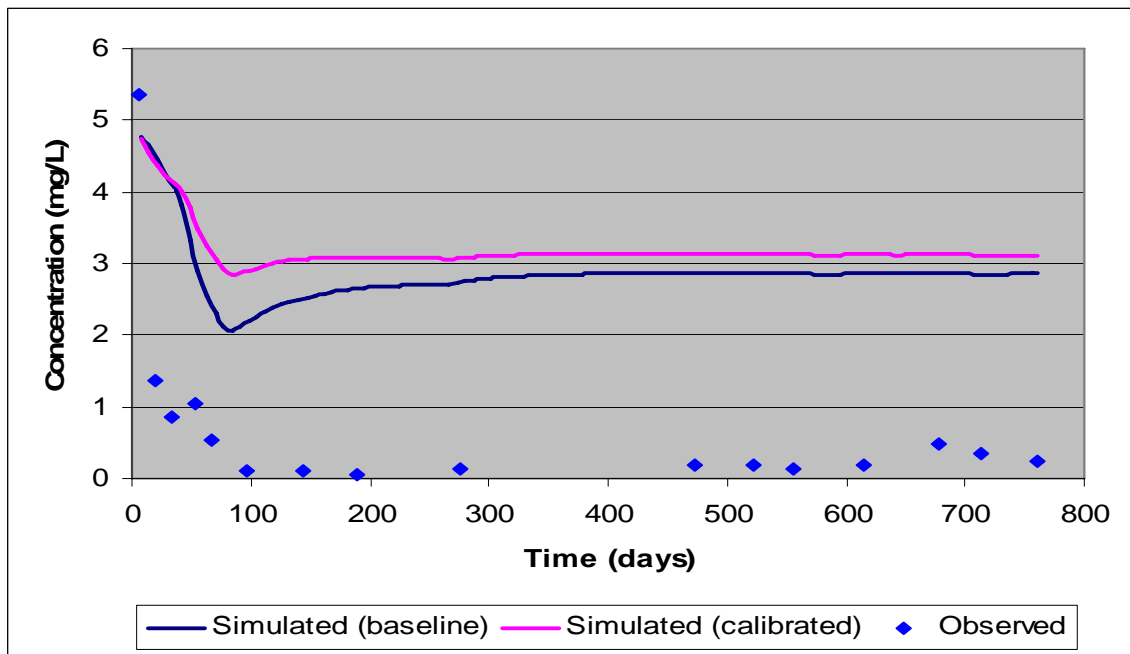


Figure 4.15 Nitrate Concentration vs Time at Well NMW7

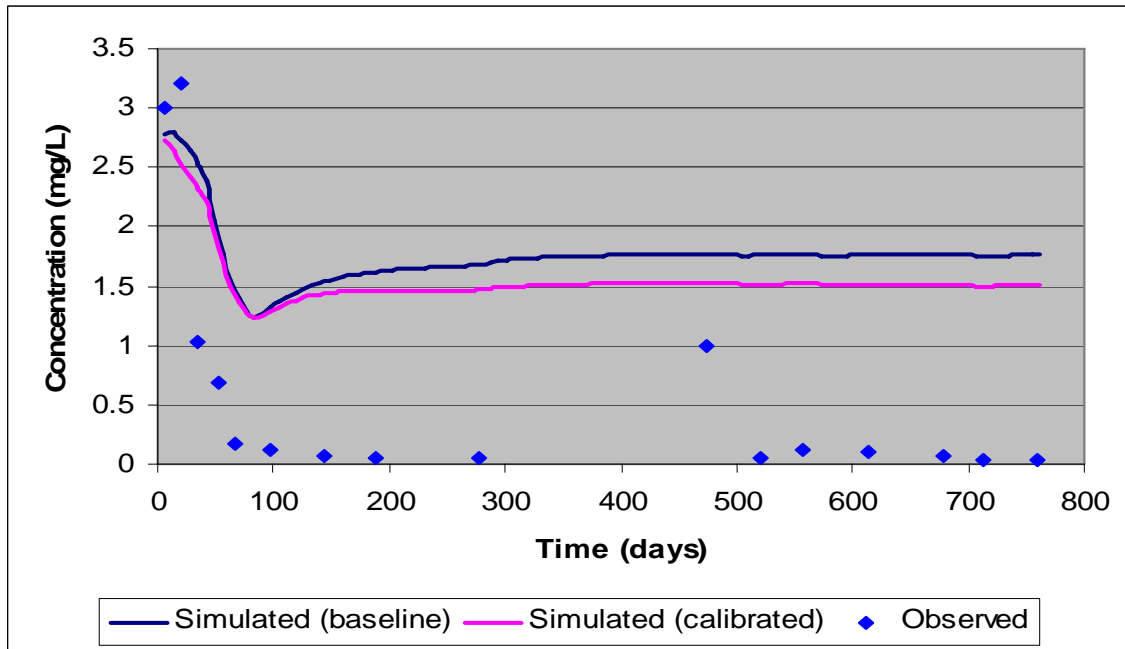


Figure 4.16 Perchlorate Concentration vs Time at Well NMW7

4.4.4 DEEP DOWNGRAIDENT MONITORING WELLS

Monitoring wells 3519 (78-103 ft bls) and NMW10 (80-100 ft bls) are deep monitoring wells located downgradient of the downflow HFTW. Thus, these wells may be good indicators of the quality of treated water leaving the downflow HFTW. Figures 4.17 – 4.19 show measured and simulated oxygen, nitrate, and perchlorate concentrations, respectively, versus time at well 3519. We see from Figures 4.17 and 4.18 that using the best-fit parameters improves the model’s fit for both oxygen and nitrate data, compared to the baseline parameters. Use of the best-fit parameters results in little improvement for the perchlorate simulations. We also note from Figure 4-19 that the measured perchlorate concentrations at this deep downgradient well are significantly higher than the concentrations predicted by the model.

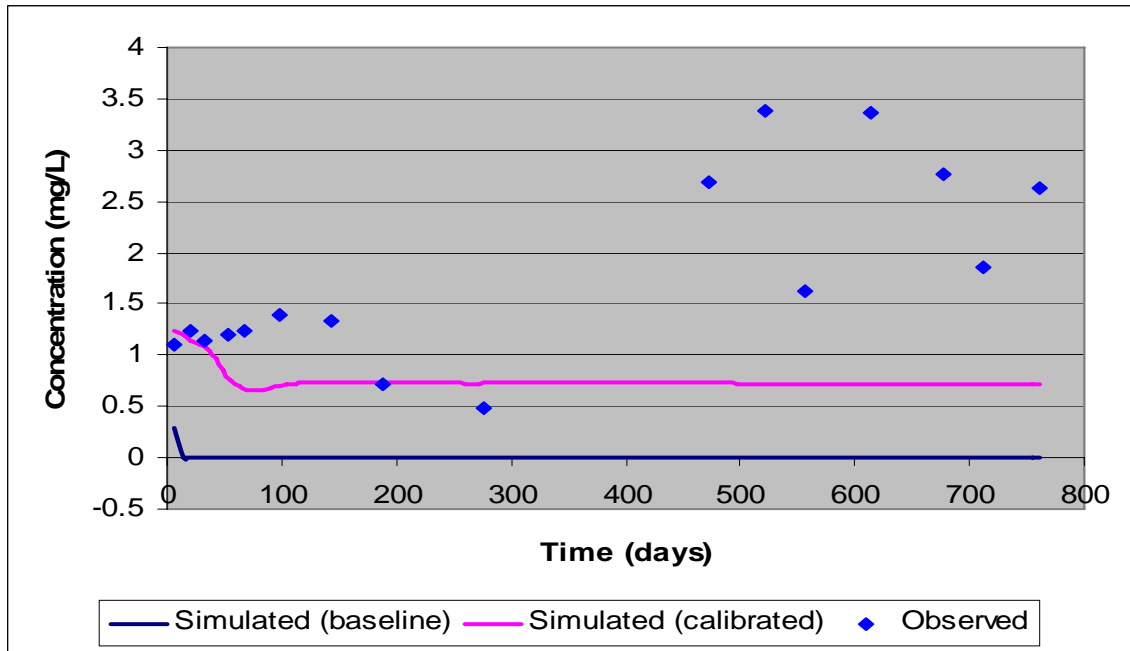


Figure 4.17 Oxygen Concentration vs Time at Well 3519

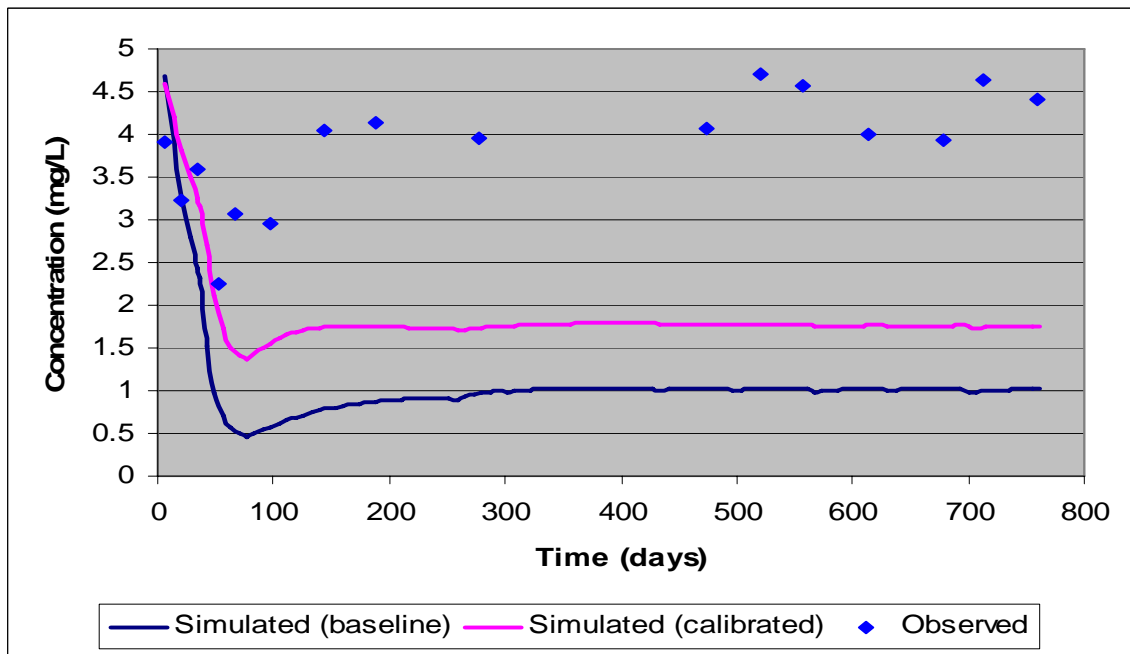


Figure 4.18 Nitrate Concentration vs Time at Well 3519

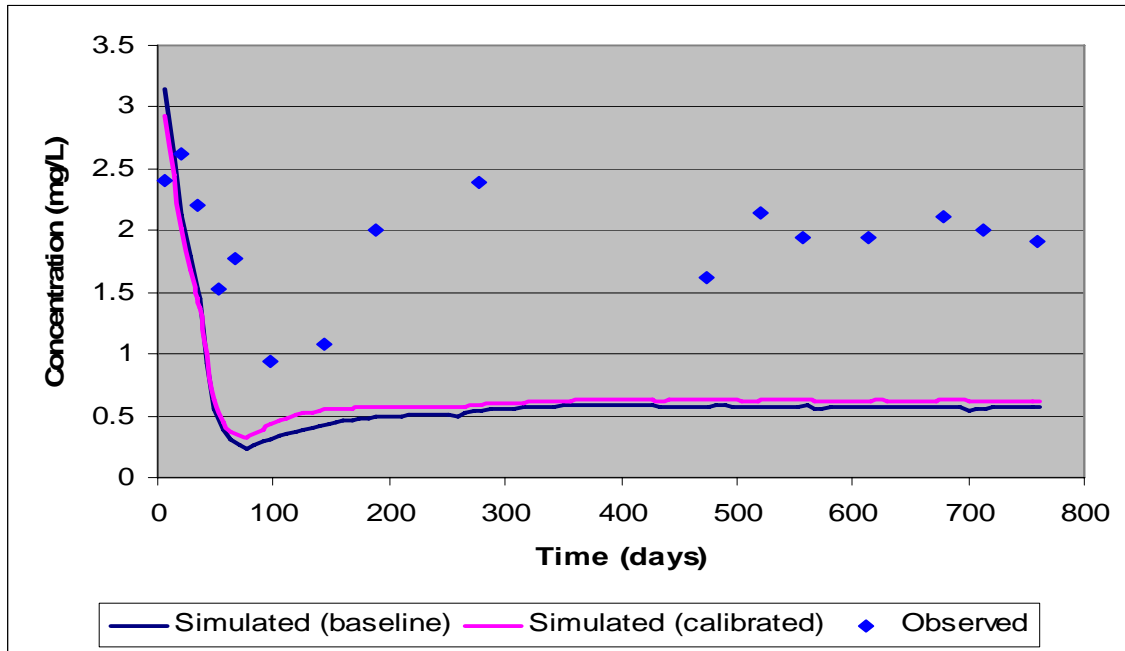


Figure 4.19 Perchlorate Concentration vs Time at Well 3519

NMW10 is a deep well located further downgradient of the downflow HFTW than 3519. Figures 4.20 – 4.22 show measured and simulated oxygen, nitrate, and perchlorate concentrations, respectively, versus time at NMW10. We see from Figure 4.20 that using the best-fit parameters improves the model fit for the oxygen data, compared to the baseline parameters, while Figure 4.21 and 4.22 show little improvement for the nitrate or perchlorate simulations. The model fits to the nitrate and perchlorate concentration data appear reasonable.

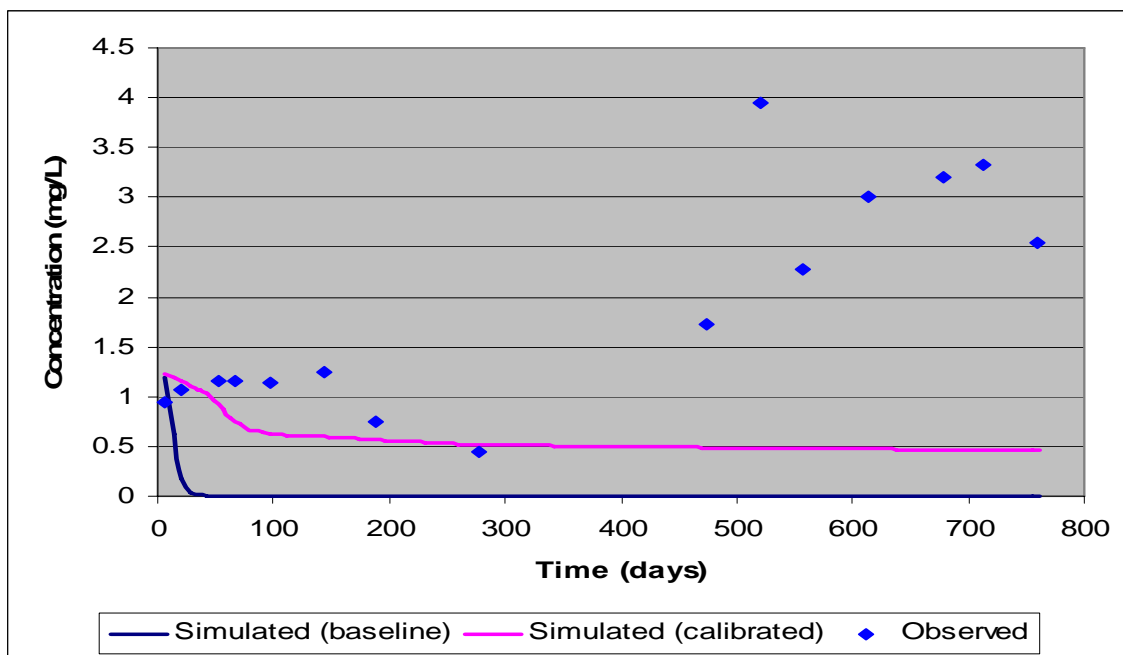


Figure 4.20 Oxygen Concentration vs Time at Well NMW10

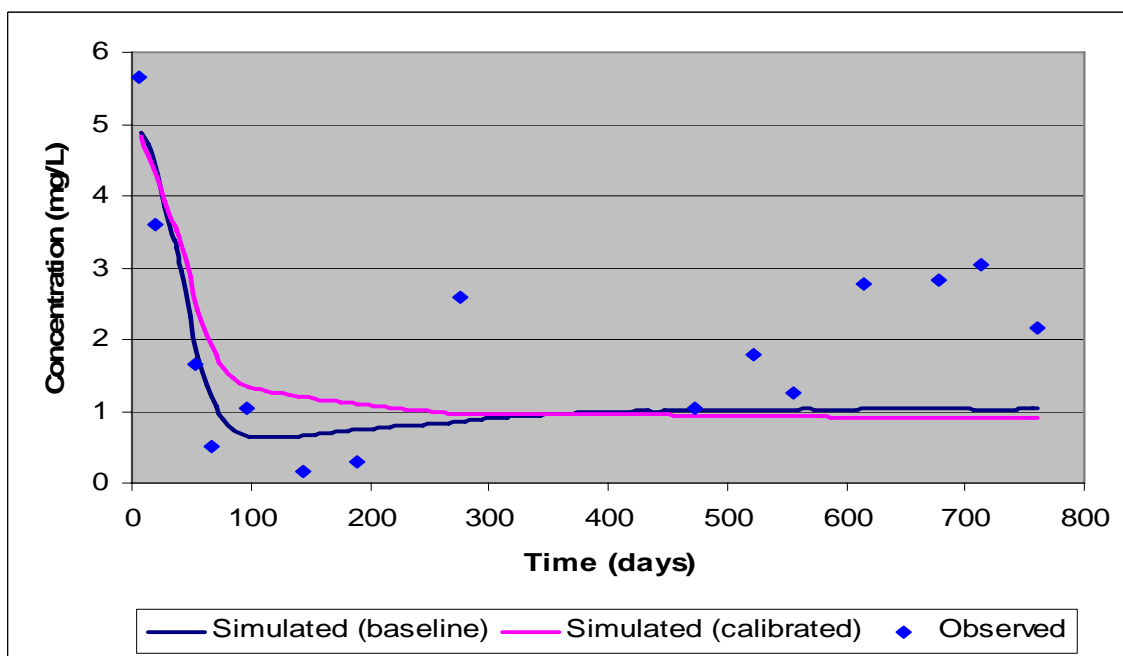


Figure 4.21 Nitrate Concentration vs Time at Well NMW10

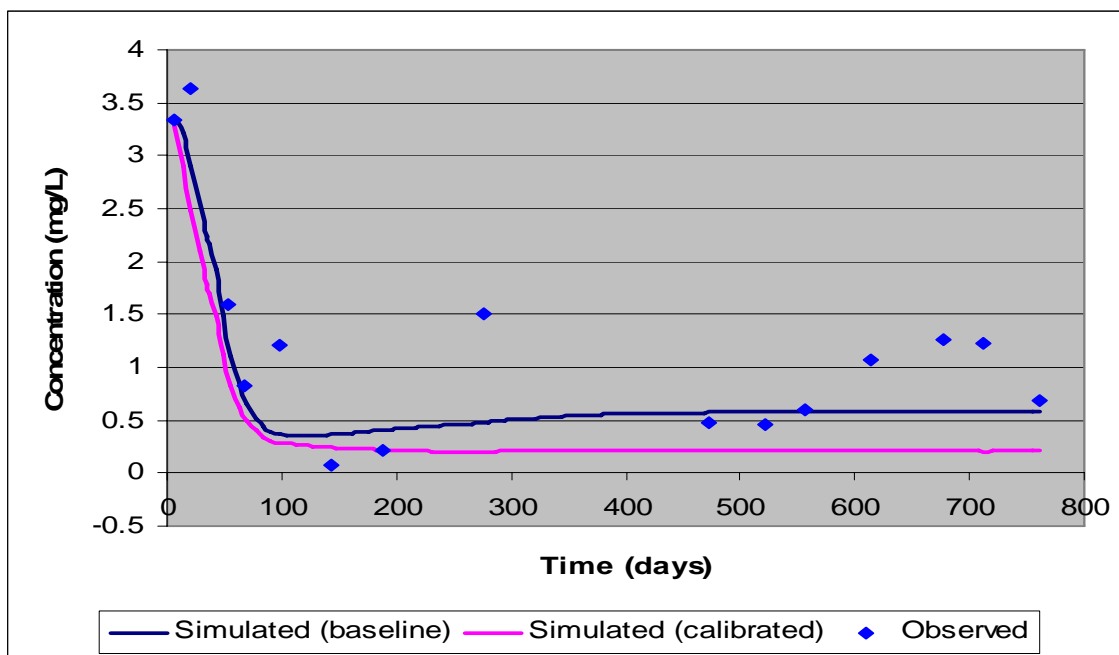


Figure 4.22 Perchlorate Concentration vs Time at Well NMW10

4.5 MODEL APPLICATION TO INVESTIGATE EFFECT OF DIFFERING SITE CONDITIONS ON TECHNOLOGY PERFORMANCE

The best-fit parameters obtained above were utilized in simulations of the technology at the two sites described in Section 3.5 and the results compared with the Aerojet site results. As there are no competing electron acceptors at Site 1, only perchlorate breakthrough curves will be evaluated at the different monitoring wells.

4.5.1 PERCHLORATE CONCENTRATION VS TIME RESULTS

Figures 4.23 through 4.28 indicate that perchlorate concentrations at Site 1 are the highest at all monitoring wells, even though there are no competing electron acceptors present at the site. A potential reason for these results is that due to the high conductivity at the site, the groundwater is flowing through the area so fast that the added substrate is being diluted to the point that an effective bioactive zone cannot be established.

The simulations at all monitoring wells show that the technology performance at Site 2 is generally similar to the performance at the Aerojet site, even with the increased concentrations of electron acceptors and low conductivity. One possible explanation is that the low conductivity of the site is restricting the amount of perchlorate entering the site while at the same time allowing the substrate-amended groundwater more time in the bioactive zones surrounding the HFTWs.

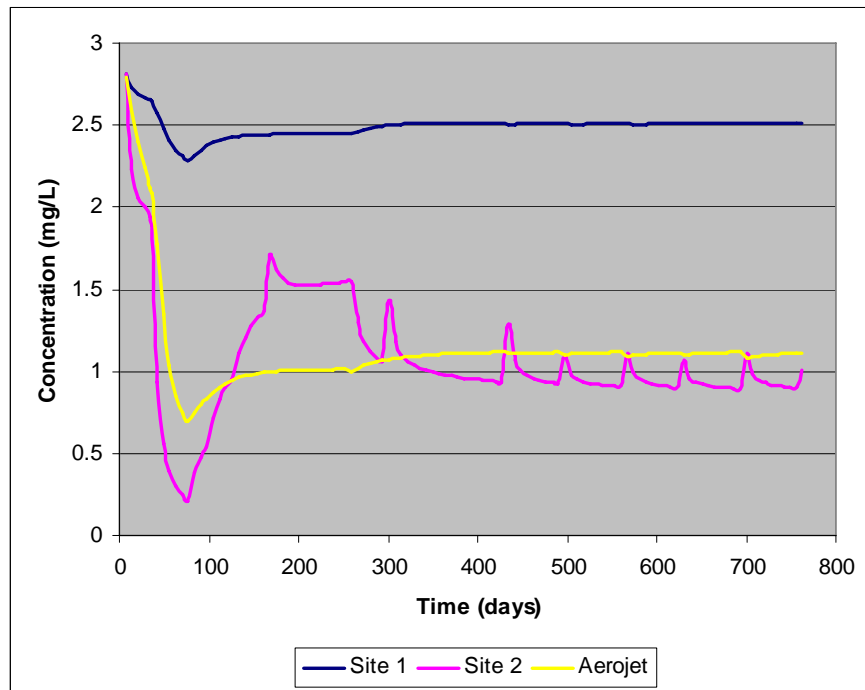


Figure 4.23 Simulated Perchlorate Concentration vs Time at Well NMW3 for Hypothetical Sites 1 and 2 and Aerojet

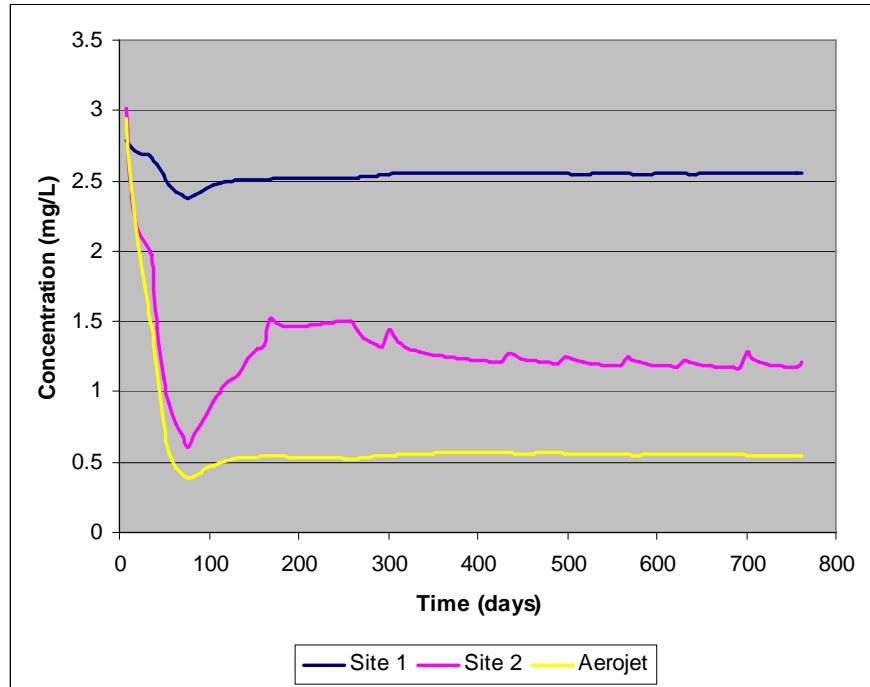


Figure 4.24 Simulated Perchlorate Concentration vs Time at Well NMW4 for Hypothetical Sites 1 and 2 and Aerojet

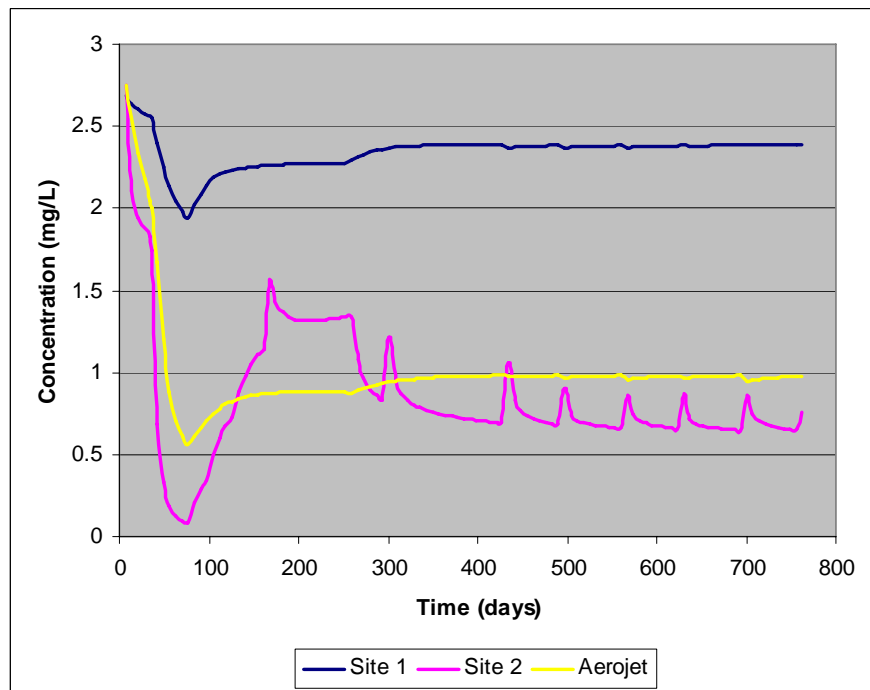


Figure 4.25 Simulated Perchlorate Concentration vs Time at Well 3632 for Hypothetical Sites 1 and 2 and Aerojet

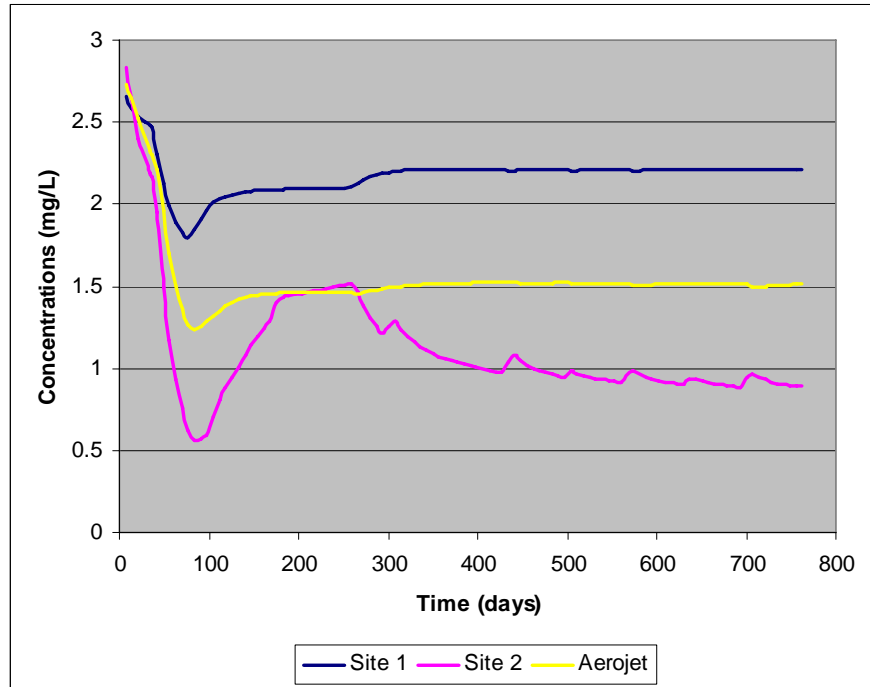


Figure 4.26 Simulated Perchlorate Concentration vs Time at Well NMW7 for Hypothetical Sites 1 and 2 and Aerojet

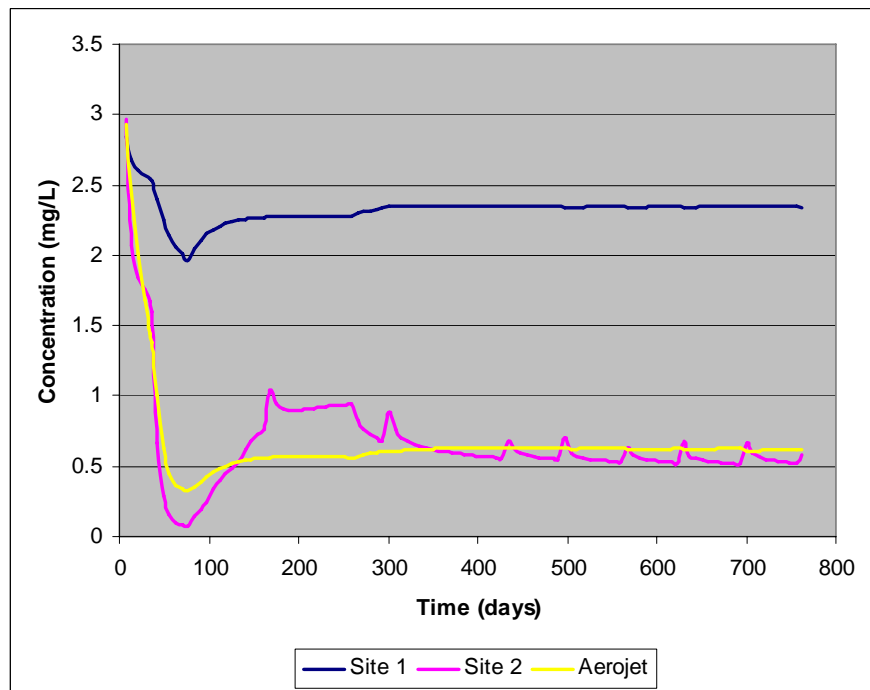


Figure 4.27 Simulated Perchlorate Concentration vs Time at Well 3519 for Hypothetical Sites 1 and 2 and Aerojet

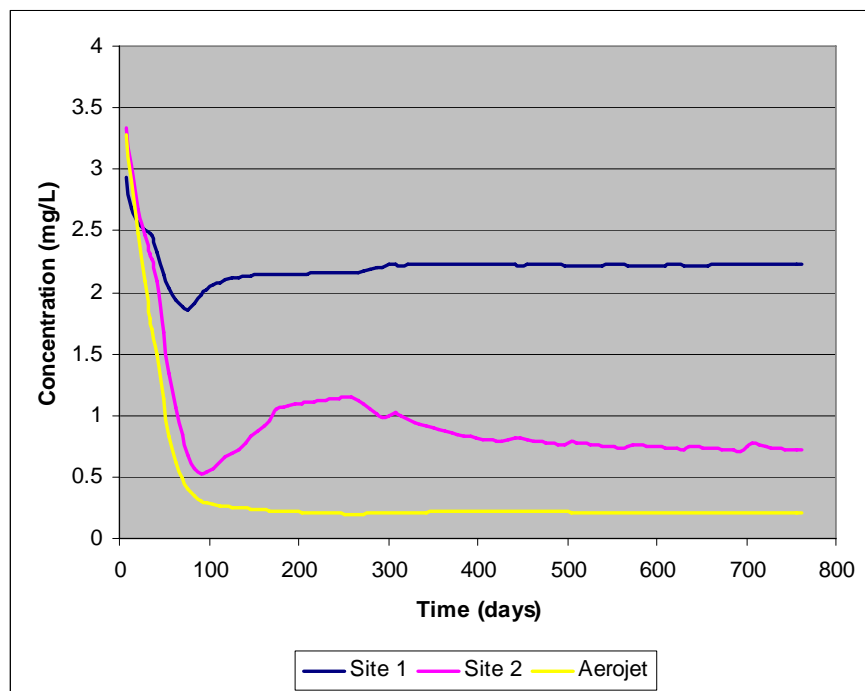


Figure 4.28 Simulated Perchlorate Concentration vs Time at Well NMW10 for Hypothetical Sites 1 and 2 and Aerojet

4.5.2 PERCHLORATE CONTOUR PLOTS

Figures 4.29 through 4.31 show perchlorate contour plots at model layer 5 and at three different times (63, 182, and 364 days, respectively) for the two hypothetical sites, as well as the Aerojet site. Layer 5 of the model corresponds with the lower screen of the HFTWs. Figure 4.29 shows that, at day 63, Site 2 with the high concentrations of electron acceptors and low hydraulic conductivity, has a smaller perchlorate “hole” than the Aerojet site. As time progresses the size of the perchlorate hole increases, though it still remains smaller than the hole at the Aerojet Site at day 182 and day 364.

The simulation results for Site 1, with no competing electron acceptors and high conductivity, show little change from day 63 through day 364. This seems to indicate that steady state is reached quickly with little additional growth of the hole. Despite the size of Site 1’s perchlorate hole, the breakthrough curves indicate that the hole is

“shallow”, i.e. perchlorate is not being reduced much below the 2.4 mg/L contour line. Based upon the size of the contour hole and the breakthrough curves it appears that the Site 2 and Aerojet perchlorate holes are much “deeper” than Site 1’s, i.e. more perchlorate is being reduced.

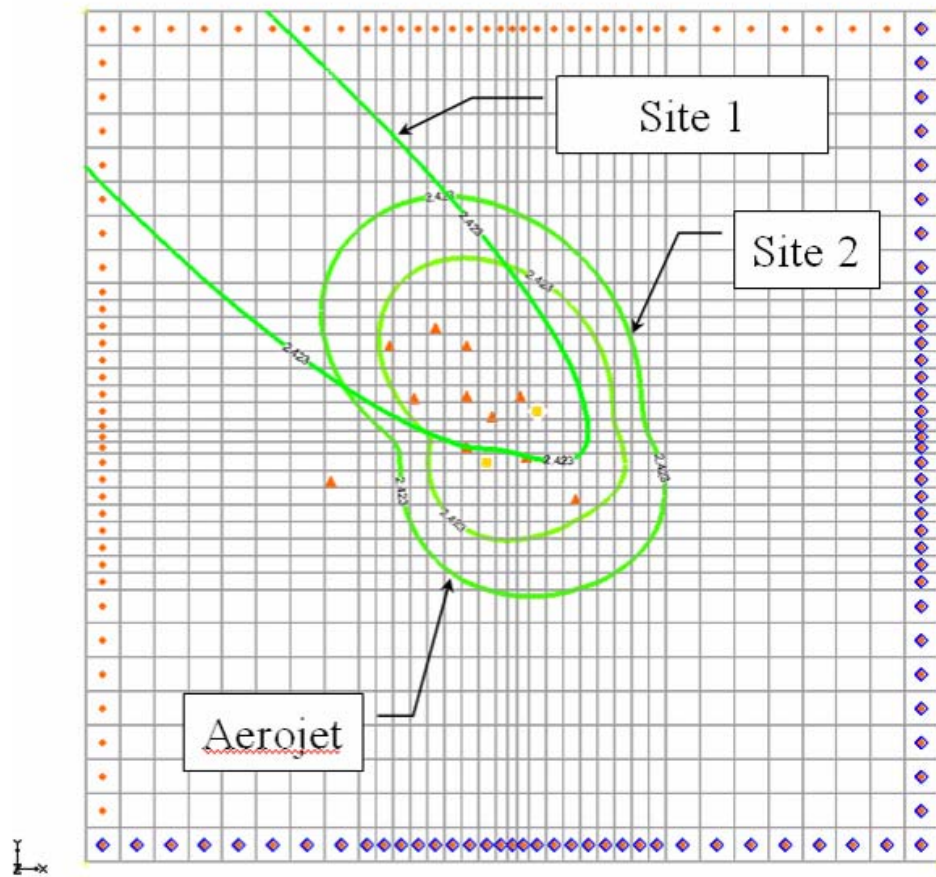


Figure 4.29 Perchlorate “Hole” (defined by 2.4 mg/L contour) at Layer 5 and Day 63

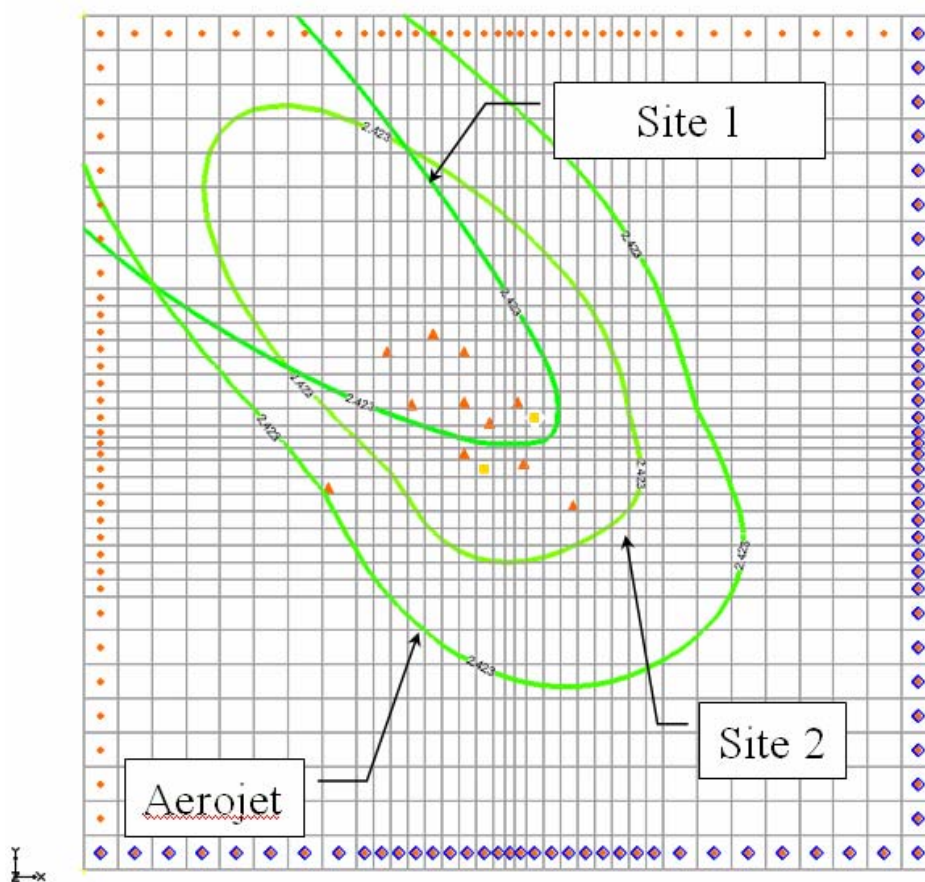


Figure 4.30 Perchlorate “Hole” (defined by 2.4 mg/L contour) at Layer 5 and Day 182

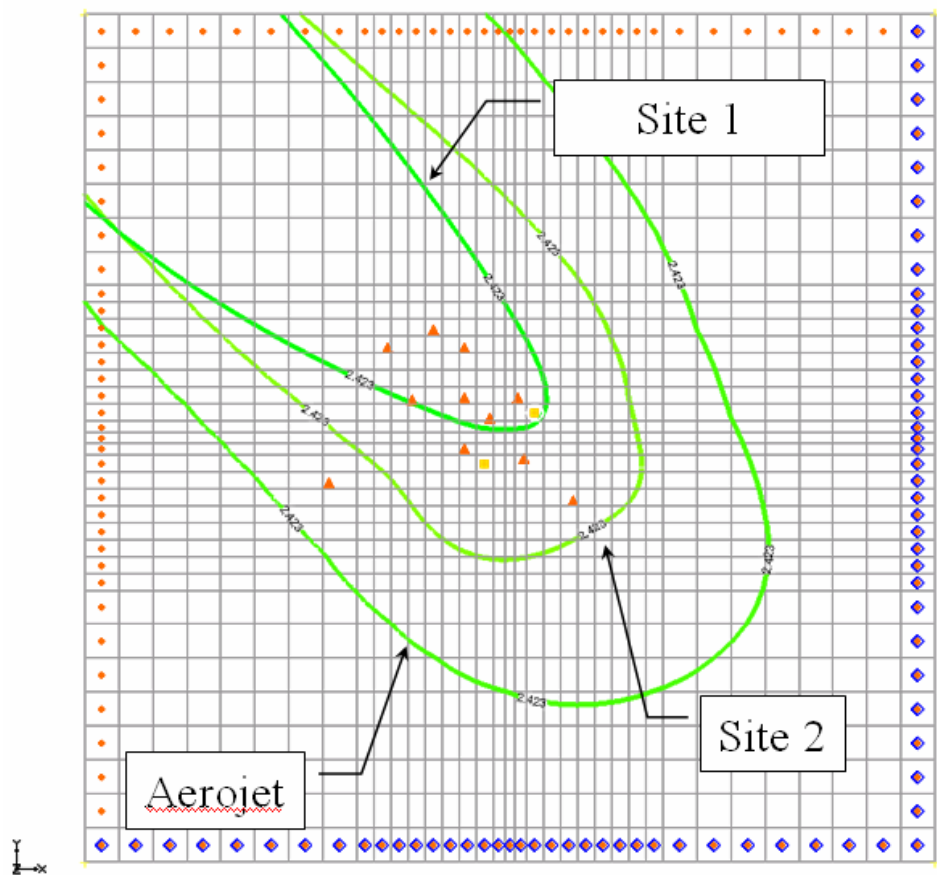


Figure 4.31 Perchlorate “Hole” (defined by 2.4 mg/L contour) at Layer 5 and Day 364

5.0 CONCLUSIONS

5.1 SUMMARY

In this thesis, data obtained from a field evaluation of an innovative technology that applied HFTWs to mix electron donor into perchlorate-contaminated groundwater to stimulate *in situ* biodegradation, were modeled. The first 113 days of field data were used to calibrate the technology model, and then the model was used to predict measured perchlorate concentrations, as well as the concentrations of competing electron acceptors, over the entire 761 days of the evaluation. The parameterized model was then used to simulate how well the technology would perform under various site conditions.

5.2 CONCLUSIONS

- **The technology model appears to simulate the overall behavior of perchlorate and competing electron acceptors at the Aerojet site.** The technology model successfully demonstrated that perchlorate reduction occurs at the site, although the accuracy of the model varies between the shallow and deep aquifers. Using the best-fit parameters obtained by calibrating the model to data measured over the initial period of the field evaluation, oxygen concentration predictions are improved over the predictions obtained using baseline parameter values, while little improvement was seen for model predictions of nitrate and perchlorate concentrations. In general, the model appears to overestimate performance of the HFTW system in the deep aquifer while underestimating its performance in the shallow aquifer. One possible reason for this may be the

accuracy with which the model simulates groundwater flow at the site. The flow model assumes steady-state and is based on fitting layer hydraulic conductivities to pump test results. It does not incorporate surface recharge or seasonal variations, and regional flow is assumed to be horizontal. These assumptions of the flow model may be the cause of the differences between measured and simulated perchlorate concentrations. In particular, the underprediction of perchlorate concentrations in the deep aquifer zones and overprediction in the shallow zones may be due to vertical (downward) flows that the model doesn't account for.

- **Specific parameters within the technology model have a greater effect on model results than others.** Sensitivity analyses indicated that the model was most sensitive to the k_{\max} parameter and insensitive to the K_i^{oxy} parameter. With k_{\max} having such a significant impact on the model results, it appears additional research is needed to measure k_{\max} more accurately. As the technology model proved insensitive to certain parameters (e.g. K_i^{oxy}), the dual-Monod assumption the model is based upon may need to be reevaluated to determine whether or not the technology model may be simplified to a simple Monod or first-order equation.
- **The technology is effective at locations with moderate levels of competing electron acceptors and low hydraulic conductivity.** Results indicated that at locations with a high hydraulic conductivity and no competing electron acceptors, the substrate either becomes too diluted or there's insufficient time to establish an effective bioactive zone within the area of interest. The model appeared to reduce

perchlorate to lower levels at the site with lower hydraulic conductivity and in the presence of competing electron acceptors.

- **A genetic algorithm that uses the RMSE of all the data as the objective function for calibration has the potential to overweight the fit of the model to measured concentration data of one electron acceptor at the expense of fitting data from the other acceptors.** By combining all model errors into one term, the genetic algorithm focused on an overall reduction in errors. Perhaps because of the way the dual-Monod multi-electron acceptor equations are structured, with oxygen's concentration impacting both nitrate and perchlorate reductions, oxygen appeared to be given additional weighting towards error reduction, so the calibrated model was better at fitting the oxygen data than the nitrate and perchlorate data.

5.3 RECOMMENDATIONS

- **Optimize the HFTW system.** Use the calibrated model from this field study to investigate how to engineer an optimized HFTW system. That is, determine the pumping rates, electron donor injection schedule and well configuration that would result in “best” (cheapest, most effective) system performance.
- **Refine the flow model.** As noted above, the flow model makes various assumptions that may result in the differences between measured and simulated perchlorate concentrations. A tracer test may be useful in better defining the flow model.

- **Modify model.** Sensitivity analyses from this study indicated that certain processes in the model, like inhibition from competing electron acceptors, may not significantly affect model results. Conversely, other processes not incorporated in this model (e.g. bioclogging) may significantly affect results. Further study and analysis of the field evaluation results are needed to contribute to model development.
- **Develop a calibration method that allows for better fitting of all the electron acceptor data simultaneously.** As noted in the conclusions, the objective function used in this study had the effect of overweighting the oxygen data at the expense of the nitrate and perchlorate data. The application of weighting factors or the development of a multi-objective optimization may improve the fit of model simulations to all data simultaneously.
- **Investigate whether genetic algorithm efficiency can be improved by limiting the number and range of parameters to be optimized.** As initially configured, the GA evaluated nine parameters over a wide range, using an inordinate amount of computer resources. Focusing the GA on the most important parameters (*e.g.* k_{\max}) over a more focused range of values may improve GA performance.

APPENDIX A: DETAILED DESCRIPTION OF THE PARR (2002) HORIZONTAL FLOW TREATMENT WELL (HFTW) TECHNOLOGY MODEL

A.1 INTRODUCTION

The technology model developed by Parr (2002) combined the biological treatment process modeled by the Envirogen dual-Monod multi-electron acceptor model coupled with the Huang and Goltz (1998) numerical HFTW model. The following is a detailed description of technology model as developed by Parr (2002). The technology model referenced previously is a combination of transport equations (A.1-A.4), the biological reaction equations (A.10-A.12) and the biomass growth equation (A.13)

A.2 FLOW AND TRANSPORT MODEL

The numerical flow and transport model used in this study is based on the model developed by Huang and Goltz to simulate aerobic biodegradation of trichlorethene in an HFTW system. It is a three-dimensional model that combines steady-state flow, advective/dispersive transport of dissolved species, equilibrium sorption, and biodegradation. The model assumes microorganisms are stationary, while oxygen, nitrate, perchlorate and the electron donor are affected by advection, dispersion, and in the case of the donor, sorption.

Equations A.1 - A.4 are the three-dimensional advection/dispersion equations used in the numerical model to describe transport of the donor and the three electron acceptors (oxygen, nitrate, and perchlorate).

$$\frac{\partial C^{\text{don}}}{\partial t} = D \cdot \nabla^2 C^{\text{don}} - \mathbf{v} \cdot \nabla C^{\text{don}} + r_{\text{don}} \quad (\text{A.1})$$

$$\frac{\partial C^{\text{oxy}}}{\partial t} = D \cdot \nabla^2 C^{\text{oxy}} - \mathbf{v} \cdot \nabla C^{\text{oxy}} + r_{\text{oxy}} \quad (\text{A.2})$$

$$\frac{\partial C^{\text{nit}}}{\partial t} = D \cdot \nabla^2 C^{\text{nit}} - \mathbf{v} \cdot \nabla C^{\text{nit}} + r_{\text{nit}} \quad (\text{A.3})$$

$$\frac{\partial C^{\text{per}}}{\partial t} = D \cdot \nabla^2 C^{\text{per}} - \mathbf{v} \cdot \nabla C^{\text{per}} + r_{\text{per}} \quad (\text{A.4})$$

Dispersion, which is not quantitatively important to this study, was modeled using numerical dispersion and is estimated in the x, y and z directions as

$$D_{x,y,z} = \frac{v_{x,y,z} \Delta(d_{x,y,z})}{2} + \frac{(v_{x,y,z})^2 \Delta t}{2} \quad (A.5)$$

The last term on the right hand side of Equations A.1 through A.4 are the sink terms for the biodegradation reactions. As applied to perchlorate remediation, the last term represent biodegradation as modeled using the dual-Monod multi-electron acceptor biological submodel described in the electron donor and electron acceptor sections.

A.3 ELECTRON DONOR

The rate of utilization of the electron donor is described below. The modified dual-Monod model attempts to simulate the effect of competition between multiple electron acceptors on donor and acceptor utilization, and microbial growth.

$$r_{\text{don}} = \frac{dC^{\text{don}}}{dt} = -X \cdot (r_{\text{don,oxy}} + r_{\text{don,nit}} + r_{\text{don,per}}) \quad (A.6)$$

Note that r_{don} is the rate of donor consumption (in units of donor mass per volume per time) in contrast to $r_{\text{don,oxy}}$, $r_{\text{don,nit}}$, and $r_{\text{don,per}}$, which are defined below as specific rates of donor utilization (in units of donor mass per biomass per time):

$$r_{\text{don,oxy}} = k_{\text{max}}^{\text{don/oxy}} \left[\frac{C^{\text{don}}}{K_s^{\text{don/oxy}} + C^{\text{don}}} \right] \cdot \left[\frac{C^{\text{oxy}}}{K_s^{\text{oxy}} + C^{\text{oxy}}} \right] \quad (A.7)$$

$$r_{\text{don,nit}} = k_{\text{max}}^{\text{don/nit}} \left[\frac{C^{\text{don}}}{K_s^{\text{don/nit}} + C^{\text{don}}} \right] \cdot \left[\frac{C^{\text{nit}}}{K_s^{\text{nit}} + C^{\text{per}}} \right] \cdot \left[\frac{K_i^{\text{oxy}}}{K_i^{\text{oxy}} + C^{\text{oxy}}} \right] \quad (A.8)$$

$$r_{\text{don,per}} = k_{\text{max}}^{\text{don/per}} \left[\frac{C^{\text{don}}}{K_s^{\text{don/per}} + C^{\text{don}}} \right] \cdot \left[\frac{C^{\text{per}}}{K_s^{\text{per}} + C^{\text{per}}} \right] \cdot \left[\frac{K_i^{\text{oxy}}}{K_i^{\text{oxy}} + C^{\text{oxy}}} \right] \cdot \left[\frac{K_i^{\text{nit}}}{K_i^{\text{nit}} + C^{\text{nit}}} \right] \quad (A.9)$$

A.4 ELECTRON ACCEPTORS

The rate of utilization of the electron acceptors is modeled below. It can be seen that these rates are directly linked to the rate of utilization of the donor through a factor (F), which is the stoichiometric yield coefficient for the electron donor-electron acceptor

reaction. Assuming $k_{\max} = k_{\max\text{don/per}} = k_{\max\text{don/nit}} = k_{\max\text{don/ox}}y$, and $K_s^{\text{don}} = K_s^{\text{don/per}} = K_s^{\text{don/nit}} = K_s^{\text{don/ox}}y$ the equations are as follows:

Oxygen

$$\begin{aligned} r_{\text{oxy}} &= \frac{dC^{\text{oxy}}}{dt} = -X \cdot (F_{\text{oxy}} \cdot r_{\text{don,ox}}y) \\ r_{\text{oxy}} &= \frac{dC^{\text{oxy}}}{dt} = -X \cdot F_{\text{oxy}} \cdot k_{\max} \left[\frac{C^{\text{don}}}{K_s^{\text{don}} + C^{\text{don}}} \right] \cdot \left[\frac{C^{\text{oxy}}}{K_s^{\text{oxy}} + C^{\text{oxy}}} \right] \end{aligned} \quad (\text{A.10})$$

Nitrate

$$\begin{aligned} r_{\text{nit}} &= \frac{dC^{\text{nit}}}{dt} = -X \cdot (F_{\text{nit}} \cdot r_{\text{don,nit}}) \\ r_{\text{nit}} &= \frac{dC^{\text{nit}}}{dt} = -X \cdot F_{\text{nit}} \cdot k_{\max} \left[\frac{C^{\text{don}}}{K_s^{\text{don}} + C^{\text{don}}} \right] \cdot \left[\frac{C^{\text{nit}}}{K_s^{\text{nit}} + C^{\text{nit}}} \right] \cdot \left[\frac{K_i^{\text{oxy}}}{K_i^{\text{oxy}} + C^{\text{oxy}}} \right] \end{aligned} \quad (\text{A.11})$$

Perchlorate

$$\begin{aligned} r_{\text{per}} &= \frac{dC^{\text{per}}}{dt} = -X \cdot (F_{\text{per}} \cdot r_{\text{don,per}}) \\ r_{\text{per}} &= \frac{dC^{\text{per}}}{dt} = -X \cdot F_{\text{per}} \cdot k_{\max} \left[\frac{C^{\text{don}}}{K_s^{\text{don}} + C^{\text{don}}} \right] \cdot \left[\frac{C^{\text{per}}}{K_s^{\text{per}} + C^{\text{per}}} \right] \cdot \left[\frac{K_i^{\text{oxy}}}{K_i^{\text{oxy}} + C^{\text{oxy}}} \right] \cdot \left[\frac{K_i^{\text{nit}}}{K_i^{\text{nit}} + C^{\text{nit}}} \right] \end{aligned} \quad (\text{A.12})$$

A.5 MICROBIAL GROWTH/DECAY

The microbial growth/decay equation utilized in the technology model is as follows:

$$\begin{aligned} \frac{dX}{dt} &= X \cdot [Y_{\text{biomass}} \cdot (r_{\text{don,ox}}y + r_{\text{don,nit}} + r_{\text{don,per}}) - b] \quad X > X_{\min} \\ \frac{dX}{dt} &= 0; \quad X \leq X_{\min} \end{aligned} \quad (\text{A.13})$$

Where $r_{\text{don,ox}}y$, $r_{\text{don,nit}}$ and $r_{\text{don,per}}$ are defined in equations A.7-A.9. Equation A.13 also incorporates a “switch” to keep the microbial population from completely dying off in areas where there is no electron donor or acceptor.

A.6 PARAMETER VALUES

Tables A.1 through A.3 represent the various kinetic, environmental and engineering parameters that Parr established (Parr, 2002).

Table A.1 Kinetic Parameters Used in Model Simulations (Parr, 2002)

Parameter	Baseline Value
k_{\max}	.21 mg donor/mg biomass/day
K_S^{don}	10.0 mg/L
K_S^{oxy}	10.0 mg/L
K_S^{nit}	15.0 mg/L
K_S^{per}	20.0 mg/L
K_i^{oxy}	10.0 mg/L
K_i^{nit}	15.0 mg/L
Y_{biomass}	.25 mg biomass/mg donor
F_{oxy}	0.83 mg oxygen/mg donor
F_{nit}	1.3 mg nitrate/mg donor
F_{per}	1.45 mg perchlorate/mg donor
b	0.01 1/day
X_{\min}	.01 mg/L

Table A.2 Environmental Parameters Used in Model Simulations (Parr, 2002)

Parameter	Baseline Value
Pore water velocity	0.279 m/day
Darcy velocity	0.0836 m/day
Horizontal hydraulic conductivity	7.6 m/day
Vertical hydraulic conductivity	0.38 m/day
Hydraulic gradient	0.011 m/m
Porosity	0.3

Table A.3 Engineering Parameters Used in Model Simulations (Parr, 2002)

Parameter	Baseline Value
Time-average electron donor concentration	600 mg/L
Donor injection pulse schedule	3 hrs on 5 hrs off
Well spacing	15 m
Well screen lengths	10 m
Pumping rate	100 m ³ /day
Well	15 m

A.7 DEFINITION OF TERMS

b	biomass decay rate (1/day)
C_{don}	concentration of the electron donor (mg/L)
C_{oxy}	concentration of the electron donor (an electron acceptor) (mg/L)
C_{nit}	concentration of the electron donor (an electron acceptor) (mg/L)
C_{per}	concentration of the electron donor (an electron acceptor) (mg/L)
$D_{x,y,z}$	dispersion in the x, y and z directions
$d_{x,y,z}$	cell size in the x, y and z directions
F_{oxy}	stoichiometric coefficient for the donor-oxygen reaction (mg oxygen/mg donor)
F_{nit}	stoichiometric coefficient for the donor-nitrate reaction (mg oxygen/mg donor)
F_{per}	stoichiometric coefficient for the donor-perchlorate reaction (mg oxygen/mg donor)
K_i^{oxy}	oxygen inhibition coefficient (mg/L)
K_i^{nit}	nitrate inhibition coefficient (mg/L)
k_{max}	maximum specific rate of substrate utilization (mg donor/mg biomass/day)

$k_{\text{maxdon/oxy}}$	maximum specific rate of substrate utilization in the presence of oxygen when donor concentration is varied and limiting (mg donor/mg biomass/day)
$k_{\text{maxdon/nit}}$	maximum specific rate of substrate utilization in the presence of nitrate when donor concentration is varied and limiting (mg donor/mg biomass/day)
$k_{\text{maxdon/per}}$	maximum specific rate of substrate utilization in the presence of perchlorate when donor concentration is varied and limiting (mg donor/mg biomass/day)
$K_S^{\text{don/oxy}}$	half saturation concentration of the electron donor in the presence of oxygen when donor (xxxxx) concentration is varied and limited (mg donor/L)
$K_S^{\text{don/nit}}$	half saturation concentration of the electron donor in the presence of nitrate when donor (xxxxx) concentration is varied and limited (mg donor/L)
$K_S^{\text{don/per}}$	half saturation concentration of the electron donor in the presence of perchlorate when donor (xxxxx) concentration is varied and limited (mg donor/L)
K_S^{oxy}	half saturation concentration when oxygen (an electron acceptor) concentration is varied and limited (mg/L)
K_S^{nit}	half saturation concentration when nitrate (an electron acceptor) concentration is varied and limited (mg/L)
K_S^{per}	half saturation concentration when perchlorate (an electron acceptor) concentration is varied and limited (mg/L)
r_{don}	rate of electron donor consumption (mg donor/L/day)
$r_{\text{don,oxy}}$	specific rate of electron donor consumption using oxygen as an electron acceptor (mg donor/mg biomass/day)
$r_{\text{don,nit}}$	specific rate of electron donor consumption using nitrate as an electron acceptor (mg donor/mg biomass/day)
$r_{\text{don,per}}$	specific rate of electron donor consumption using perchlorate as an electron acceptor (mg donor/mg biomass/day)
r_{oxy}	rate of oxygen consumption (mg oxygen/L/day)

r_{nit}	rate of nitrate consumption (mg nitrate/L/day)
r_{per}	rate of perchlorate consumption (mg perchlorate/L/day)
t	time (days)
$v_{x,y,z}$	groundwater velocity in the x, y and z directions
X	concentration of active biomass (mg/L)
X_{min}	minimum concentration level of active biomass (mg/L)
Y_{biomass}	the biomass yield per mass of donor consumed (mg biomass/mg electron donor)

APPENDIX B: MONITORING WELL BREAKTHROUGH GRAPHS

This Appendix includes graphs showing all oxygen, nitrate, and perchlorate concentration data observed at all monitoring wells. In addition, model simulations utilizing the baseline Aerojet parameters and the best-fit parameters determined by calibration with the GA are shown on the graphs. Baseline and best-fit parameters are available in Table 4.2. The simulations using the best-fit parameter values are indicated on the graphs by the lines labeled “Simulated (calibrated)”.

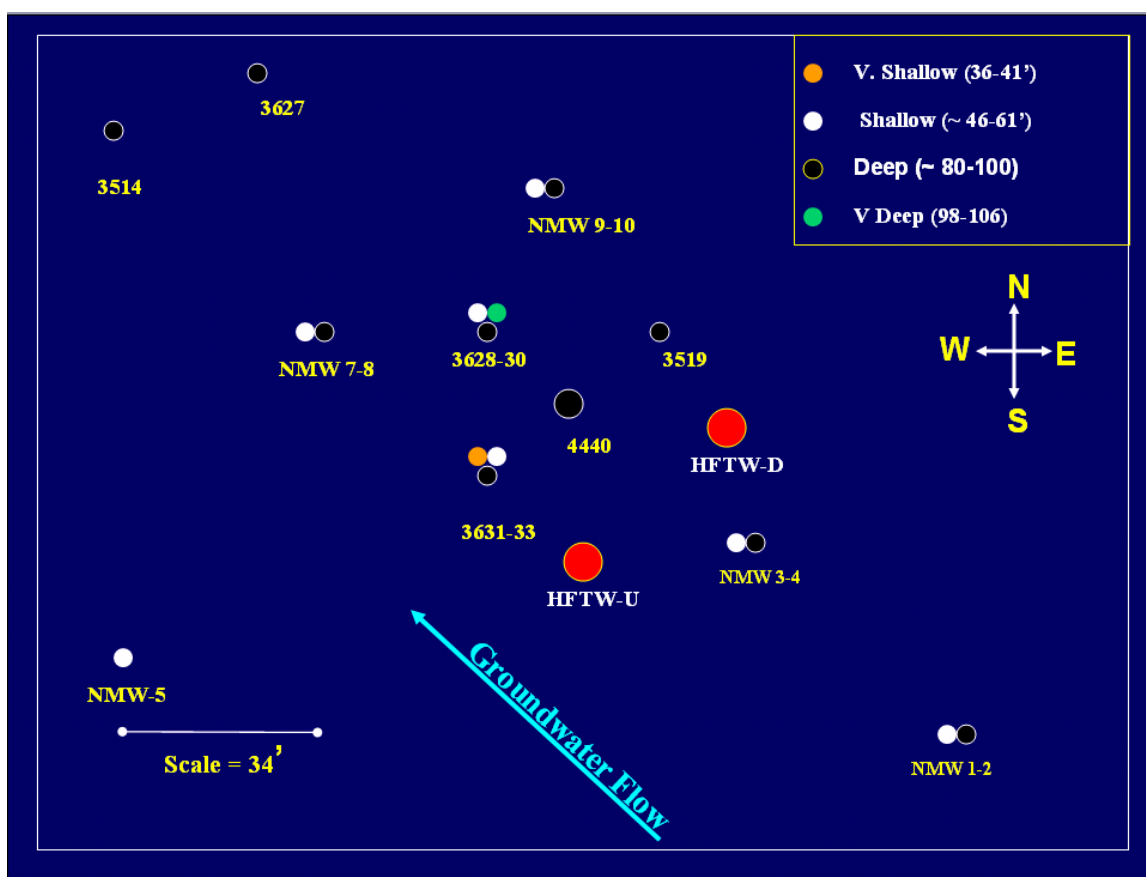


Figure B.1 Aerojet HFTW and Monitoring Well Site Layout

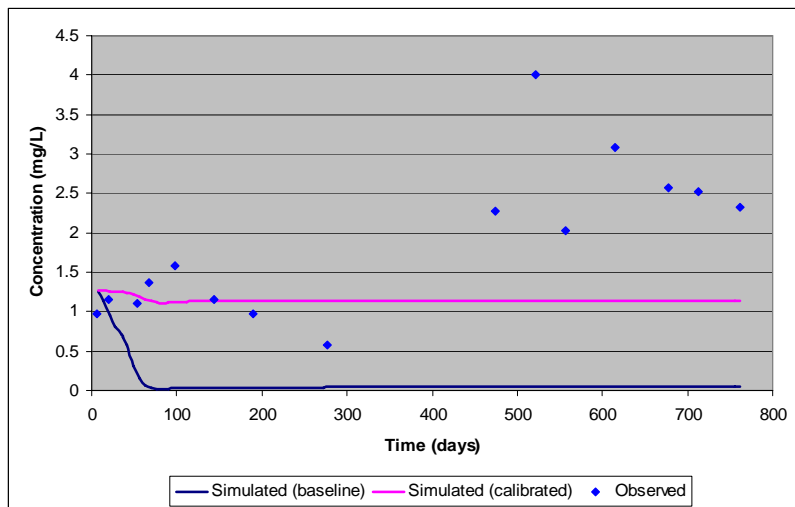


Figure B.2 NMW1 Oxygen Breakthrough

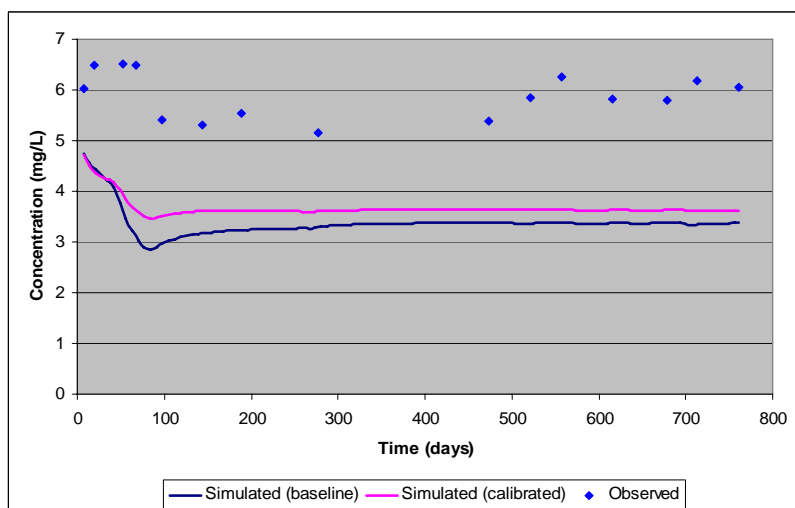


Figure B.3 NMW1 Nitrate Breakthrough

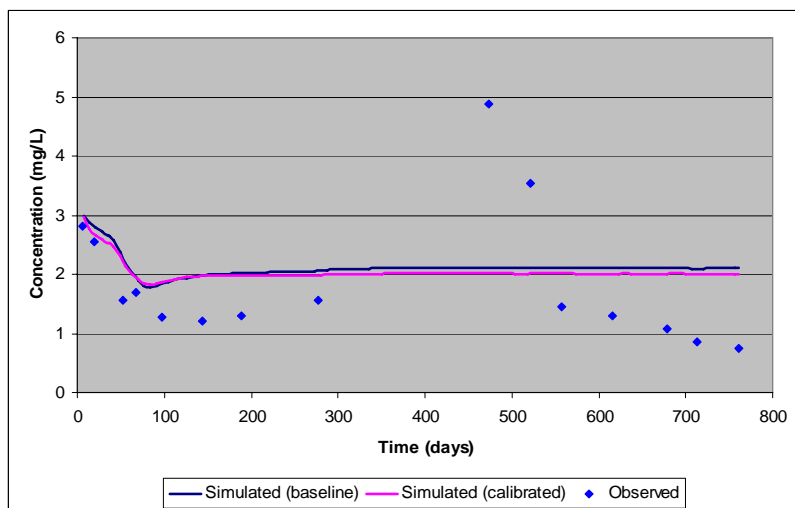


Figure B.4 NMW1 Perchlorate Breakthrough

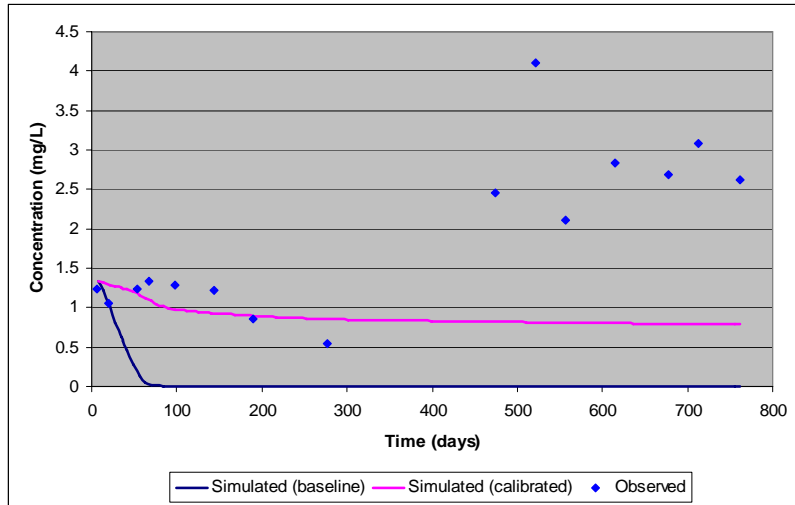


Figure B.5 NMW2 Oxygen Breakthrough

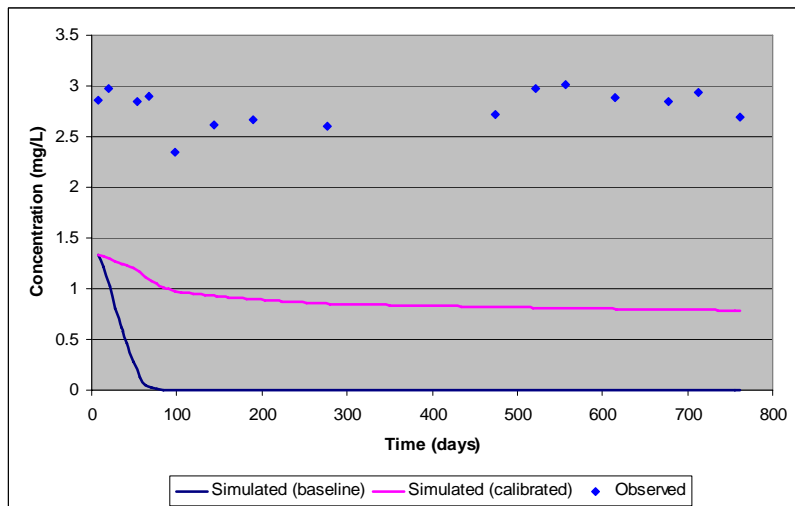


Figure B.6 NMW2 Nitrate Breakthrough

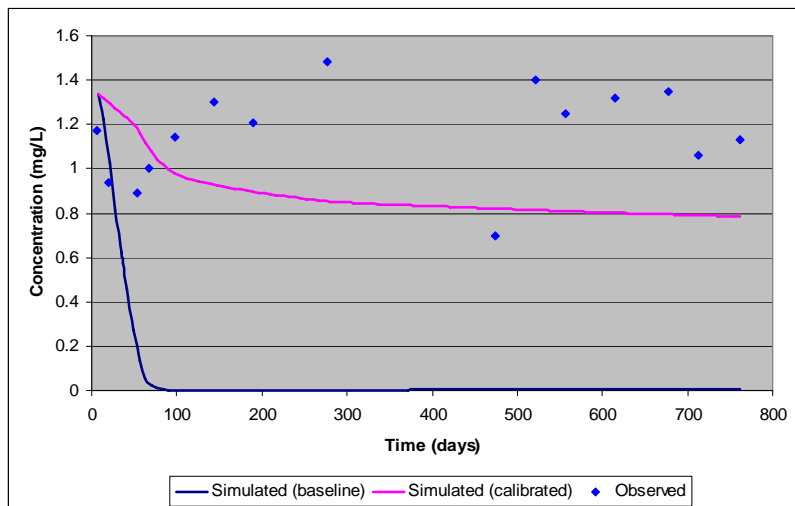


Figure B.7 NMW2 Perchlorate Breakthrough

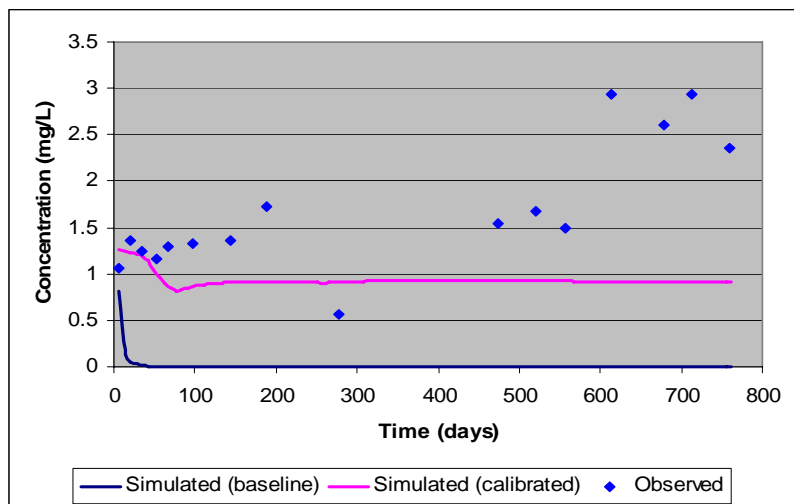


Figure B.8 NMW3 Oxygen Breakthrough

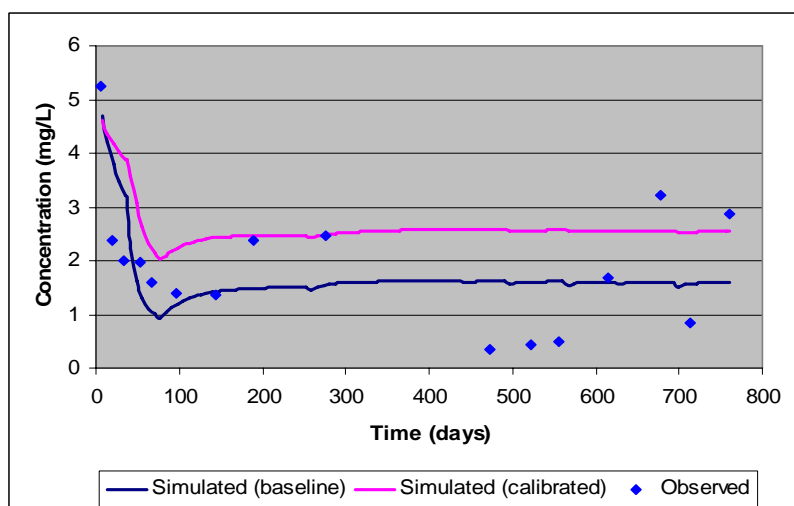


Figure B.9 NMW3 Nitrate Breakthrough

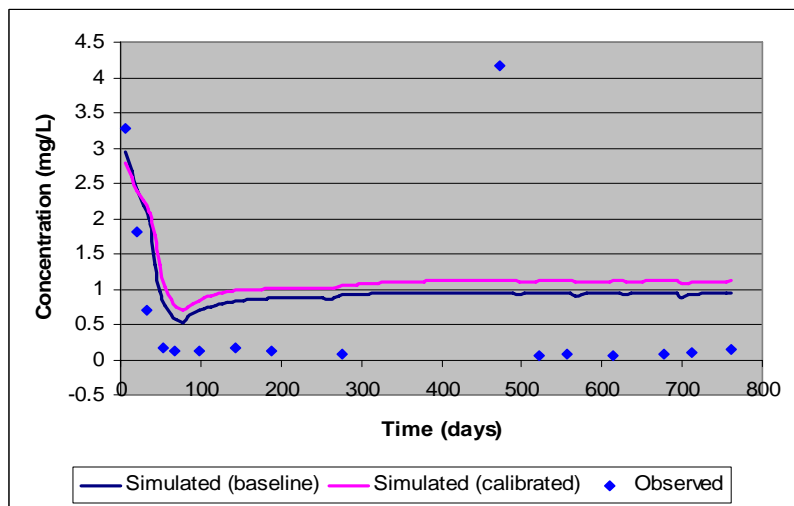


Figure B.10 NMW3 Perchlorate Breakthrough

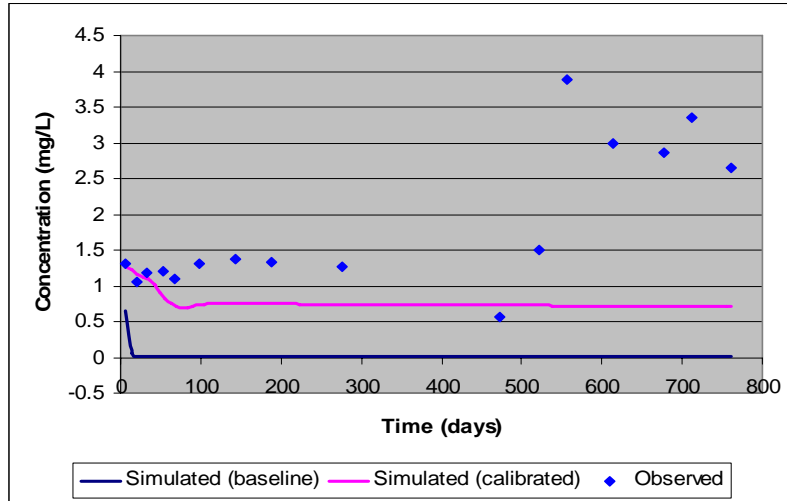


Figure B.11 NMW4 Oxygen Breakthrough

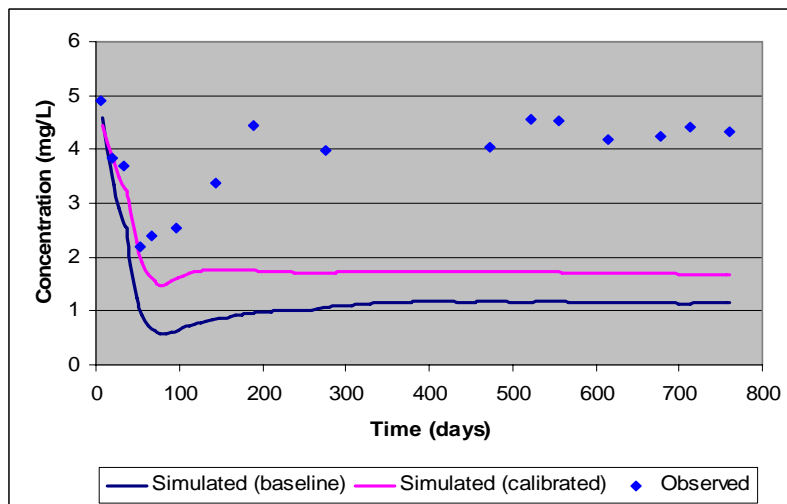


Figure B.12 NMW4 Nitrate Breakthrough

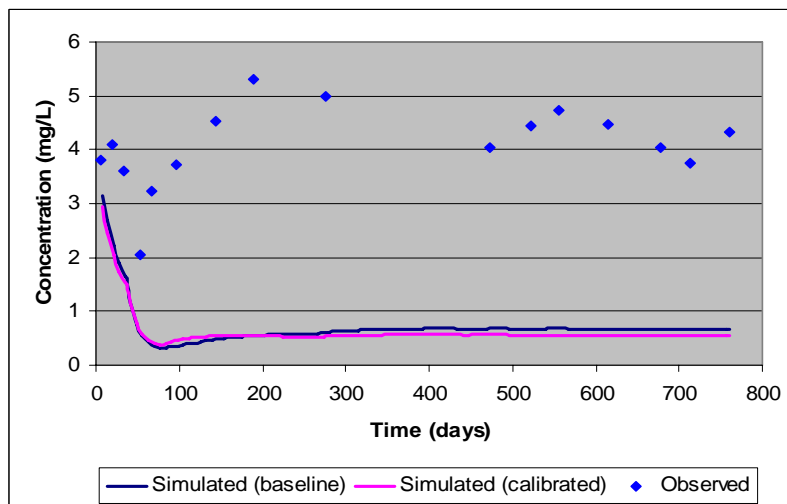


Figure B.13 NMW4 Perchlorate Breakthrough

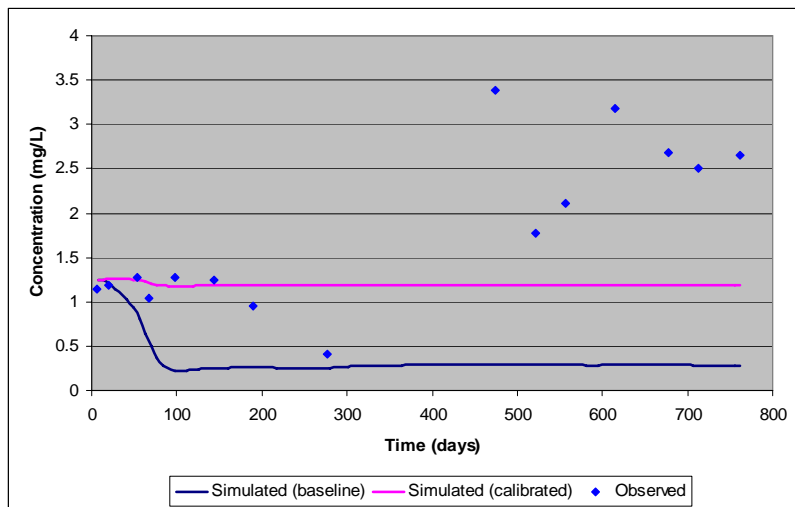


Figure B.14 NMW5 Oxygen Breakthrough

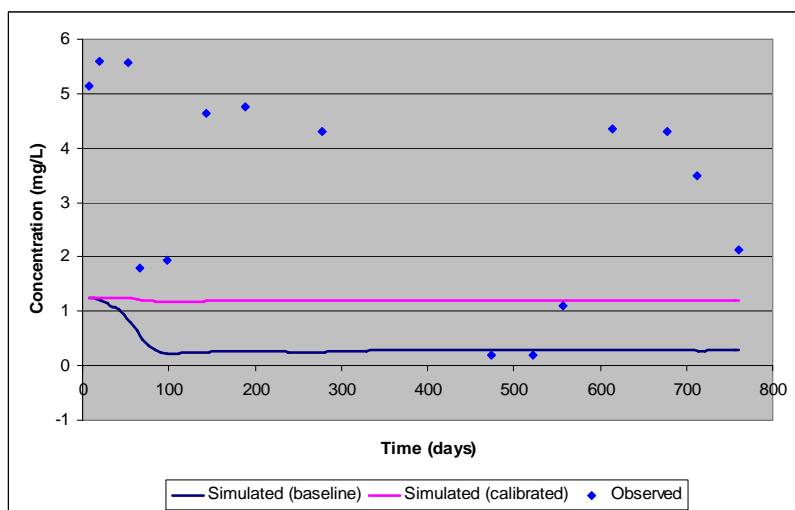


Figure B.15 NMW5 Nitrate Breakthrough

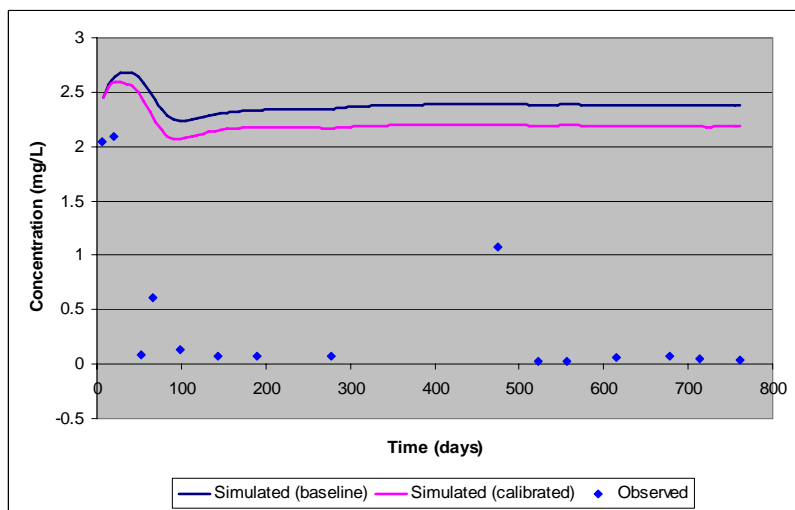


Figure B.16 NMW5 Perchlorate Breakthrough

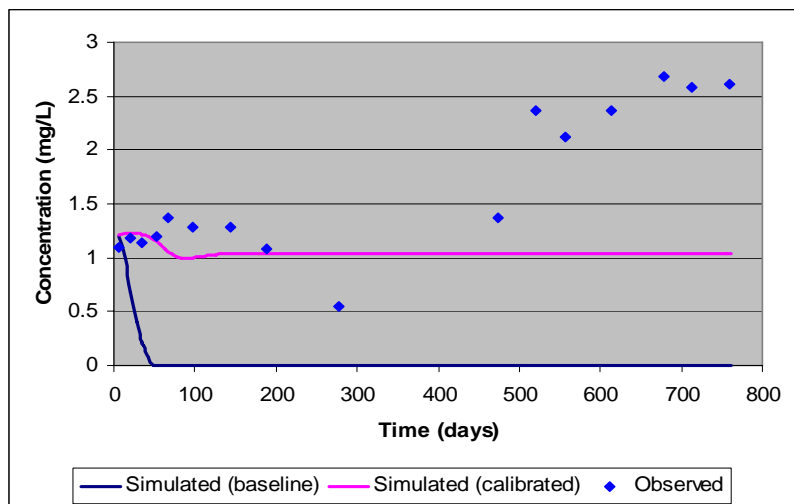


Figure B.17 NMW7 Oxygen Breakthrough

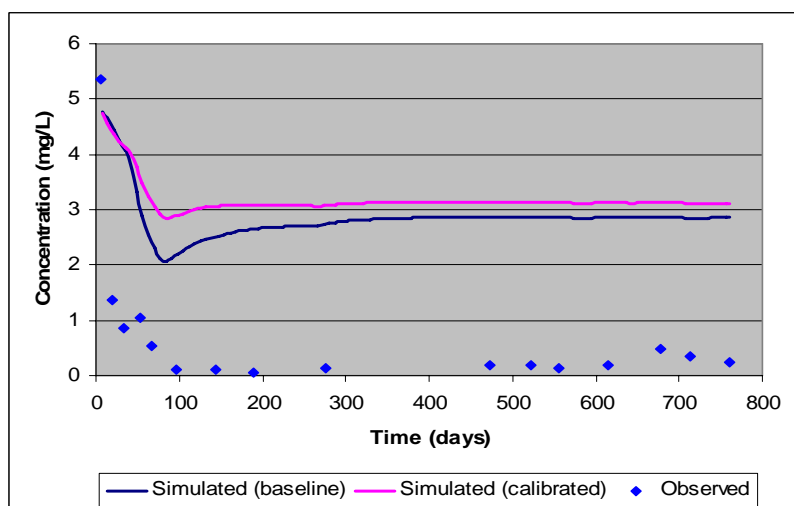


Figure B.18 NMW7 Nitrate Breakthrough

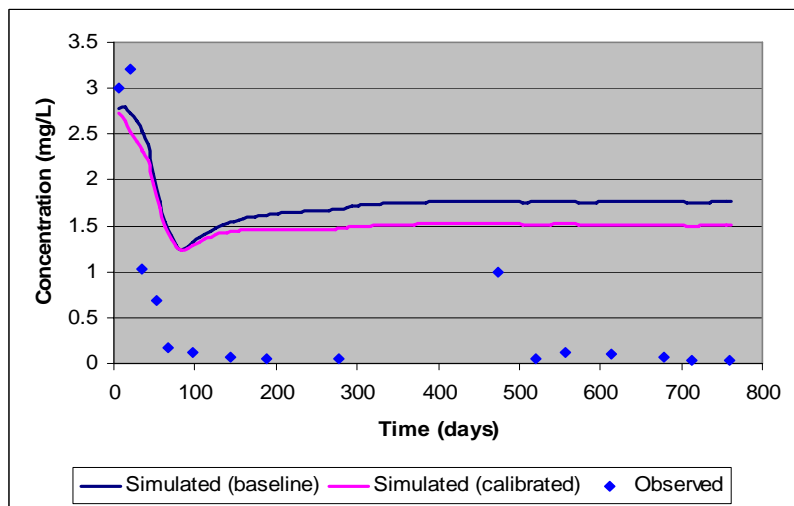


Figure B.19 NMW7 Perchlorate Breakthrough

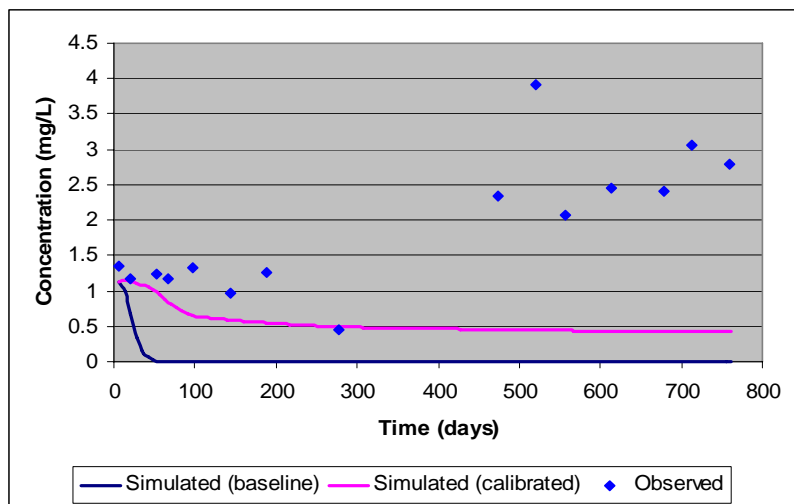


Figure B.20 NMW8 Oxygen Breakthrough

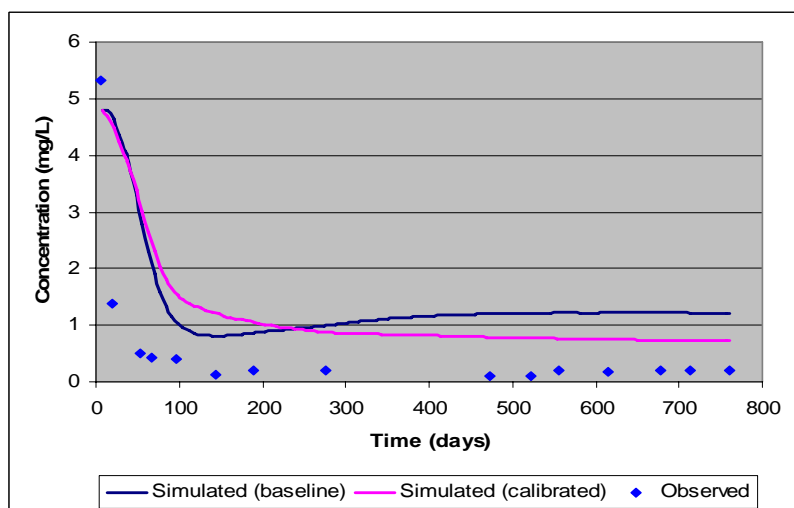


Figure B.21 NMW8 Nitrate Breakthrough

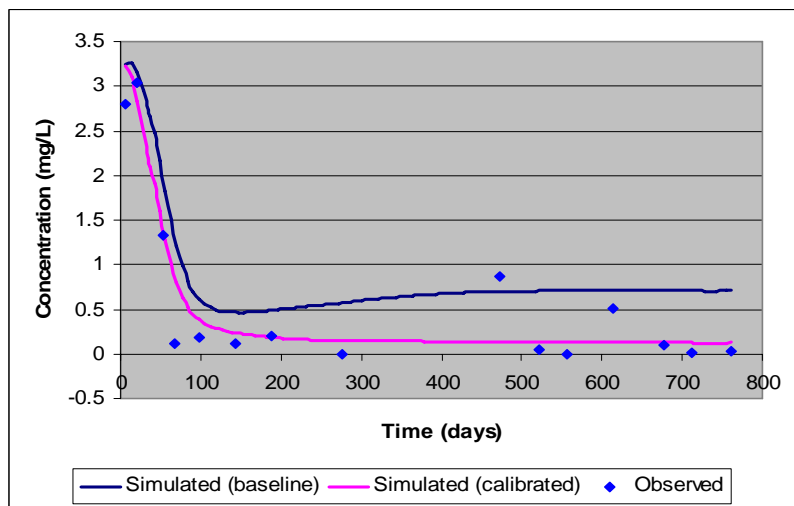


Figure B.22 NMW8 Perchlorate Breakthrough

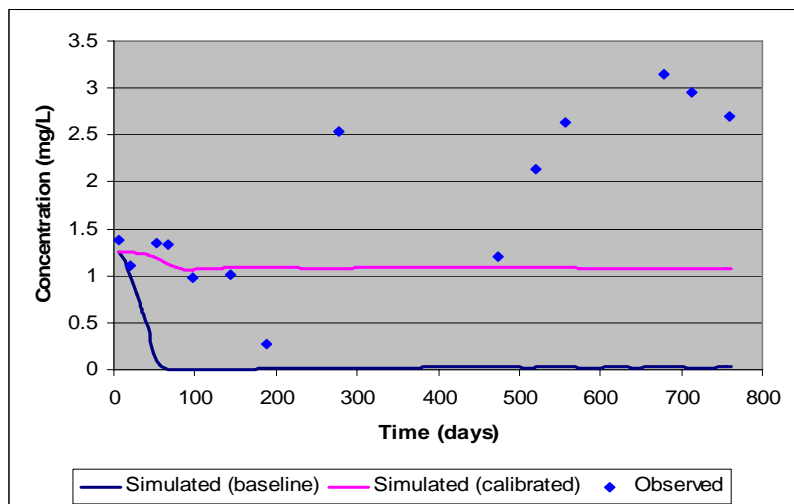


Figure B.23 NMW9 Oxygen Breakthrough

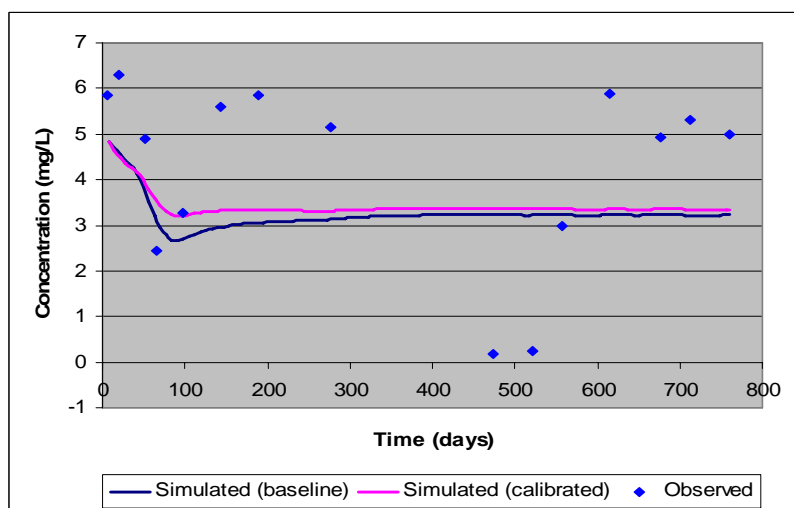


Figure B.24 NMW9 Nitrate Breakthrough

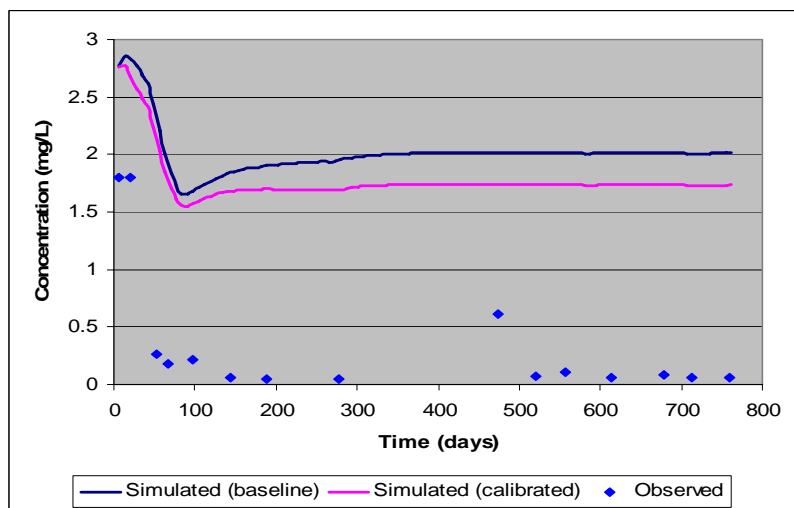


Figure B.25 NMW9 Perchlorate Breakthrough

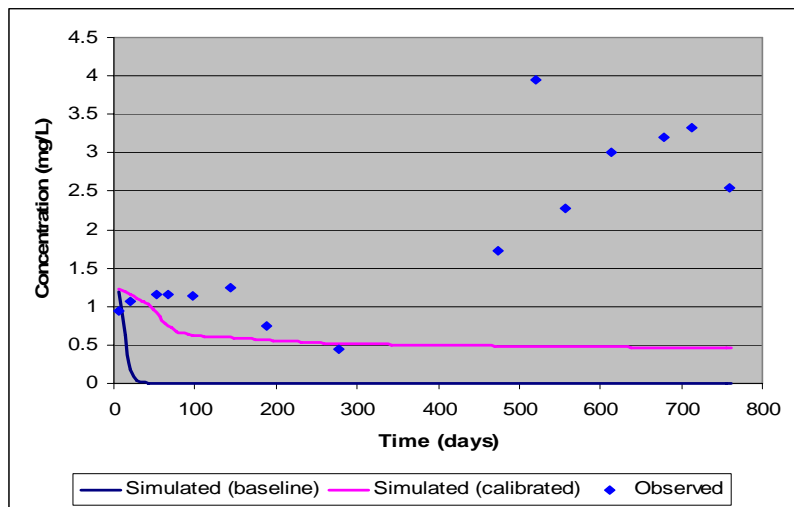


Figure B.26 NMW10 Oxygen Breakthrough

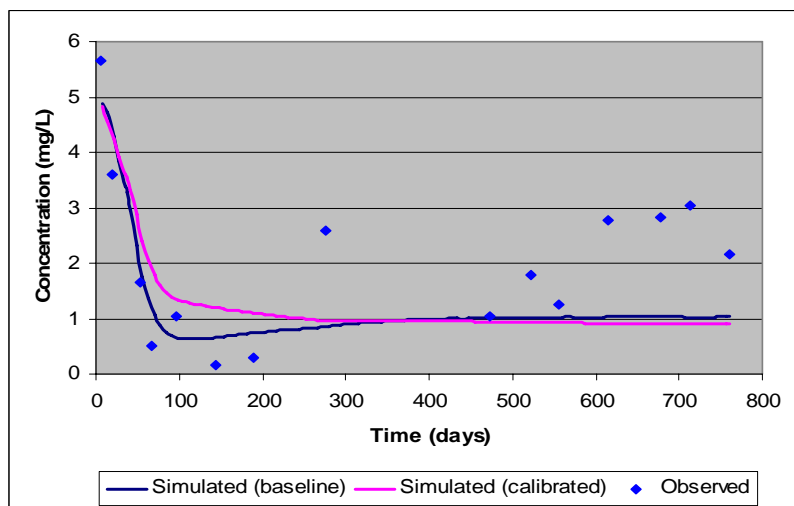


Figure B.27 NMW10 Nitrate Breakthrough

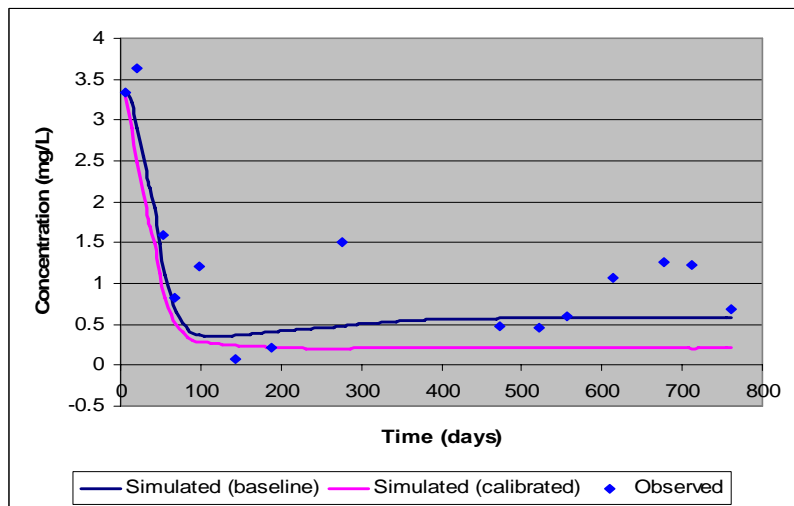


Figure B.28 NMW10 Perchlorate Breakthrough

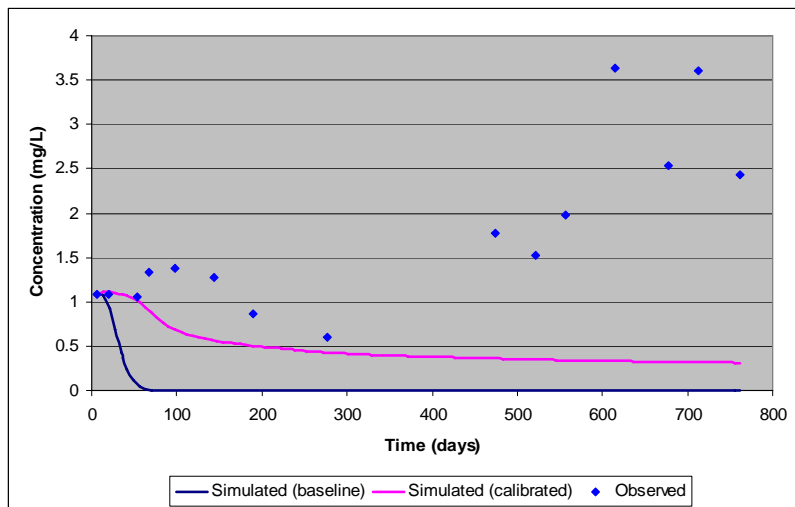


Figure B.29 3514 Oxygen Breakthrough

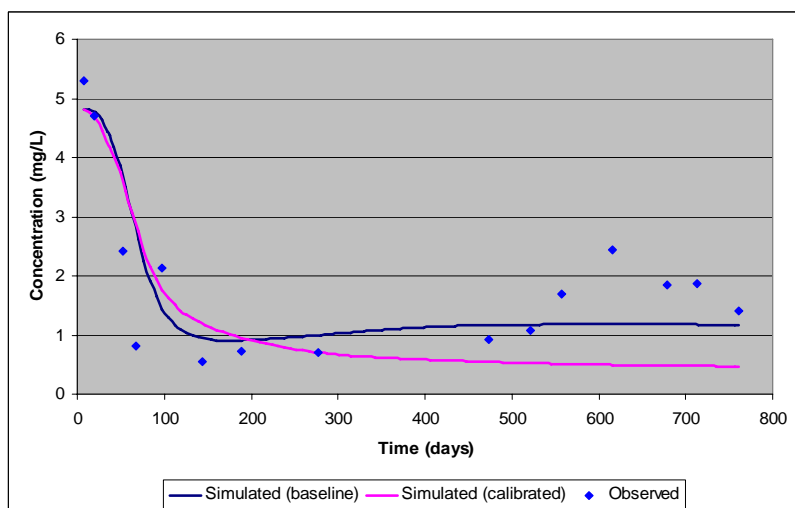


Figure B.30 3514 Nitrate Breakthrough

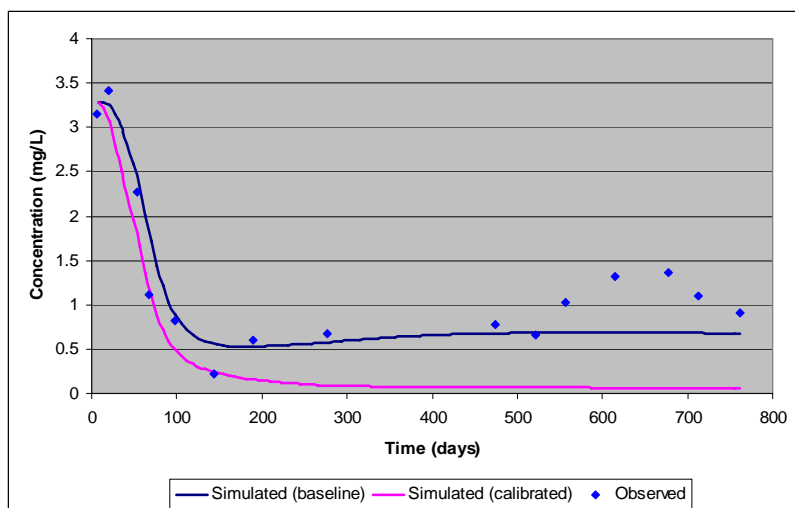


Figure B.31 3514 Perchlorate Breakthrough

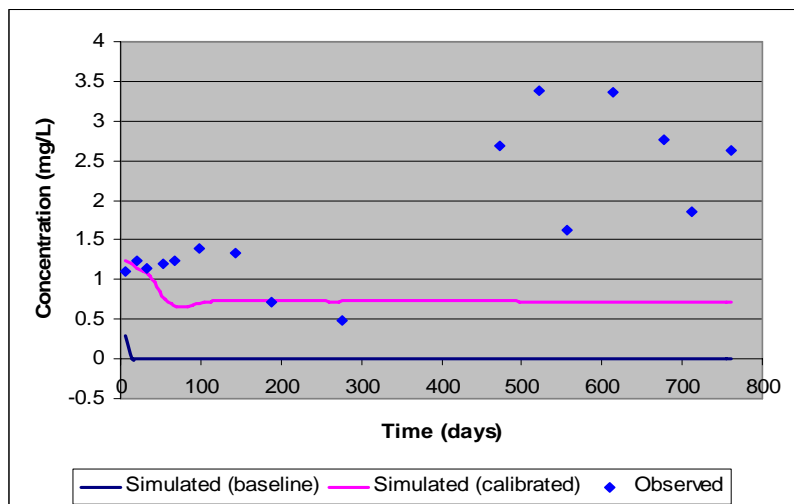


Figure B.32 3519 Oxygen Breakthrough

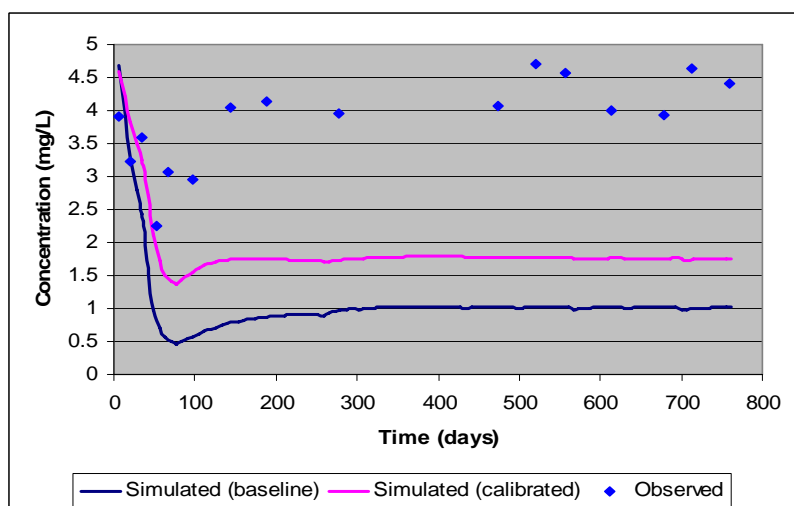


Figure B.33 3519 Nitrate Breakthrough

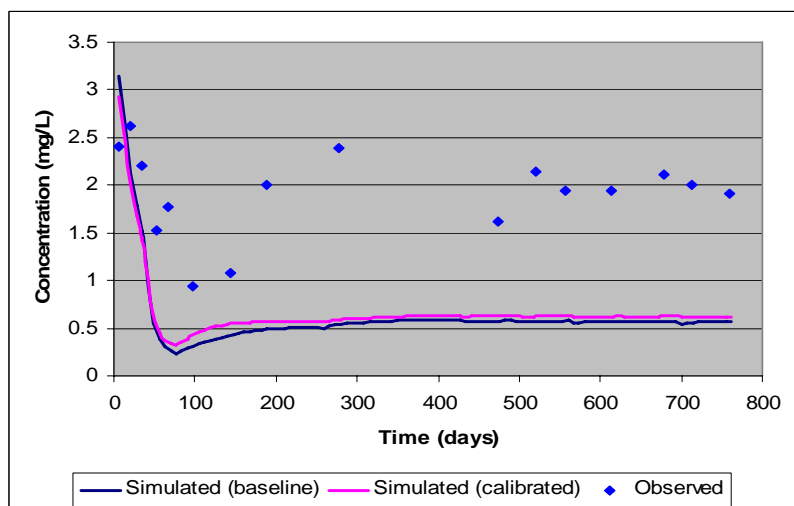


Figure B.34 3519 Perchlorate Breakthrough

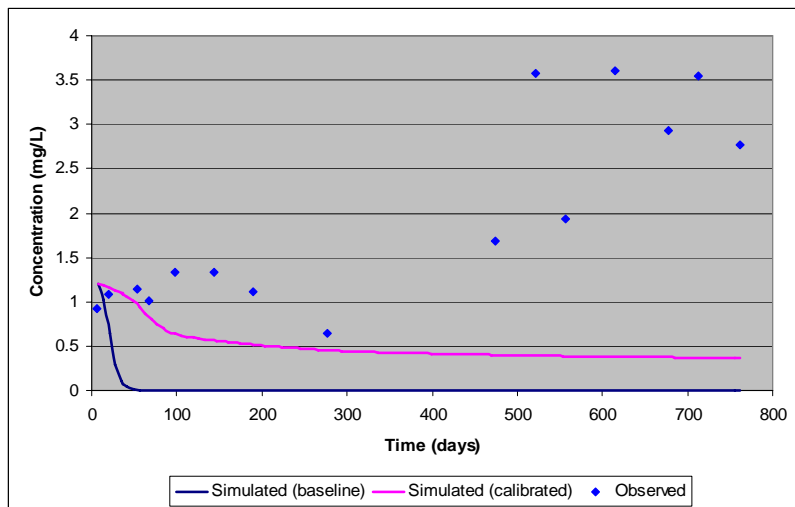


Figure B.35 3627 Oxygen Breakthrough

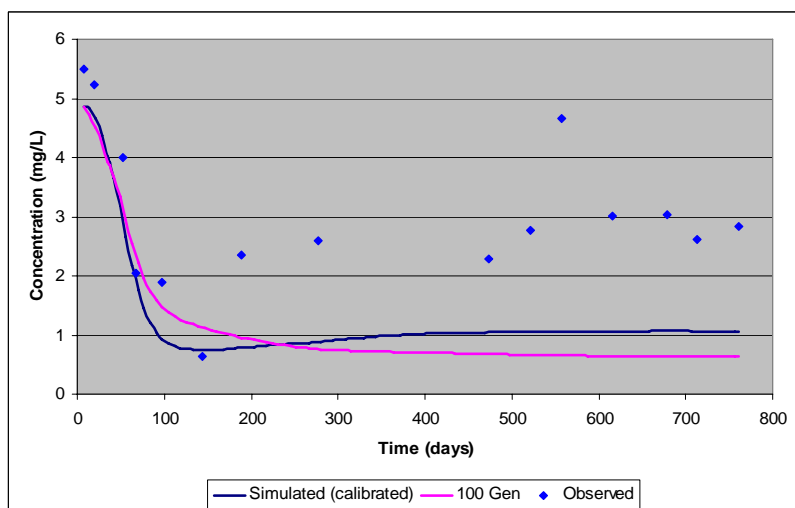


Figure B.36 3627 Nitrate Breakthrough

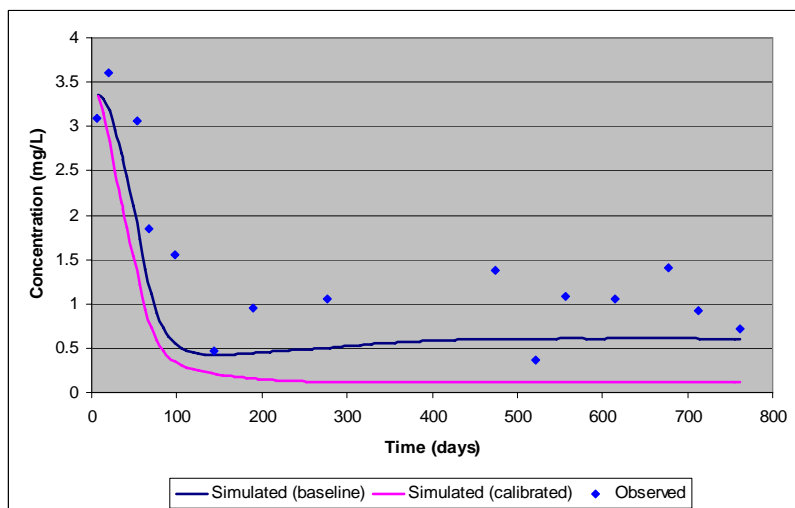


Figure B.37 3627 Perchlorate Breakthrough

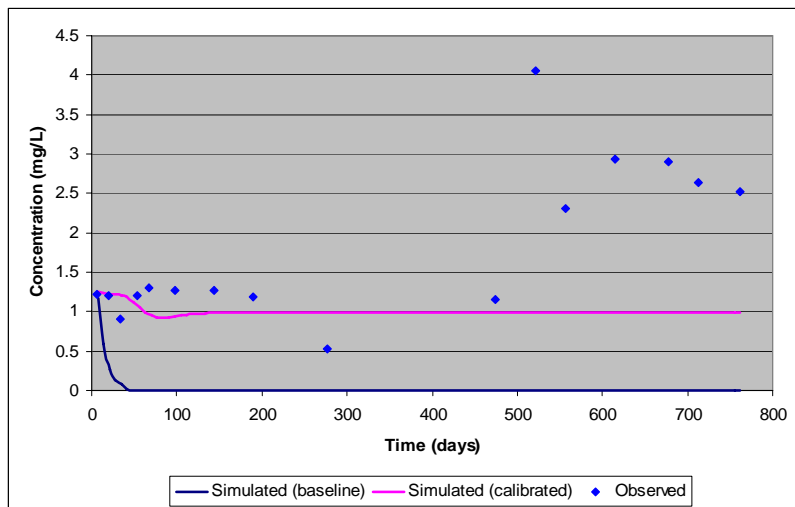


Figure B.38 3628 Oxygen Breakthrough

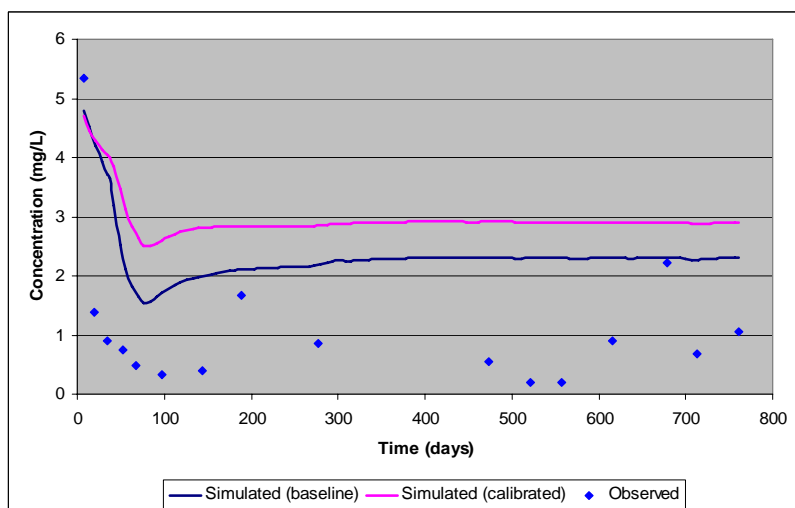


Figure B.39 3628 Nitrate Breakthrough

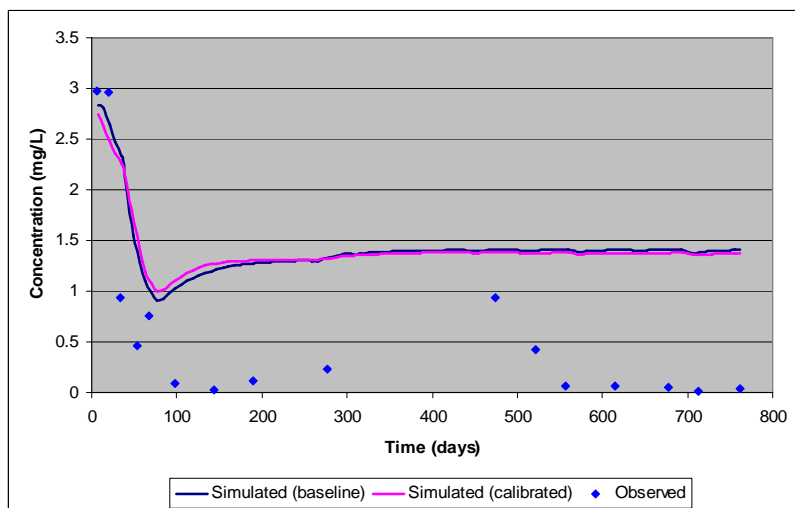


Figure B.40 3628 Perchlorate Breakthrough

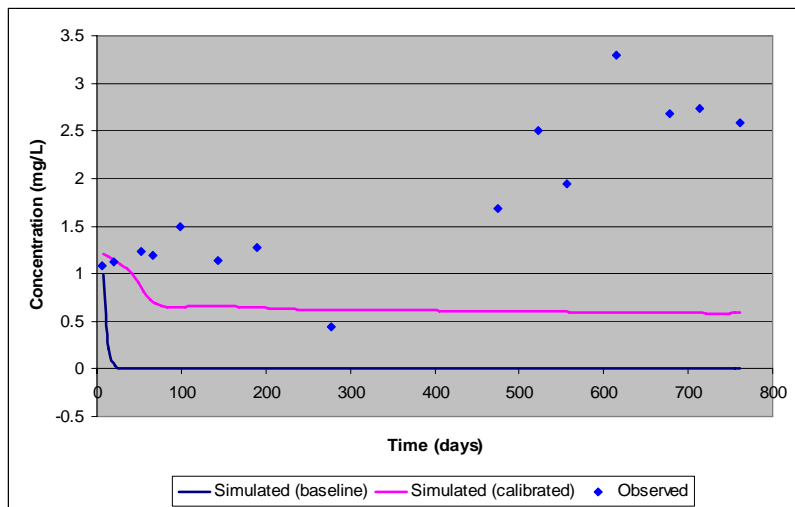


Figure B.41 3629 Oxygen Breakthrough

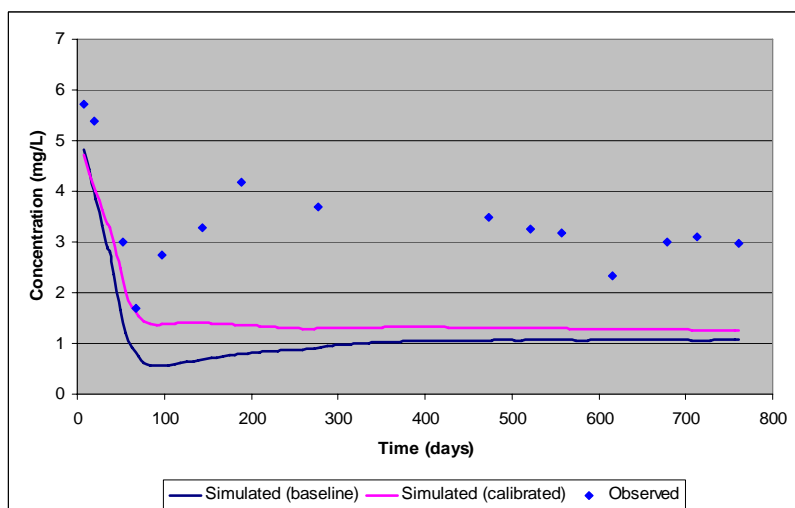


Figure B.42 3629 Nitrate Breakthrough

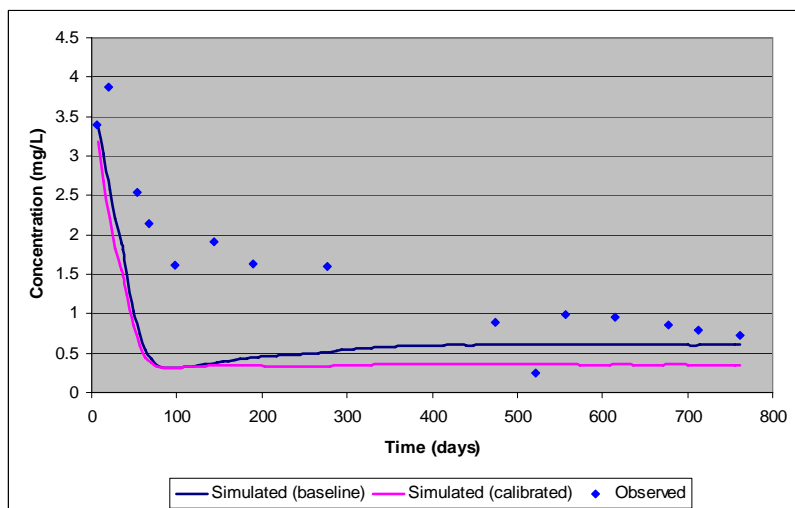


Figure B.43 3629 Perchlorate Breakthrough

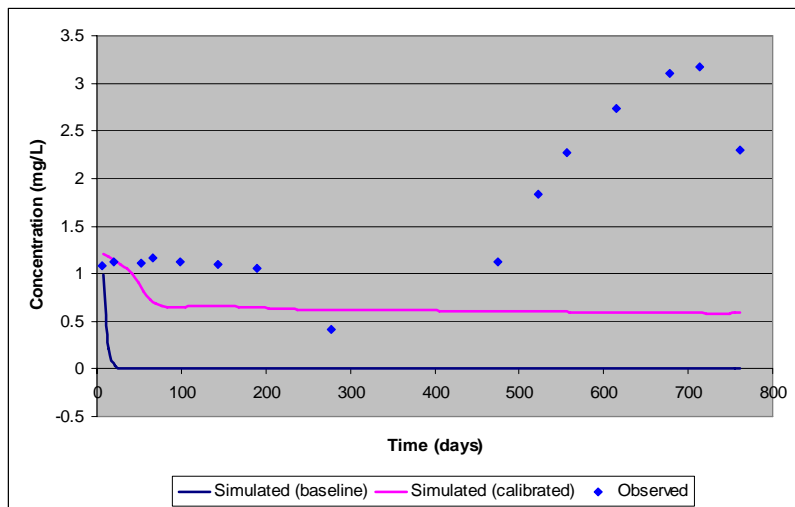


Figure B.44 3630 Oxygen Breakthrough

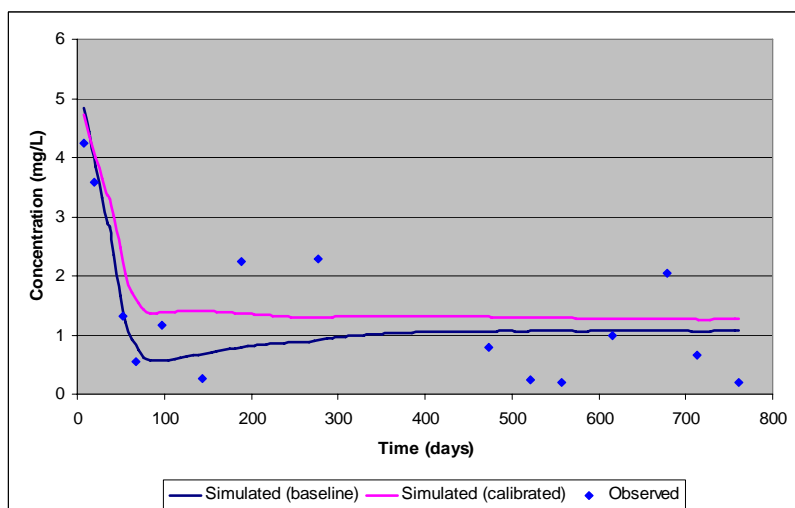


Figure B.45 3630 Nitrate Breakthrough

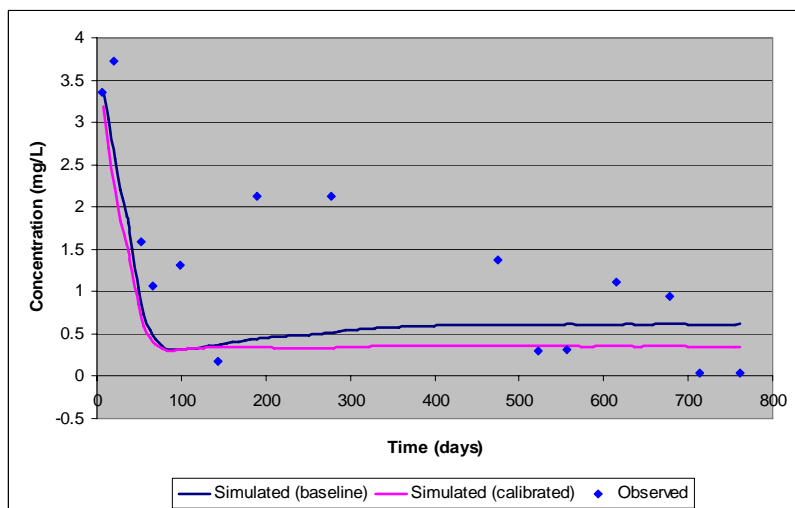


Figure B.46 3630 Perchlorate Breakthrough

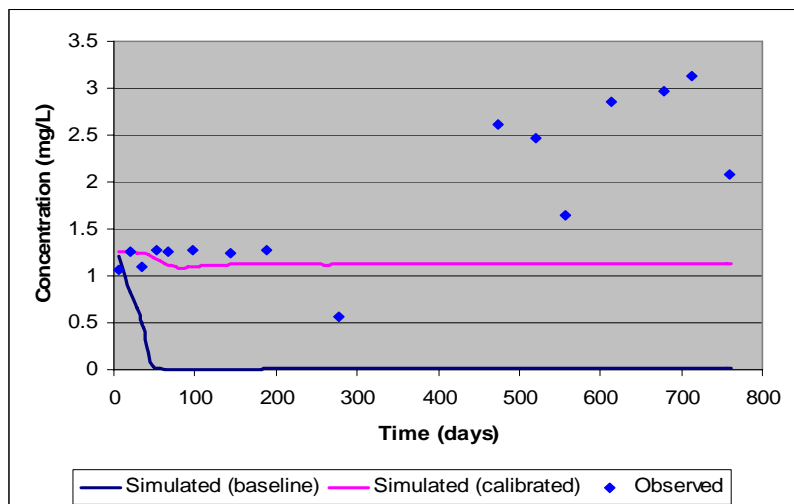


Figure B.47 3631 Oxygen Breakthrough

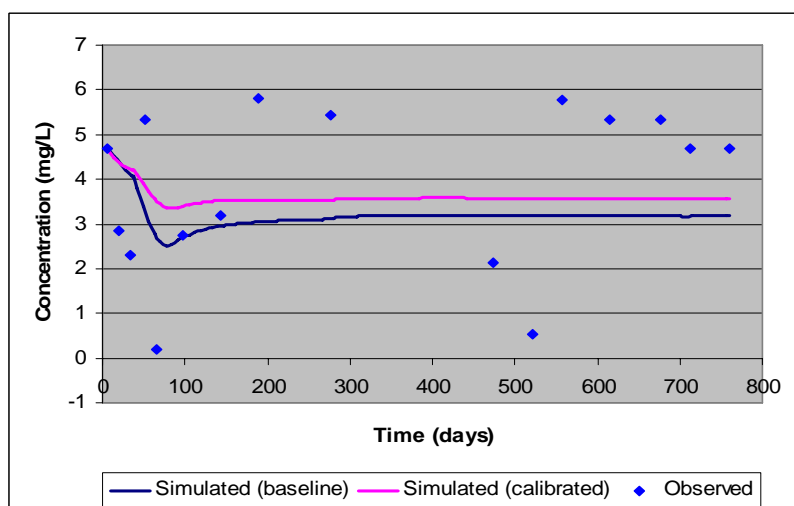


Figure B.48 3631 Nitrate Breakthrough

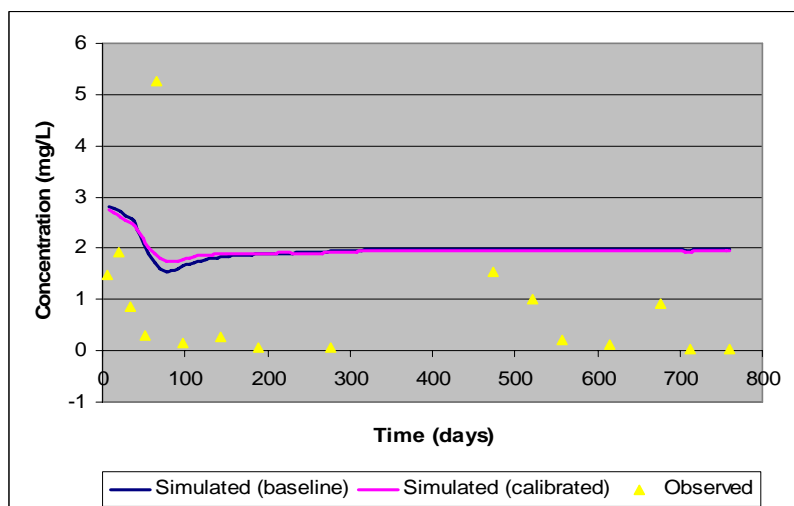


Figure B.49 3631 Perchlorate Breakthrough

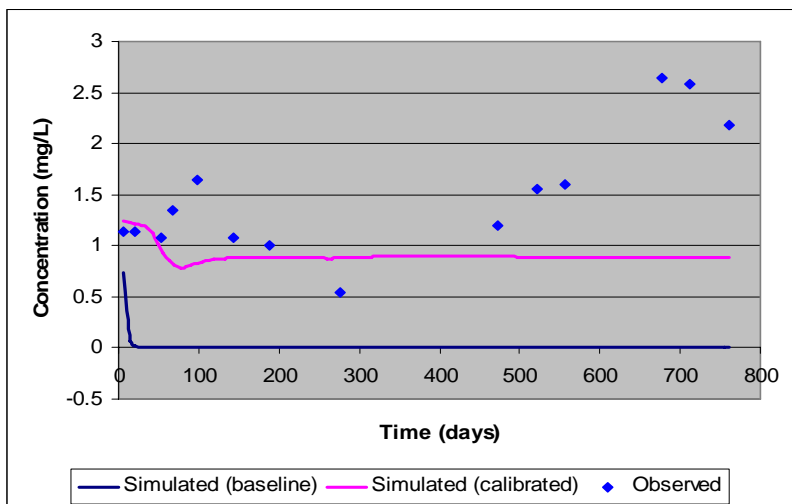


Figure B.50 3632 Oxygen Breakthrough

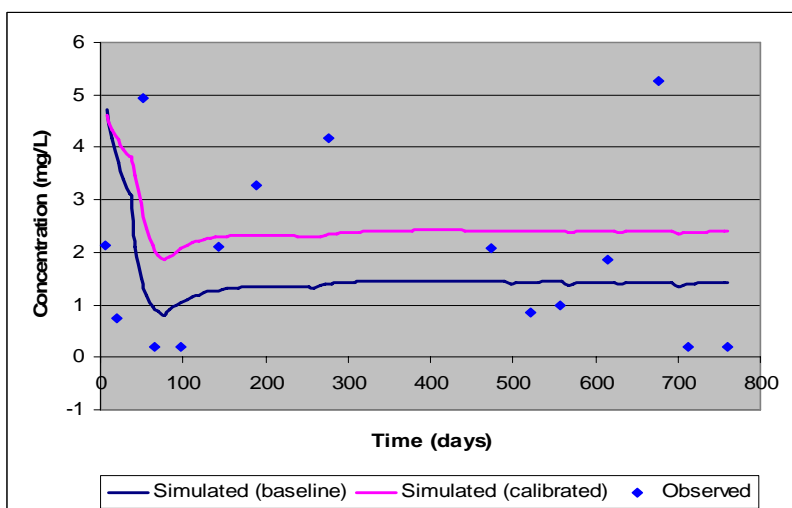


Figure B.51 3632 Nitrate Breakthrough

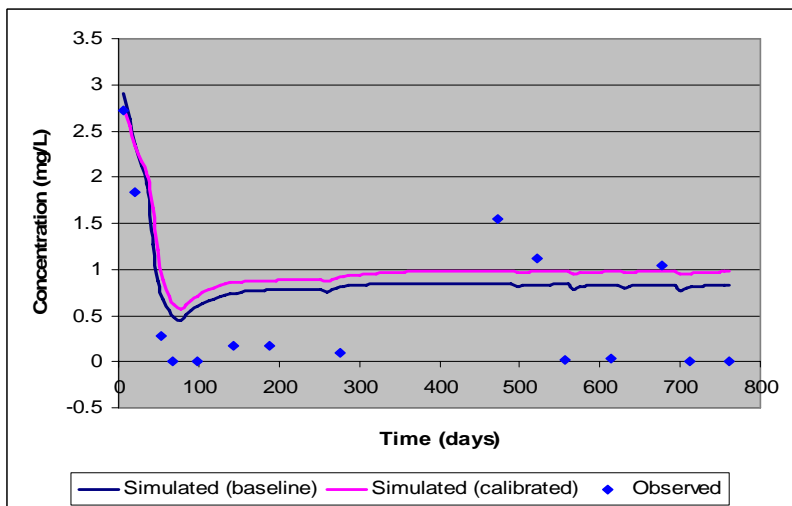


Figure B.52 3632 Perchlorate Breakthrough

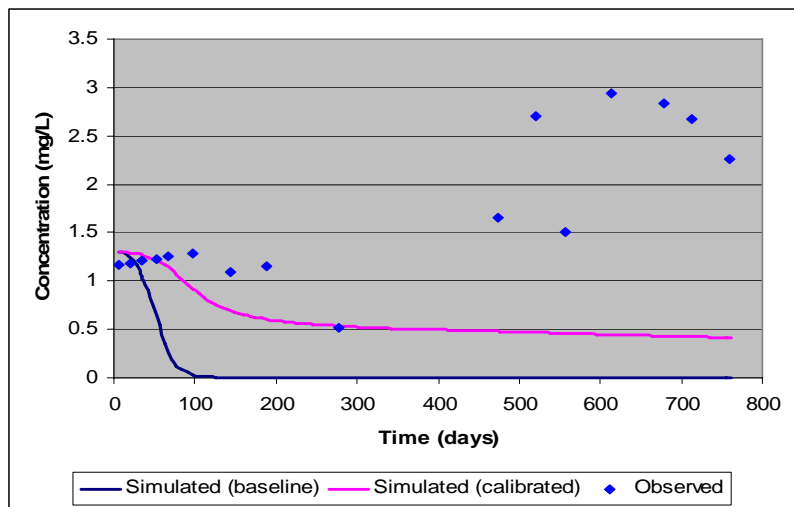


Figure B.53 3633 Oxygen Breakthrough

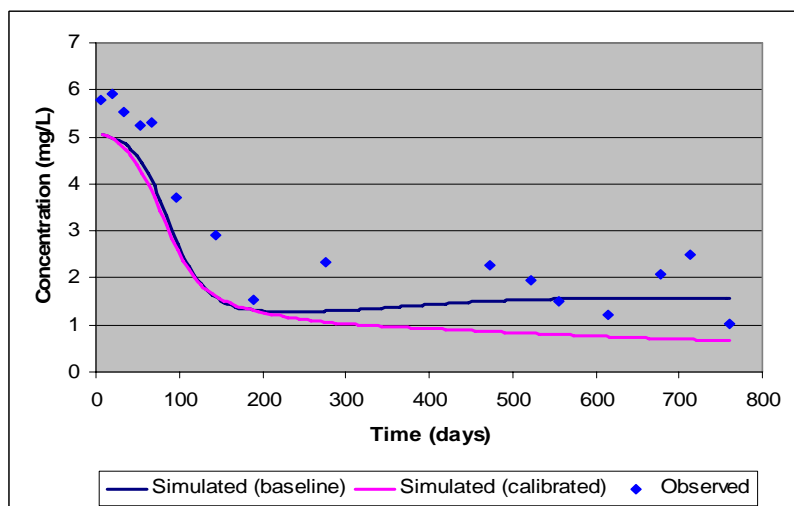


Figure B.54 3633 Nitrate Breakthrough

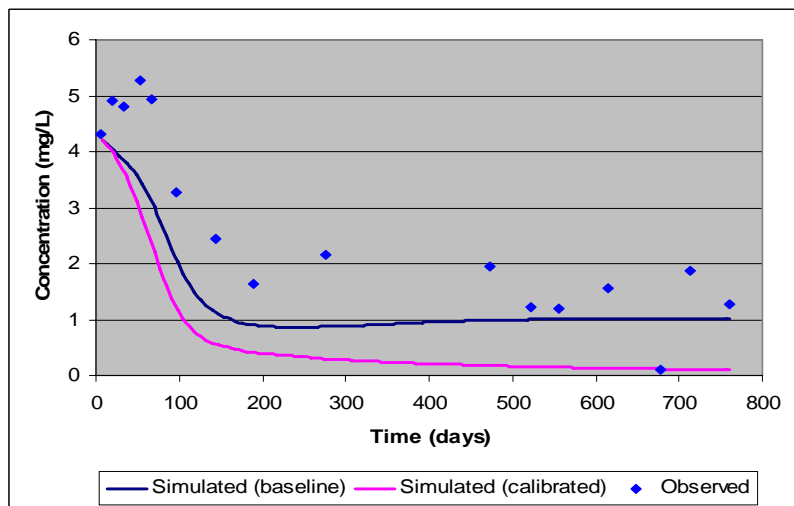


Figure B.55 3633 Perchlorate Breakthrough

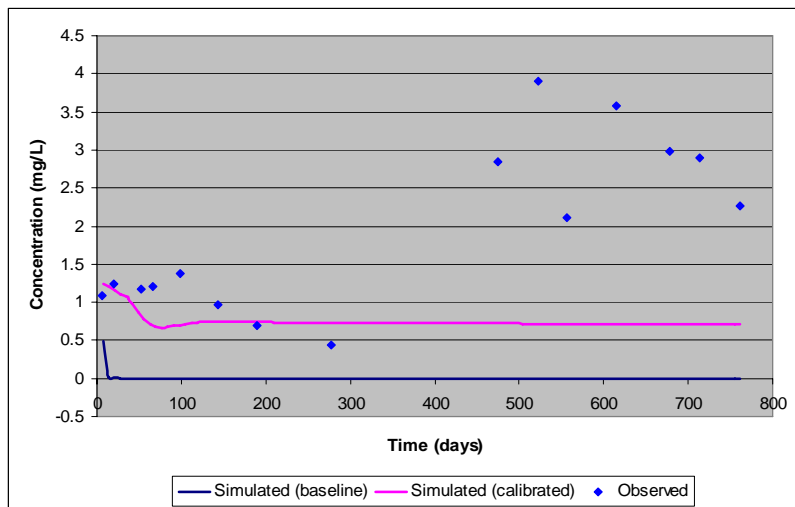


Figure B.56 4440 Oxygen Breakthrough

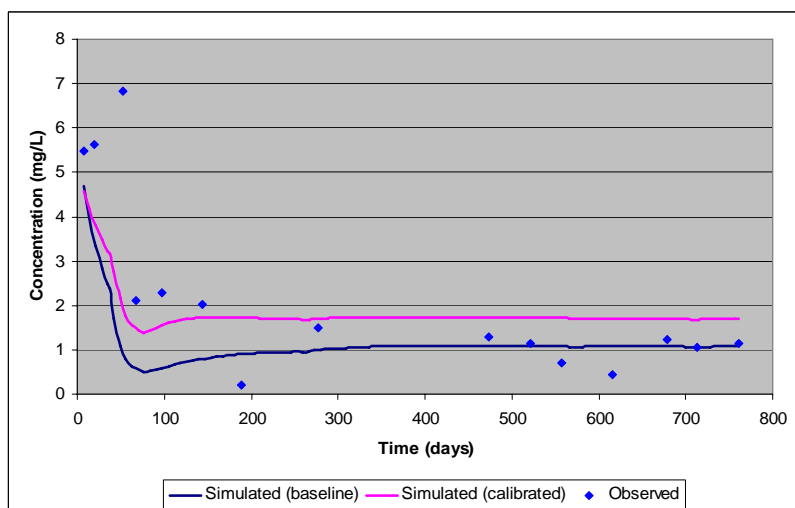


Figure B.57 4440 Nitrate Breakthrough

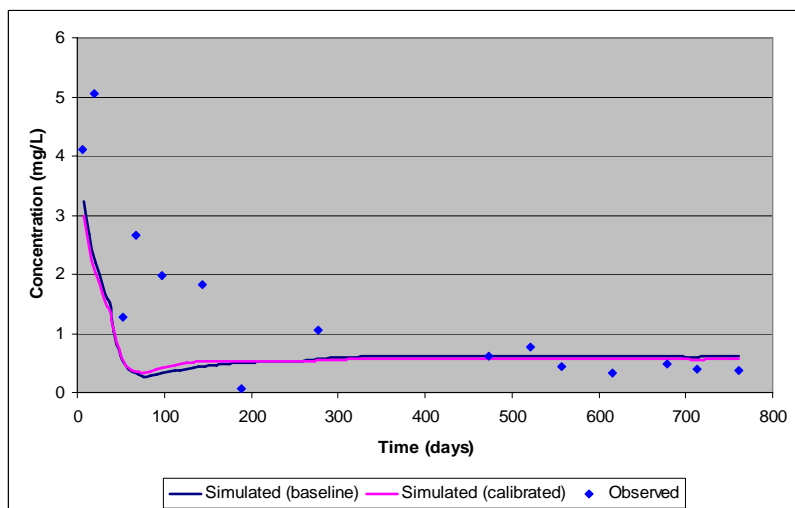


Figure B.58 4440 Perchlorate Breakthrough

BIBLIOGRAPHY

- Air Force Center for Environmental Excellence (AFCEE), 2006. "Perchlorate Treatment Technology Fact Sheet: *In situ* Anaerobic Bioremediation." August, 2006.
- Arizona Department of Environmental Quality (ADEQ), Arizona Department of Health Services (ADHS). Arizona Department of Water Resources (ADWR), Arizona Department of Agriculture (ADA). Perchlorate in Arizona: Occurrence Study of 2004. December, 2004.
- Bäck T. Evolutionary Computing. *Evolutionary Computation 1: Basic Algorithms and Operators*. Institute of Physics Publishing. Bristol and Philadelphia, PA. 2000.
- Brandhuber P, Clark S. Perchlorate Occurrence Mapping. Prepared for the American Water Works Association. Denver, CO: HDR Engineering. 2004.
- California Department of Health Services (CDHS). Perchlorate in California Drinking Water: Overview and Links. Department of Health Services, Sacramento, California. 2007.
<http://www.dhs.ca.gov/ps/ddwem/chemicals/perchl/perchlindex.htm>
- Chosa, P.G. Modeling a Field Application of *In situ* Bioremediation of Perchlorate-Contaminated Groundwater Using Horizontal Flow Treatment Wells (HFTWs). MS Thesis, AFIT/GEM/ENV/04M-05, 2004. School of Engineering and Management, Air Force Institute of Technology, (AU), Wright-Patterson AFB, OH. March 2004.
- Christ, J. A., M.N. Goltz, and Huang J., Development and Application of an Analytical Model to Aid Design and Implementation of *In situ* Remediation Technologies, *Journal of Contaminant Hydrology*, 37(3): 295-317, 1999.
- Clement, T. P. "A modular computer model for simulating reactive multi-species transport in three-dimensional ground water systems." Pacific Northwest National Laboratory, PNNL-SA-11720. Richland WA: PNNL. 1997.
- Coates, J.D., Michaelidou, U., O'Connor, S.M., Bruce, R.A., and Achenbach, L.A. The diverse microbiology of (per)chlorate reduction. In E.T. Urbansky, Ed., Perchlorate in the Environment. New York: Kluwer Academic/Plenum Publishers, pp. 257–270. 2000.
- Collopy, F. and Armstrong, J. S. "Error Measures For Generalizing About Forecasting Methods: Empirical Comparisons", *International Journal of Forecasting*, 8, 69-80, 1992.

- Cox, E.E., Edwards, E., and Neville, S. *In situ* Bioremediation of Perchlorate in Groundwater, *Perchlorate in the Environment*. Ed. Urbansky, E. T.; Kluwer Academic/Plenum Publishers, New York, 2000.
- Cunningham, J.A., Hoelen, T.P., Hopkins, G.D., LeBron, C.A., Reinhard, M. Hydraulics of recirculating well pairs for ground water remediation. *Ground Water*. 42 (6), 880–889. 2004.
- Eiben A.E. and Smith J.E. *Introduction to Evolutionary Computing*. New York : Springer, 2003.
- Envirogen. *In situ* Bioremediation of Perchlorate. SERDP project CY-1136 Final Report. 21 May, 2002.
- Environmental Modeling Systems, Inc. (EMS-I). GMS 6.0 Overview. 2007.
http://www.ems-i.com/GMS/GMS_Overview/gms_overview.html
- Environmental Security Technology Certification Program (ESTCP). *In situ* Bioremediation of Perchlorate Using Horizontal Flow Treatment Wells: ESTCP Technology Demonstration Plan Project CE-0227 Final. United States Department of Defense. December, 2003.
- Eshelman L.J. Genetic Algorithms. *Evolutionary Computation 1: Basic Algorithms and Operators*. Institute of Physics Publishing. Bristol and Philadelphia, PA. 2000.
- Ground-Water Remediation Technologies Analysis Center (GWRTAC). *Perchlorate Treatment Technologies*, 1st ed. Technology Status Report. 2001.
- Harbaugh, A., Banta, E.R., Hill, M.C., & McDonald, M.G., MODFLOW-2000, The U.S. Geological Survey (USGS) Modular Ground-Water Model – User Guide to Modularization Concepts and the Ground-Water Flow Process., USGS, Reston, VA, 2000.
- Hassan A. Validation of Numerical Ground Water Models Used to Guide Decision Making. *Ground Water*. 42 (2): 277-290. 2004.
- Hatzinger, P.B. and J. Diebold. Interim Project Report: ESTCP Field Pilot Perchlorate Treatment-Horizontal Flow Treatment Wells Shaw Project 683024. Shaw Environmental, Inc. 2005.
- Hatzinger, P.B., Whittier M.C., Arkins M.D., Bryan C.W., Guarini W.J. *In-Situ* and Ex-Situ Bioremediation Options for Treating Perchlorate in Groundwater. *Remediation Journal*, 12 (2): 69-86, 2002.
- Hatzinger, P.B., Huang, J., Goltz, M.N., Chosa, P.G., Diebold, J., Farhan, Y., Parr, J.C., and S. Neville. Field Evaluation of *In situ* Bioremediation of Perchlorate-

- Contaminated Groundwater: Modeling and Preliminary Results. Unpublished research paper. 2005.
- Huang J. Personal communication. 2006-2007.
- Huang, J. and M.N. Goltz. A Model Of *In situ* Bioremediation Which Includes The Effect Of Rate Limited Sorption And Bioavailability. Proceedings of the 1998 Conference on Hazardous Waste Research, pp 297-295, Snow Bird, UT, 19-21 May, 1998.
- Interstate Technology and Regulatory Council (ITRC). Perchlorate: Overview of Issues, Status, and Remedial Options. September, 2005.
- Kingscott, J., Weisman, R.J. Cost Evaluation for Selected Remediation Technologies. *Remediation Journal*, 12 (2): 99-116, 2002.
- Logan, B. E., A Review of Chlorate- and Perchlorate-Respiring Microorganisms. *Bioremediation Journal*, 2(2): 69-79, 1998
- Logan, B. E. Assessing the Outlook for Perchlorate Remediation, *Environmental Science and Technology* 35(23): 482A-487A. 2001.
- Massachusetts Department of Environmental Protection (MassDEP). Drinking Water Standard. 2006.
<http://mass.gov/dep/water/drinking/percinfo.htm>
- McCarty, P. L., Goltz, M. N., Hopkias, G.D., Dolan, M. E., Allan, J. P., Kawakami, B.T., and Carrothers, T. J.. Full-scale evaluation of *in-situ* cometabolic degradation of trichloroethylene in groundwater through toluene injection. *Environmental Science and Technology*, 32, 88-100. 1998
- National Research Council (NRC). Health Implications of Perchlorate Ingestion. National Research Council of the National Academies. National Academies Press, Washington, D.C. January, 2005. <http://www.nap.edu/catalog/11202.html>.
- Nevada Division of Environmental Protection (NDEP). Defining a Perchlorate Drinking Water Standard. October, 2006.
- Parr, J.C. Application of Horizontal Flow Treatment Wells for *In situ* Treatment of Perchlorate Contaminated Groundwater. MS Thesis, AFIT/GEE/ENV/02M-08, 2002. School of Engineering and Management, Air Force Institute of Technology, (AU), Wright-Patterson AFB, OH, March 2002.
- Schwartzenbach, R.P., P.M. Gschwend, and D.M. Imboden. Environmental Organic Chemistry. John Wiley and Sons, pp. 488, 539, 540, 1993.

- Shaw Environmental and Infrastructure (Shaw). *In situ* Bioremediation of Perchlorate Using Horizontal Flow Treatment Wells. ESTCP Technology Demonstration Plan, Project CU-0224 Final. 2003.
- Shaw Environmental and Infrastructure. Aerojet Field Data. Excel Spreadsheet. December, 2006.
- Schwartzenbach, R.P., P.M. Gschwend, and D.M. Imboden. *Environmental Organic Chemistry*. John Wiley and Sons. 1993.
- Trumpolt, C. W., Crain, M., Cullison, G. D., Flanagan, S. J. P., Siegel, L., & Lathrop, S. Perchlorate: Sources, Uses and Occurrences in the Environment. *Remediation Journal*, 16(1), 65-89. 2005.
- United States Air Force (USAF). *Air Force Guidance on Actions Related to Perchlorate*. June, 2006.
- United States Department of Defense (DoD). *Policy on DoD Required Actions Related to Perchlorate*. January, 2006.
- United States Environmental Protection Agency. "Announcement of the drinking water contaminant candidate list"; notice. *Federal Register*. 63:10274-87. 1998.
- United States Environmental Protection Agency (EPA). "Drinking Water Contaminant Candidate List and Regulatory Determinations". 2006.
<http://www.epa.gov/safewater/ccl/index.html>
- United States Environmental Protection Agency. Known Perchlorate Releases in the US. Excel Spreadsheet. March, 2005.
http://www.epa.gov/ogwdw000/ucmr/data/ucmr_list1and2chem.zip
- United States Environmental Protection Agency. "Perchlorate and Perchlorate Salts". Integrated Risk Information Management System. 2005.
<http://www.epa.gov/iris/subst/1007.htm>
- United States Environmental Protection Agency. Perchlorate Environmental Contamination: Toxicological Review and Risk Characterization Based on Emerging Information. External Review Draft. NCEA-1-0503. Washington, DC: Office of Research and Development; 2002.
- United States Environmental Protection Agency. Perchlorate Treatment Technology Update. Federal Facilities Forum Issue Paper. May 2005.
- United States Environmental Protection Agency. Request for National Academy of Sciences review of the health impacts of perchlorate. Official memorandum. March, 2003.

- United States Environmental Protection Agency. "Terms of Environment: Glossary, Abbreviations and Acronyms". 2006.
<http://www.epa.gov/OCEPAterms/rterms.html>
- United States Environmental Protection Agency. "UCM Rounds 1 and 2 and the Six Year Review Data". 2005.
http://www.epa.gov/safewater/ucmr/data/r1r26yr_ptables.zip
- United States Environmental Protection Agency Office of Solid Waste and Emergency Response (OSWER). "Assessment Guidance for Perchlorate". 2006.
http://www.epa.gov/fedfac/pdf/perchlorate_guidance.pdf
- United States Government Accounting Office (GAO). 2005. "Perchlorate: A System to Track Sampling and Cleanup Results Is Needed." GAO-05-462. May, 2005.
<http://www.gao.gov/new.items/d05462.pdf>.
- Urbansky, E. T., Perchlorate Chemistry: Implications for Analysis and Remediation. *Bioremediation Journal*, 2: 81-95, 1998
- Urbansky, E. T., Perchlorate as an Environmental Contaminant. *Environmental Science and Pollution Research*, 9(3): 187-192, 2002.
- Xu, J. Y., Y. Song, B. Min, L. Steinberg, and B. E. Logan. "Microbial Degradation of Perchlorate: Principles and Applications," *Environmental Engineering Science* 20(5): 405–22. 2003.

Vita

Major Roland E. Secody graduated from Tuba City High School in Tuba City, Arizona. He entered undergraduate studies at the United States Air Force Academy, Colorado where he graduated with a Bachelor of Science degree in Civil Engineering in June 1994. He received his regular commission and entered active duty in June 1994. Following his commissioning, Maj Secody has had assignments in the Air Force Materiel Command, Pacific Air Forces, and the United States Air Forces in Europe, and four deployments to Saudi Arabia, Oman and Iraq. In September of 2005, he entered the Graduate School of Engineering and Management, Air Force Institute of Technology. Upon graduation, he will be assigned to United States Forces Korea, at Yongsan Army Garrison, Republic of Korea.

REPORT DOCUMENTATION PAGE				Form Approved OMB No. 074-0188	
<p>The public reporting burden for this collection of information is estimated to average 1 hour per response, including the time for reviewing instructions, searching existing data sources, gathering and maintaining the data needed, and completing and reviewing the collection of information. Send comments regarding this burden estimate or any other aspect of the collection of information, including suggestions for reducing this burden to Department of Defense, Washington Headquarters Services, Directorate for Information Operations and Reports (0704-0188), 1215 Jefferson Davis Highway, Suite 1204, Arlington, VA 22202-4302. Respondents should be aware that notwithstanding any other provision of law, no person shall be subject to a penalty for failing to comply with a collection of information if it does not display a currently valid OMB control number.</p> <p>PLEASE DO NOT RETURN YOUR FORM TO THE ABOVE ADDRESS.</p>					
1. REPORT DATE (DD-MM-YYYY) 22-03-2007		2. REPORT TYPE Master's Thesis		3. DATES COVERED (From – To) Sep 2005 – Mar 2007	
4. TITLE AND SUBTITLE Modeling <i>In Situ</i> Bioremediation of Perchlorate-Contaminated Groundwater				5a. CONTRACT NUMBER	
				5b. GRANT NUMBER	
				5c. PROGRAM ELEMENT NUMBER	
6. AUTHOR(S) Roland E. Secody, Major, USAF				5d. PROJECT NUMBER	
				5e. TASK NUMBER	
				5f. WORK UNIT NUMBER	
7. PERFORMING ORGANIZATION NAMES(S) AND ADDRESS(S) Air Force Institute of Technology Graduate School of Engineering and Management (AFIT/EN) 2950 Hobson Way, Building 640 WPAFB OH 45433-7765				8. PERFORMING ORGANIZATION REPORT NUMBER AFIT/GEM/ENV/07-M13	
9. SPONSORING/MONITORING AGENCY NAME(S) AND ADDRESS(ES) Air Force Center for Environmental Excellence Environmental Security Technology Certification Program Attn: Dr. Doris Anders Attn: Dr. Andrea Leeson 3300 Sidney Brooks 901 N. Stuart St., Ste 303 Brooks City-Base, TX 78235 Arlington, VA 22203 (210)-536-5667 DSN 240-5667 (703) 696-2118				10. SPONSOR/MONITOR'S ACRONYM(S) AFCEE/TDE ESTCP	
				11. SPONSOR/MONITOR'S REPORT NUMBER(S)	
12. DISTRIBUTION/AVAILABILITY STATEMENT APPROVED FOR PUBLIC RELEASE; DISTRIBUTION UNLIMITED.					
13. SUPPLEMENTARY NOTES					
14. ABSTRACT Perchlorate-contaminated groundwater is a significant problem for the Department of Defense and the United States Air Force. An innovative technology was recently developed which uses dual-screened treatment wells to mix an electron donor into perchlorate-contaminated groundwater in order to effect <i>in situ</i> bioremediation of the perchlorate by indigenous perchlorate reducing bacteria without the need to extract the contaminated water from the subsurface. In this study, a model that simulates operation of the technology is calibrated and validated using 761 days of observational data obtained from a field-scale technology evaluation project. A genetic algorithm was used with the first 113 days of data to derive a set of best-fit parameters to describe perchlorate reduction kinetics for the electron donor, citrate, utilized in the evaluation study. The calibrated parameter values were then used to predict technology performance from day 114 through day 761. Measurements of goodness-of-fit statistics indicate the model appears to qualitatively reproduce the salient characteristics of the observed data when utilizing the new best-fit parameter values. Therefore, it appears the model may be a useful tool for designing and operating this technology at other perchlorate-contaminated sites.					
15. SUBJECT TERMS Perchlorate, groundwater contamination, bioremediation, technology model, genetic algorithm, calibration					
16. SECURITY CLASSIFICATION OF:			17. LIMITATION OF ABSTRACT UU	18. NUMBER OF PAGES 126	19a. NAME OF RESPONSIBLE PERSON Mark N. Goltz, AD-24, DAF(ENV)
REPORT U	ABSTRACT U	c. THIS PAGE U			19b. TELEPHONE NUMBER (Include area code) (937) 255-3636, ext 4638 email: mark.goltz@afit.edu